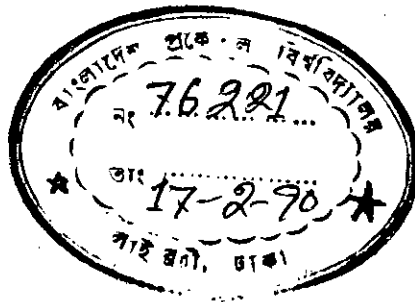


MICROWAVE BANDPASS FILTERS
USING COUPLED TEM-LINES
IN COMB GEOMETRY

A

Thesis

submitted to the Department of Electrical and Electronic
Engineering, B.U.E.T. Dhaka, in partial fulfilment of the
requirements for the degree of Master of Science in
Engineering (Electrical and Electronics).



QUAZI DEEN MOHD KHOSRU

January 1990



#76221#

Declaration

I hereby declare that this work has been done by me and this has not been submitted elsewhere for the award of any degree or diploma or for publication.



(Quazi Deen Mohd Khosru)

The thesis "Microwave bandpass filters using coupled TEM-lines in comb geometry" submitted by Quazi Deen Mohd Khosru, Roll No. 871339P, Session '85-86 to the Department of Electrical and Electronic Engineering, B.U.E.T. has been accepted as satisfactory for partial fulfilment of the requirements for the degree of Master of Science in Engineering (Electrical and Electronic Engineering).

Board of Examiners:

1. Saiful Islam, MScEng., PhD, CEng, MIEE, FIEE
Professor,
Department of EEE.
Bangladesh University of
Engineering and Technology,
Dhaka 1000. Chairman
and Supervisor *Saiful Islam*
19.1.90
2. Md. Abdul Matin, M.Sc.Engg., Ph.D., FIEB
Professor and Head,
Department of EEE.
Bangladesh University of
Engineering and Technology,
Dhaka 1000. Member
(Ex-officio) *M. A. Matin*
19.1.1990
3. K. Mohiuddin Ahmed, M.Sc.Engg., Ph.D., MIEB
Associate Professor,
Department of EEE.
Bangladesh University of
Engineering and Technology,
Dhaka 1000. Member *M. A. Matin*
19.1.90
4. Muhammad Ali Chowdhury, M.Sc.Engg., Ph.D.
Assistant Professor,
Department of EEE.
Bangladesh University of
Engineering and Technology,
Dhaka 1000. Member *M. A. Chowdhury*
19.1.90
5. Shamsuddin Ahmed, M.Sc.Engg., Ph.D.
Professor and Head,
Department of EEE.
ICTVTR, Gazipur. Member
(External) *Shamsuddin*

Acknowledgement

The author feels pleasure to have the opportunity to express his profound gratitude to Dr. Saiful Islam, Professor, Department of Electrical and Electronic Engineering, B.U.E.T. for his ceaseless guidance, valuable suggestions and cooperation which played a significant role in carrying out this work. Sincere thanks once again goes to him without saying for his expert opinion and active help in solving out the problems the author had to come across in fabrication and measurement.

The author also takes the privillage to acknowledge his indebtedness to Dr. M. Abdul Matin, Professor and Head, Department of Electrical and Electronic Engineering, B.U.E.T., for his all-out encouragement and cooperation at all stages of this work.

Thanks are also due to Mr. Molla Ahmed Ali and Mr. Hussain Ali of Machine shop for their sincere assistance in machining brass plates and constructing the filter.

Finally, the author rounds up this chapter throwing petals of thanks over every body who had even the least involvement with this work some how or other.

Contents

	<u>Page</u>
Declaration	(i)
Approval	(ii)
Acknowledgement	(iii)
Contents	(iv)
Abstract	(vii)
List of principal symbols	(viii)
<u>Chapter 1 Introduction</u>	
1.1 Historical background	1
1.2 Objective of this work	5
1.3 Brief introduction to this thesis	5
<u>Chapter 2 Low pass to bandpass transformation</u>	
2.1 Introduction	8
2.2 Method of transformation	8
2.3 Conversion of filter elements	11
2.4 Summary	14
<u>Chapter 3 Methods of filter synthesis</u>	
3.1 Introduction	15
3.2 Different methods of filter synthesis	15
3.3 Definition of image impedance and propagation function	16
3.4 Image parameter method	19
3.5 Insertion loss method	23
3.6 Summary	25
<u>Chapter 4 Parallel coupled TEM lines and its equivalent circuits</u>	
4.1 Introduction	26

	Page
4.2 Different types of parallel coupled lines	26
4.3 Coupling with thick rectangular bars	28
4.4 Unsymmetrical parallel coupled lines	32
4.5 Arrays of parallel coupled lines	35
4.6 Transmission lines as resonators and its lumped constant equivalent circuits	37
4.7 Parallel coupled line filter section and its equivalent circuit	39
4.8 Summary	43
 <u>Chapter 5 Conversion of prototype filter circuit using impedance/admittance inverters</u>	
5.1 Introduction	44
5.2 Definition of impedance and admittance inverter	44
5.3 Equivalent forms of prototype filter using inverters	45
5.4 Derivation of the expressions for inverter parameters	47
5.5 Some inverter circuits	50
5.6 Summary	53
 <u>Chapter 6 Comb-line geometry and its equivalent circuit</u>	
6.1 Introduction	55
6.2 Comb-line bandpass filter	55
6.3 Equivalent circuit of comb-line filter	58
6.4 Summary	62
 <u>Chapter 7 Design equations of comb-line filter</u>	
7.1 Introduction	63
7.2 Design equations	63
7.3 Derivation of design equations	65
7.4 Summary	72

	Page
<u>Chapter 8 Design of the experimental filter</u>	
8.1 Introduction	74
8.2 Design procedure	74
8.3 Computation of widths of rectangular bars and separation between adjacent bars	77
8.4 Summary	79
<u>Chapter 9 Fabrication and measurement of the experimental filter</u>	
9.1 Introduction	80
9.2 Fabrication of the experimental filter	80
9.3 Measurement of insertion loss characteristics	84
9.4 Method of tuning	94
9.5 Summary	94
<u>Chapter 10 Discussions and conclusions</u>	
Discussions and conclusions	96
Suggestions for future work	99
<u>References</u>	100
<u>Appendices</u>	
Appendix-A Program to calculate capacitance values	102
Appendix-B Program to calculate widths of resonators	103
Appendix-C Table of measured attenuation characteristics (before tuning)	104
Appendix-D Table of measured attenuation characteristics (after tuning)	105
Appendix-E Table of measured attenuation characteristics (after tuning) with connection to input and output terminals interchanged	106

Abstract

A method for designing microwave narrowband bandpass filters having Chebychev characteristics is presented. The method utilizes a lowpass to bandpass transformation to achieve the lumped bandpass filter circuit from the desired lumped lowpass prototype element values. An equivalent circuit of the lumped bandpass filter consisting of J-inverters and shunt resonators is then developed. Equivalent circuit of the admittance inverters and the shunt resonators are next obtained using the previously published theory and equivalent circuits. Parallel coupled TEM lines in the configuration of rectangular bars between two parallel ground planes have been used for fabricating the filter. The parallel coupled lines of such a filter are grounded on the same side and open circuited on the other side which results in comb geometry. Lumped parallel plate capacitances are added to the open circuit ends of the parallel coupled lines to complete the design. The parallel coupled lines are one eighth wavelength long at the passband center frequency which makes this type of filter more compact compared to the quarter wavelength resonator filters.

Based on the developed analytic design method a computer programme for PC in basic has been prepared for designing this type of combline filters. With the help of this computer programme a five resonator 10% bandwidth Chebychev filter has been designed for 1.68 GHz center frequency. From the line parameters thus obtained, the physical dimensions of the filter are next computed with the help of previously published graphs and analytical expressions. Using these values an experimental filter has been fabricated and measured in the laboratory. The designed parameters and the measured results are presented.

List of principal symbols

ω	radian frequency variable for bandpass filter
ω'	radian frequency variable for low pass prototype filter
W	fractional bandwidth
ω_0	midband frequency
g_k	low pass prototype filter element values
γ	image propagation function
α	image attenuation factor
β	image phase factor
P_i	incident power
ρ	reflection co-efficient
Γ	input reflection co-efficient for lossless network
Y_{oo}	odd mode admittance
Y_{oe}	even mode admittance
v	velocity of light in the medium of propagation
ϵ	absolute dielectric constant
ϵ_r	relative dielectric constant
η_0	intrinsic impedance of free space
w_k	widths of rectangular bars
t	thickness of rectangular bars
b	distance between adjacent bars
$J_{k,k+1}$	admittance inverter parameters
$B_k(\omega)$	comb line filter resonator functions
C'_{fe}	fringing capacitance
$C_{k,k+1}$	coupling capacitances
C_k	self capacitances
C_k^s	lumped capacitances
Y_A	terminating admittances
Y_{ak}	line admittances

CHAPTER-1

Introduction

1.1 Historical Background:

A good number of publications in the field of microwave bandpass filters are available in various journals and periodicals. Here, attention has been given only to those papers which deal with filters having physical structure similar to the one employed in this study i.e. the structures having parallel coupled lines between parallel ground plates.

A number of structures consisting of arrays of parallel conductors between ground planes were analyzed by Bolljahn and Matthaei [1]. The structure included interdigital line, meander line, a form of helix. The results of their study indicated that certain structure has special merit for use as filter. They [1] showed that interdigital line structure has very interesting band-pass filter properties. Before this discovery, interdigital line structures had been regarded as slow-wave structures. Matthaei [2] gave an approximate design procedure of bandpass filters using interdigital arrays of resonator line elements between parallel ground planes. He presented two approximate design procedures both of which permit design directly from lumped element low-pass, prototype filters for Chebychev response. Both design procedures could work either

for narrow or wide-band filters, but one of the procedures gave more practical dimensions for filters having wide bandwidth (e.g. an octave), while the other could give more practical dimensions for filters having narrow or moderate bandwidth. Matthaei[2] claimed that the resulting filters were very compact, had relatively noncritical manufacturing tolerances, and strong stop bands with the second pass band centered at three times the center frequency of the first pass band. For finding out the physical dimensions of the structure from static capacitance values he[2] used the expressions and curves of Getsinger [3]. He[2] presented the dimensions and measured performance curves for a ten percent bandwidth and an octave bandwidth designs.

An exact theory of interdigital line network and related coupled structures were presented by Wenzel [4]. According to Wenzel, an exact theory is desirable when optimum network performance or special network configurations are required and the use of exact synthesis procedures allow greater flexibility in design and fabrication. At the same time, the accurate determination of practical circuit limitations are made possible. He[4] reviewed the theory of parallel coupled line arrays and discussed the derivation of exact equivalent circuits from the equivalent matrix using modern network synthesis techniques. He[4] also introduced the theory of equivalent coupled structures in order to avoid the lengthy analysis required for the impedance matrix approach. He[4] showed how to find the equivalent networks

for interdigital lines simply by inspection. The techniques presented by Wenzel [4] were simple to apply and allowed to obtain a given transmission line response in a variety of line configurations. He presented the practical drawing of the design of an experimental interdigital filter. He used a combination of coaxial interdigital realization in order to get relatively wide line spacings. His paper contains information in details and discussions on both theoretical and practical aspects. Despite his claim that the design procedure was exact he had to find out the length of the input and output lines by means of almost trial and error method. Moreover he arbitrarily shortened the interdigital line sections by about one fifth of an inch. He also used tuning screws to achieve the desired characteristics. However, he ultimately succeeded in constructing one such filter that came out with satisfactory performance. Wenzel also used the results of Getsinger [3] to obtain the physical dimensions from the matrix of static capacitance.

A design procedure for a practical digital elliptic function filter capable of providing either band-pass or bandstop characteristics was presented by Horton and Wenzel [5]. They gave examples to illustrate typical design procedure for both band-pass and band stop applications. However, they presented experimental results only for an octave band-stop design. Regarding its advantages, they mentioned about its high selectivity in a very compact configuration as because the realization was in the form of a

coaxial and interdigital form. About its remarkable drawback they mentioned that the structure is inherently wide band and is not suitable for narrow band designs due to physical limitations. Moreover, the structure requires series internal stubs and therefore involves more machined parts.

Rhodes [6] presented a design procedure for narrow-band bandpass TEM-line elliptic function filter. He proposed the realization in the form of a stepped-impedance digital n-wire line which is one-half of a wave length long at center frequency and short circuited to ground at both ends. The digital line is stepped in impedance along any arbitrary prescribed plane in the filter. Rhodes presented a detailed design procedure for the construction of the two characteristic admittance matrices which described the digital n-wire line from the low-pass prototype element values. He also showed that the normalized impedance values of the elements in the filter are all of the order of unity and independent of the actual bandwidth of the filter except for the input and output transformer elements. He gave a numerical example and experimental results on a seventh-degree 1-percent bandwidth filter with a center frequency at 3.7 GHz and demonstrated the significant improvements which may be obtained from the half-wave stepped digital elliptic filter over most of the other forms of microwave TEM-line narrow-band bandpass filters. Another important feature of Rhodes [6] filter is its compactness and inherent physical rigidity which makes it attractive for applications where

size, weight, and stability under mechanical vibrations are important. The only unfavourable factor of the structure is its incapability to reject harmonics. However, he[6] suggested that the inclusion of quasi-low-pass filters directly into the end blocks of the filter through single interdigital sections would attenuate the harmonics without increasing the external size of the filters and at the same time, the advantages of the filter remain unaffected.

1.2 Objective of this work:

The first objective of this thesis is to develop an analytic design technique for a narrowband bandpass filter which is compact in size. The second objective is to prepare a program for desktop personal computers(PC) so that one can obtain the line parameters of the filter by simply providing the low pass prototype element values as input. The last objective is to verify the design method by designing, fabricating and measuring an experimental filter.

1.3 Brief introduction to this thesis:

The method to obtain bandpass characteristics from a low pass prototype filter specifications has been described in chapter two of this dissertation. It also includes the deduction of the bandpass filter elements due to the transformation.

In chapter three various methods of filter synthesis is discussed in details.

Chapter four contains some important information regarding parallel coupled TEM lines and their equivalent circuits. Various configurations like coupling with thick rectangular bars, unsymmetrical parallel coupled lines, arrays of parallel coupled lines have been discussed individually in this chapter.

The concept of both impedance and admittance inverters are given in chapter five. It contains the derivation of inverter parameters in terms of prototype circuit element values and at the same time the conversion of prototype filter circuit using admittance inverters have been taken into account. Some inverter circuits are also shown in this chapter.

The introduction to microwave band pass filter in comb geometry is presented in chapter six. The salient features of comb-line band pass filter has been discussed there. How an approximate equivalent circuit of comb-line filter can be obtained by replacing parallel coupled lines with their electrically equivalent open-wire line circuit has also been shown.

Chapter seven contains the design equations of comb-line filter. The mathematical expressions to calculate various design parameters are tabulated there. Derivations of these equations considering relevant circuit elements are also presented in this chapter.

Chapter eight presents the design of the experimental filter which is an important part of the objectives of this

work. Details of design procedure has been presented. Various designed parameters and physical dimensions thus obtained are tabulated in this chapter. A complete diagram of the experimental filter to be constructed is also shown there.

The experimental part of the work is described in chapter nine. It includes the fabrication and measurement techniques. A complete description about the construction of the experimental filter is given in this chapter. Photographs of the constructed filter are also shown there. The method of measurement and tuning procedure is described briefly. The plots of insertion loss against frequency obtained under two tuning conditions are also presented in this chapter.

Discussions on results and limitations are presented in chapter ten. Conclusions and suggestion for further work have also been included in this chapter.

Computer programs to determine the values of normalised capacitances and the physical dimensions of the resonator elements are presented in appendices. It also contains the tables of the measured attenuation characteristics of the fabricated filter.

CHAPTER-2

Low pass to Bandpass Transformation

2.1 Introduction:

The method to obtain bandpass characteristics from a low-pass prototype filter specifications has been discussed in this chapter. The low pass filter with cut off at $\omega = 1$ and terminated in a normalised unity load impedance may be used as a basis for the design of band-pass filter with arbitrary resistive load termination. For this reason it is referred to as a prototype filter [7]. The details of low pass to bandpass transformation technique is presented in the following sections.

2.2 Method of transformation :

Figure 2.1 shows the low-pass prototype circuit and the frequency response of the filter. To obtain a bandpass filter corresponding to the low-pass prototype consider a change of variable according to

$$\omega' = f(\omega) = (\omega_0/(\omega_2 - \omega_1)) \{ (\omega/\omega_0) - (\omega_0/\omega) \} \quad \text{--- (2.1)}$$

where ω' and ω are the frequency variables for low-pass and bandpass respectively. This equation may be solved for ω as

$$\omega = \omega' \{ (\omega_2 - \omega_1) / 2 \} \pm \sqrt{ \{ \omega'^2 (\omega_2 - \omega_1) / 2 + \omega_0^2 \} } \quad \text{--- (2.2)}$$

If we choose $\omega_0^2 = \omega_1 \omega_2$, we get

$$\omega = \omega' (\omega_2 - \omega_1) / 2 \pm (1/2) \{ \sqrt{ \{ \omega'^2 (\omega_2 - \omega_1)^2 + 4\omega_1 \omega_2 \} } \} \quad \text{--- (2.3)}$$

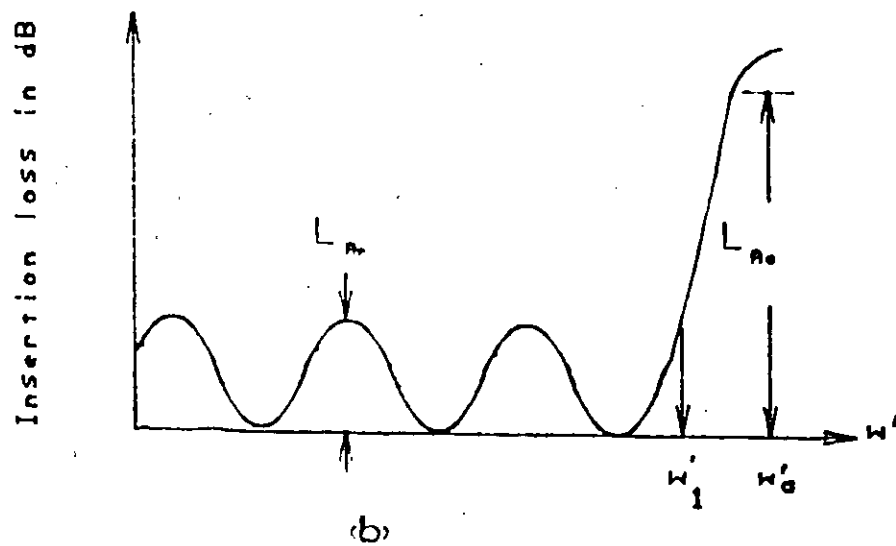
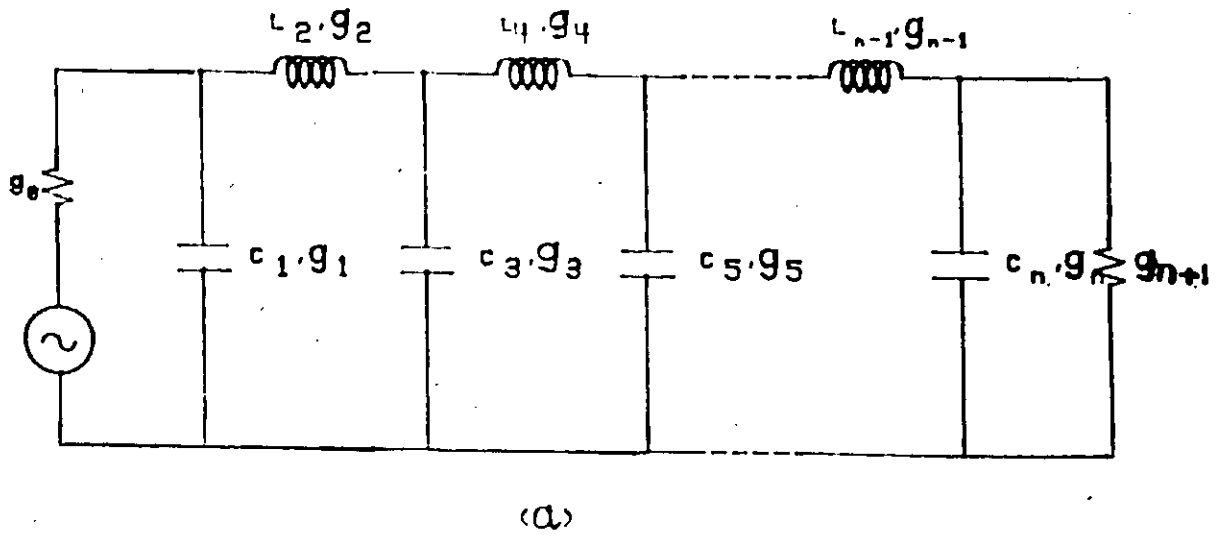


Fig. 2.1 Low-pass prototype filter

(a) Low-pass filter circuit

(b) Attenuation characteristics of the filter

The point $\omega' = 0$ is seen to map into the points $\omega = \pm\omega_0$ and $\omega' = \pm 1$ maps into the four points $\pm\omega_2$ and $\pm\omega_1$. Thus the prototype filter passband between ± 1 maps into passband extending from ω_1 to ω_2 and $-\omega_1$ to $-\omega_2$ which represents bandpass filter with band centers at $\pm\omega_0$ equal to the geometric mean of ω_1 and ω_2 as illustrated in figure 2.2.

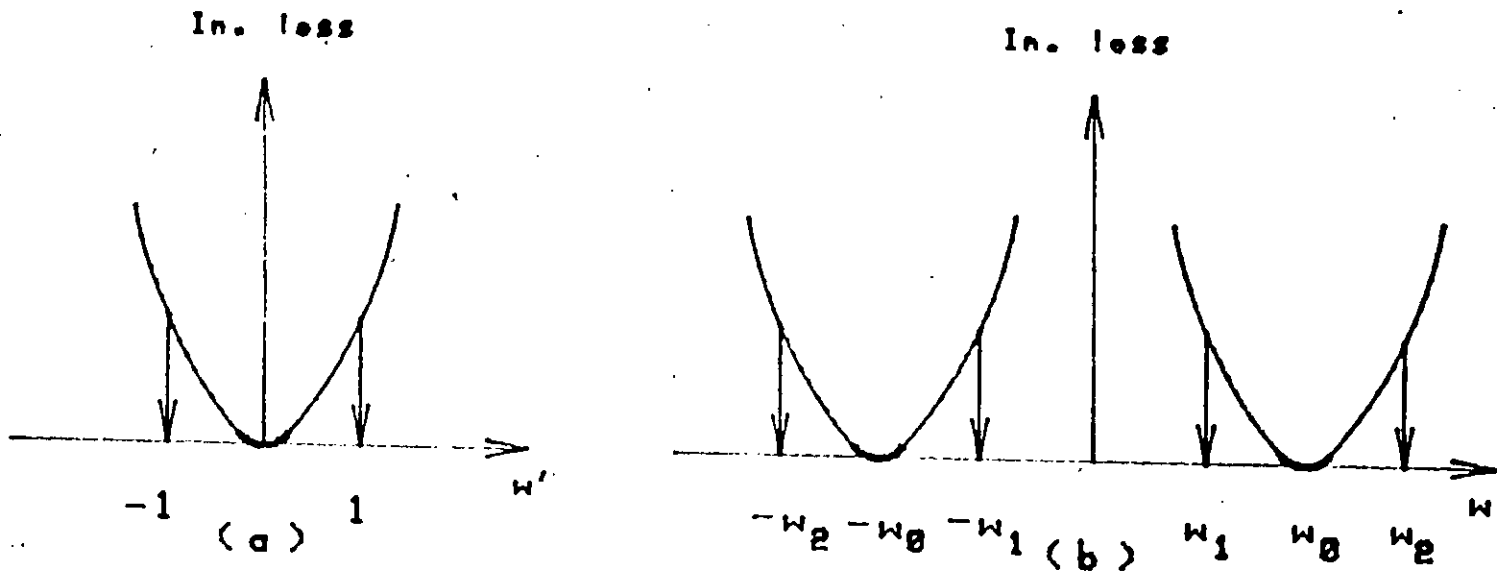


Fig. 2.2 Low-pass to bandpass transformation

(a) Low-pass response

(b) Response after low-pass to bandpass transformation

2.3 Conversion of filter elements:

The required filter elements may be deduced by considering the frequency behaviour of the prototype element and the low-pass circuit may be transformed to a corresponding lumped-element bandpass circuit using the frequency transformation

$$\omega' = (\omega_1'/W) \left\{ (\omega/\omega_0) - (\omega_0/\omega) \right\} \quad \text{--- (2.4)}$$

where $\omega_0 = \sqrt{\omega_1\omega_2}$ is known as resonance frequency and $W = (\omega_2 - \omega_1)/\omega_0$ is called fractional bandwidth.

Then the series reactance of the prototype lowpass filter circuit becomes

$$\begin{aligned} \omega' L &= \omega_1'/\omega \left\{ (\omega/\omega_0) - (\omega_0/\omega) \right\} L \\ &= \omega L' - 1/\omega C' \end{aligned} \quad \text{--- (2.5)}$$

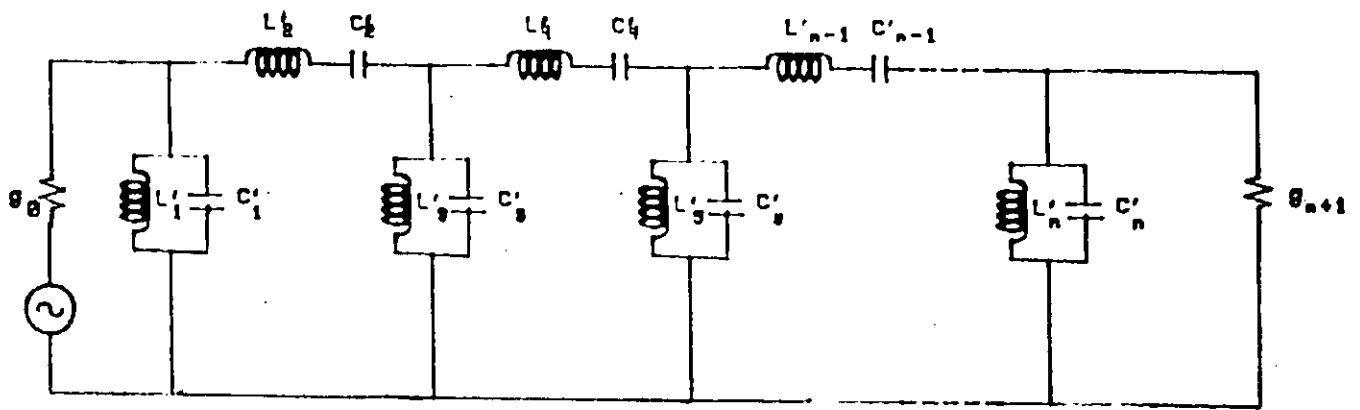
where $L' = (\omega_1'/W\omega_0)L$ and $C' = W/\omega_1'\omega_0L$

Similarly the shunt reactance $\omega' C$ transforms as follows

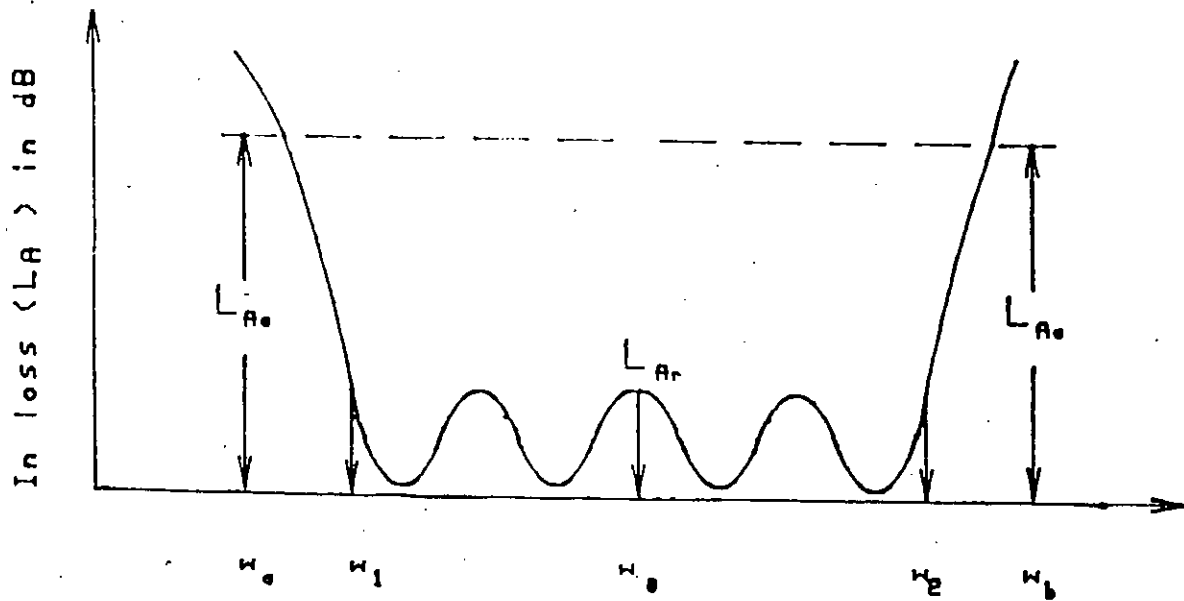
$$\begin{aligned} \omega' C &= (\omega_1'/W) \left\{ (\omega/\omega_0) - (\omega_0/\omega) \right\} C \\ &= \omega C'' - 1/\omega L'' \end{aligned} \quad \text{--- (2.6)}$$

where $C'' = (\omega_1'/W\omega_0)C$ and $L'' = W/\omega_1'\omega_0C$

So it is obvious that the series element in the lowpass prototype becomes a series combination of L and C and the shunt element becomes a parallel combination of L and C when it is transformed into bandpass filter i.e. all the reactive elements of low-pass prototype filter transform into corresponding resonators on low pass to bandpass transformation. The resultant filter network and the response thus obtained is illustrated in figure 2.3 below.



(a)



(b)

Fig. 2.3 Bandpass filter

(a) Bandpass filter circuit obtained from lowpass prototype using lowpass to bandpass transformation

(b) Attenuation characteristics of the bandpass filter

Figure 2.1(a) shows the typical low-pass prototype under discussion. It also defines the manner in which the element values g_k are to be specified for the purpose of this discussion. And figure 2.1(b) shows a typical Chebychev response such as can be achieved by filters of this type. It is to be noted that n is the number of reactive element in the prototype and that, including the resistor termination the element values range from g_0 to g_{n+1} . An important point is that a low-pass prototype with n reactive elements leads to a band-pass filter with n resonators. Figure 2.3(b) shows the band-pass filter response that corresponds to the low-pass prototype response. The band-pass filter response will have the same type of pass-band characteristic as the prototype, but the width of the band-pass filter pass-band can be specified arbitrarily.

From the low-pass to band-pass transformation, the attenuation characteristic of the low-pass prototype as a function of ω' can be mapped to the band-pass filter attenuation characteristic as a function of the band-pass filter radian frequency variable ω . Since the attenuation is the same for both the lowpass and band-pass filters at frequencies ω' and ω , respectively, which are related as given by the mapping, the band-pass filter attenuation characteristic can be predicted from the specifications of the lowpass filter.

2.4 Summary :

The low pass to band pass transformation technique has been discussed in details. Considering a lumped low pass prototype filter circuit and its response, the transformed band pass filter circuit and the corresponding response were obtained. Both the filter circuits and their respective responses are presented. Using the mapping given for the band pass filter radian frequency variable, the attenuation characteristics of the band pass filter can be obtained from the given specifications of the low pass prototype filter.

CHAPTER-3

Methods of Filter Synthesis

3.1 Introduction:

At low frequencies the building blocks for filters are ideal inductor and capacitors. These elements have very simple frequency characteristics and very general and complete synthesis procedure has been developed for the design of filters utilizing them. That is why it is possible to synthesize filters directly with a wide variety of prescribed frequency characteristics. But the filter design problem at microwave frequencies where distributed parameter elements must be used is much more complicated, and no complete theory or synthesis procedure exists. Microwave filter is realized by replacing all inductors and capacitors by suitable microwave circuit elements that have similar frequency characteristics over the frequency range of interest. Two different techniques of filter synthesis have been discussed in this chapter.

3.2. Different methods of filter synthesis:

There are essentially two low-frequency filter synthesis techniques [7] in practice. They are

- i) Image parameter method
- ii) Insertion loss method.

The Image Parameter method provides a filter design having

the required passband and stopband characteristics, but does not specify the exact frequency characteristics over each region. While the Insertion-loss method begins with a complete specifications of a physically realizable frequency characteristics, and from this a suitable filter network is synthesized. The image parameter method suffers from the shortcomings that a good deal of cut-and-try procedures must often be restored to in order to obtain an acceptable overall frequency characteristics. For this reason, the Insertion-loss method is preferable .

3.3. Definition of image impedance and image propagation function:

The image view point for the analysis of circuits is much the same as the wave view point commonly used for the analysis of transmission lines. In fact, for the case of a uniform transmission line the characteristic impedance of the line is also its image impedance[8], and if r_t is the propagation constant per unit length then $r_t l$ is the image propagation function for a line of length l .

Consider the case of a two port symmetrical network but for the sake of generality, is assumed to be unsymmetrical with different impedance characteristics at End1 than at End2. Figure 3.1 shows the case of an infinite number of identical networks of this type connected in such a manner as at each junction either End1s are connected together or End2s. Since the chain of networks extends to

infinity in each direction, the same impedance Z_{I1} is seen looking both left and right at a junction of the two End1s, while at a junction of two End2s another impedance Z_{I2} will be seen when looking either left or right. These impedances, as indicated in figure 3.1 are defined as the image impedances for End1 and End2 respectively. For an unsymmetrical network they are generally unequal.

It is to be noted that because of the fashion the infinite chain of networks in figure 3.1 are connected, the impedances seen looking left and right at each junction are always equal, hence there is never any reflection of a wave passing through a junction. Thus, from the wave point of view, the networks in figure 3.1 are all perfectly matched. If a wave is set to propagating towards the right, through the chain of networks, it will be attenuated as determined by the propagation function of each network, but will pass on from network to network without reflection. The image impedances are actually impedance of infinite networks, and as such they should be expected to have a mathematical form different from that of the rational impedance functions obtained for finite, lumped-element networks. In the cases of lumped element filter structures, the image impedances are usually irrational function. While in the cases of microwave filter structures which involve transmission line elements, the image impedances are usually both irrational and transcendental.

However, a cascade connection of lossless two-port

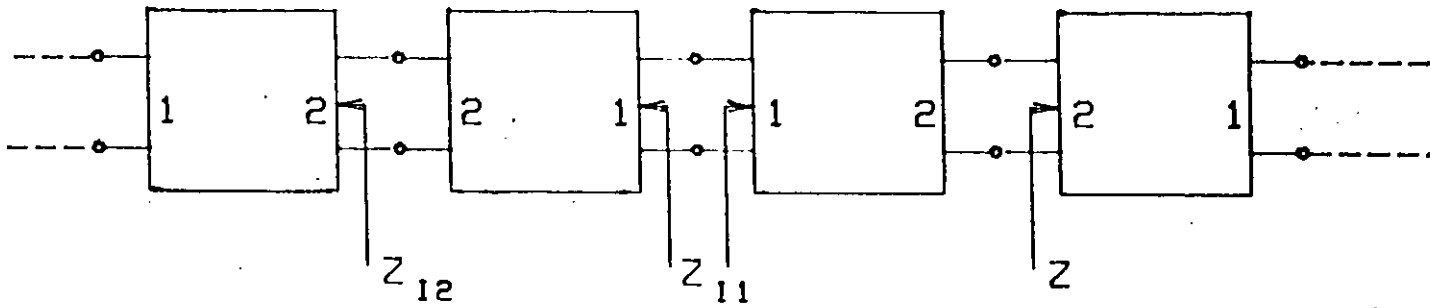


Figure 3.1 Infinite chain of identical networks used for defining image impedance and image propagation function

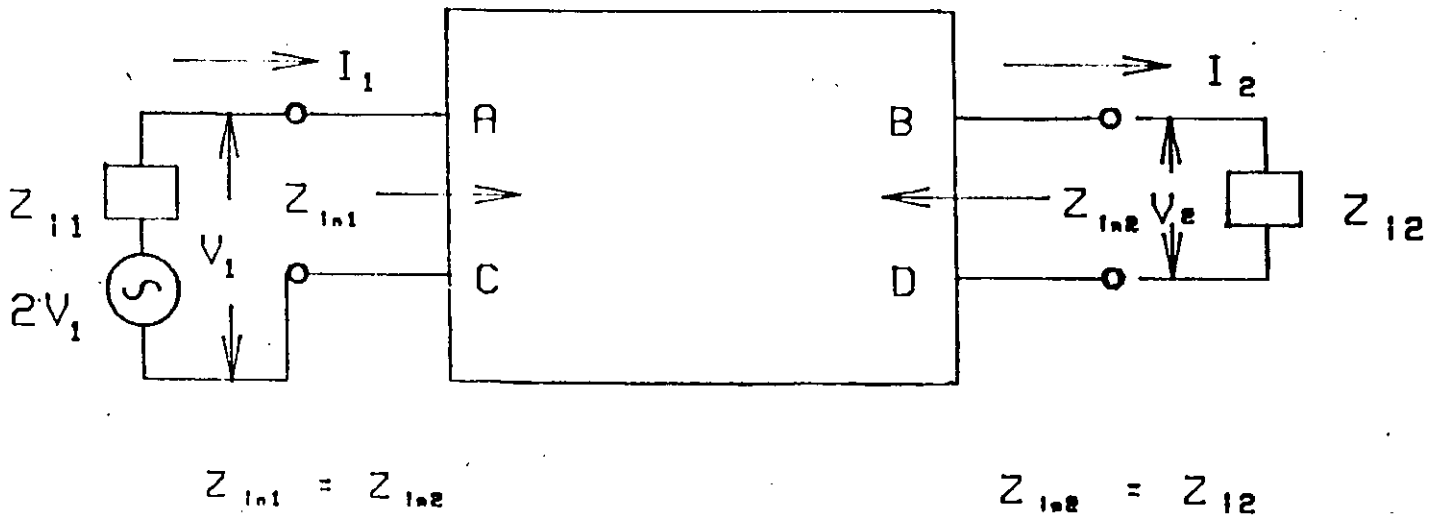


Figure 3.2 Image parameters for a two port network

networks behaves similar to a transmission line. For unsymmetrical networks two characteristic impedance occur and each section has a propagation factor. A periodic structure of this form has pass band and stopband characteristics and is therefore a bandpass filter. Usually, a filter must operate between resistive load terminations and to ensure this either symmetrical networks or matching section at input and output are used.

3.4 Image parameter method:

Consider a single two-port network with parameters A,B,C and D. Let the output be terminated in a load Z_{i2} and the input be terminated in a load Z_{i1} as shown in figure 3.2. For particular values of Z_{i1} and Z_{i2} , known as the image impedances, the input impedance at port 1 equals Z_{i1} and that at port 2 equals Z_{i2} . These impedances then provide matched terminations for the two port network, and if they are real they also provide a maximum power transfer when the generator has an internal impedance equal to the image impedance. The governing equations for the two-port network are

$$V_1 = AV_2 + BI_2 \quad \dots\dots\dots(3.1)$$

$$I_1 = CV_2 + DI_2 \quad \dots\dots\dots(3.2)$$

and hence

$$V_1/I_1 = Z_{in,1} = (AV_2+BI_2)/(CV_2+DI_2)=(AZ_{i2}+B)/(CZ_{i2}+D)$$

If we solve for V_2 and I_2 in terms of V_1 and I_1 , we obtain

$$V_2 = DV_1 - BI_1 \quad \dots\dots\dots(3.3)$$

$$I_2 = -CV_1 + AI_1 \quad \dots\dots\dots(3.4)$$

we thus have

$$-(V_2/I_2) = Z_{in,2} = -(DV_1 - BI_1) / (-CV_1 + AI_1) = (DZ_{i1} + B) / (CZ_{i1} + A)$$

The requirement that $Z_{i1} = Z_{in,1}$ and $Z_{i2} = Z_{in,2}$ gives

$$Z_{i1}(CZ_{i2} + D) = AZ_{i2} + B \quad \dots\dots\dots(3.5)$$

$$Z_{i2}(CZ_{i1} + A) = DZ_{i1} + B \quad \dots\dots\dots(3.6)$$

A simultaneous solution of these equations gives -

$$Z_{i1} = \sqrt{(AB/CD)} \quad \dots\dots\dots(3.7)$$

$$Z_{i2} = \sqrt{(BD/AC)} \quad \dots\dots\dots(3.8)$$

Also we find that $Z_{i2} = (D/A) Z_{i1}$.

If a generator with internal impedance Z_{i1} is connected at port 1 and the output port 2 is terminated in a load Z_{i2} as shown in figure 3.2, the voltage and current transfer ratios are readily found from the relations

$$V_2 = DV_1 - BI_1 = (D - B/Z_{i1})V_1$$

$$I_2 = -CV_1 + AI_1 = (-CZ_{i1} + A)I_1$$

where V_1 is the voltage across the network terminals at port 1 while the generator voltage is $2V_1$.

Thus we find that

$$V_2/V_1 = \sqrt{(D/A)} [\sqrt{(AD)} - \sqrt{(BC)}] \quad \dots\dots\dots(3.9)$$

$$I_2/I_1 = \sqrt{(A/D)} [\sqrt{(AD)} - \sqrt{(BC)}] \quad \dots\dots\dots(3.10)$$

In a similar manner the transfer constants from port 2 to port 1 are found to be

$$V_1/V_2 = \sqrt{(A/D)} [\sqrt{(AD)} + \sqrt{(BC)}] \quad \dots\dots\dots(3.11)$$

$$I_1/I_2 = \sqrt{(D/A)} [\sqrt{(AD)} + \sqrt{(BC)}] \quad \dots\dots\dots(3.12)$$

The image propagation factor is defined as

$$e^{-r} = \sqrt{(AD)} - \sqrt{(BC)}$$

whence it is found that

$$e^r = \sqrt{(AD)} + \sqrt{(BC)}$$

and

$$\text{Cosh } r = \sqrt{(AD)}$$

$$\text{Sinhr} = \sqrt{(BC)}$$

where $r = \alpha + j\beta$, is the image propagation function, α is the image attenuation in nepers and β is the image phase in radians. The factor (A/D) is interpreted as an impedance transformation ratio and may be viewed as an ideal transformer of turns ratio $\sqrt{(A/D)}$.

For a lossless network, A and D are real and B and C are imaginary. In the passband of a filter, r is pure imaginary and equal to $j\beta$, and this occurs for $|AD| < 1$. Also, in the passband, the image impedances are pure real, whereas in a stopband they are pure imaginary. In a passband, B and C must be of the same sign, so that $BC = j|B|j|C| = -|BC|$ will make Sinhr pure imaginary. Thus the solution for Z_{i1} and Z_{i2} will be real and positive since AD must be positive to give a real solution for $\text{Cosh } r$. Hence the image impedances are real in a passband.

If N two-port networks are connected in cascade and these have propagation constants r_n , with $n=1, 2, \dots, N$, and the voltage transformation ratios $T_1, T_2, T_3, \dots, T_N$ and the output section is terminated in an impedance equal to its output image impedance, the overall voltage transfer ratio is

$$V_N/V_1 = \prod_{n=1}^N T_n e^{-r_n} \quad \text{with } n=1, 2, 3, \dots, N \quad \dots \dots \dots (3.13)$$

provided also that the output image impedance of any section is equal to the input image impedance of the adjacent section. With this filter network terminated in a load impedance of the output section, and with the generator at the input having an internal impedance Z_{i1} , the overall network is matched for maximum power transfer. The filter operates between impedance levels of Z_{iN} and Z_{i1} , which provide an overall impedance ratio change of the amount

$$Z_{iN}/Z_{i1} = \prod_{n=1}^N T_n^2 \quad \dots\dots\dots(3.14)$$

In the image-parameter method of filter design, the two-port parameters A,B,C,D are chosen to provide the required passbands and stopbands. In addition, the image parameters are chosen equal to the terminating impedances at the center of the passband. The shortcomings of the filter are now apparent, because the image impedances are functions of frequency and normally do not remain equal to the terminating impedances over the whole desired passband. This mismatch results in some loss in transmission within the passband. And the amount of this loss can not be prescribed or determined before the filter has been designed. Moreover, there is no means available for controlling the rate at which the attenuation builds up with frequency beyond the edges of the passband apart from increasing the number of filter sections.

3.5 Insertion-loss method:

In general the insertion loss is defined as the ratio of the power delivered to the load when connected directly to the generator to the power delivered when the filter is inserted. The power loss ratio of a network is defined as the available or incident power divided by the actual power delivered to the load. If the incident power is P_i and ρ is the reflection co-efficient, then the reflected power is $\rho^2 P_i$ and the power delivered to the load is $(1-\rho^2)P_i$. Hence the power loss ratio is obtained as

$$P_{LR} = 1/(1-\rho^2) = 1/(1-|\Gamma|^2) \quad \dots\dots\dots(3.15)$$

and $\rho = \sqrt{[(P_{LR}-1)/P_{LR}]}$ \dots\dots\dots(3.16)

where Γ is the input reflection co-efficient for a lossless network terminated in a resistive load. Thus the insertion loss measured in decibels is

$$L = 10 \log P_{LR} \quad \dots\dots\dots(3.17)$$

When the terminating resistive load impedance equals the internal impedance of the generator at the input end.

The insertion-loss method of filter design begins by specifying the power loss ratio P_{LR} or the magnitude of the reflection co-efficient $|\Gamma|=\rho$ as a function of ω . A network that will give the desired power loss ratio is then synthesized. It must be kept in mind that a completely arbitrary $\Gamma(\omega)$ can not be chosen since it may not correspond to a physical network. The restrictions to be imposed on $\Gamma(\omega)$ are known as the conditions for physical realizability. Some of the conditions are discussed below.

For a passive network it is clear that the reflected power can not exceed the incident power. Hence one restriction on $\Gamma(\omega)$ is $|\Gamma(\omega)| \leq 1$. If the normalized input impedance of the network is

$$Z(\omega) = R(\omega) + jX(\omega) \quad \text{--- (3.18)}$$

we have

$$\Gamma(\omega) = (Z_{in} - 1)/(Z_{in} + 1) = \{R(\omega) - 1 + jX(\omega)\} / \{R(\omega) + 1 + jX(\omega)\} \quad \text{--- (3.19)}$$

Again, since R is an even function of ω and X is an odd function of ω , hence we have

$$\Gamma(-\omega) = \Gamma^*(\omega) \quad \text{--- (3.20)}$$

Thus

$$|\Gamma(\omega)|^2 = \rho^2(\omega) = \Gamma\Gamma^* = \Gamma(\omega)\Gamma(-\omega) \quad \text{--- (3.21)}$$

It is apparent from this relation that $\rho^2(\omega) = \rho^2(-\omega)$ is an even function of ω and must therefore contain only even powers of ω . Now any low frequency impedance function such as impedance of a network made up of resistors, capacitors and inductors can be expressed as the ratio of two polynomials in ω . Consequently, Γ can also be expressed as the ratio of two polynomials. It follows that $\rho^2(\omega)$ can then be expressed in the form

$$\rho^2(\omega) = M(\omega^2) / [M(\omega^2) + N(\omega^2)] = [(R-1)^2 + X^2] / [(R+1)^2 + X^2] \quad \text{--- (3.22)}$$

where M and N are real and non negative polynomials in ω^2 .

The power loss ratio can now be expressed as

$$\begin{aligned} P_{LR} &= 1 + M(\omega^2) / N(\omega^2) \\ &= 1 + \{[R(\omega) - 1]^2 + [X(\omega)]^2\} / 4R(\omega) \quad \text{--- (3.23)} \end{aligned}$$

From the above expression it is obvious that $N(\omega^2)$ must be an even polynomial in ω since it equals $4R(\omega)$. Hence we can

write $N(\omega^2) = Q^2(\omega)$, which is clearly an even polynomial in ω . If we denote $N(\omega^2)$ by the even polynomial $P(\omega^2)$, we have

$$P_{LR} = 1 + P(\omega^2)/Q^2(\omega) \dots\dots\dots (3.24)$$

The conditions specified on P_{LR} upto this point are necessary conditions in order that the network may be physically realizable. The condition that the power loss ratio be expressible in the above form is also a sufficient condition for the network to be realizable.

3.6 Summary :

Due to the complex frequency behaviour of microwave circuit elements, it is difficult to develop a complete synthesis procedure to design filters for microwave communication systems. In spite of numerous difficulties some useful techniques have been developed and two such techniques were described in details. Both the methods are essentially low frequency filter synthesis techniques. Image parameter method of filter design provides the pass band and stop band characteristics, but does not specify properly the behaviour over each region. On the other hand, the insertion loss method provides required specifications for a physically realizable filter. The concept of image impedance and image propagation function has also been discussed.

CHAPTER-4

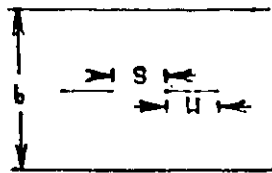
Parallel Coupled TEM Lines and its equivalent circuits

4.1 Introduction:

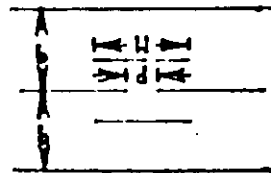
The natural coupling existing between parallel conductors is being utilized by strip-line[9] components such as directional couplers, filters, balun, delay lines. The nature of various types of coupled lines has been described broadly in the subsequent sections of this chapter.

4.2 Different types of parallel coupled lines :

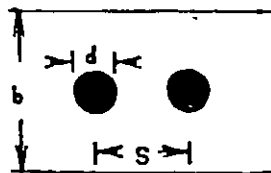
A number of examples of parallel-coupled lines are shown in figure 4.1. The (a), (b) and (c) configurations shown are primarily useful in applications where weak coupling between the lines is desired. The (d), (e), (f) and (g) configurations are useful where strong coupling between the lines is desired. The characteristics of coupled lines can be specified in terms of their even and odd mode impedances[8] i.e. Z_{oe} and Z_{oo} respectively. Z_{oe} is defined as the characteristic impedance of one line to ground when equal currents are flowing in the two lines. While Z_{oo} is defined as the characteristic impedance of one line to ground when equal and opposite currents are flowing in the two lines.



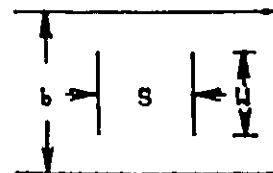
(a)



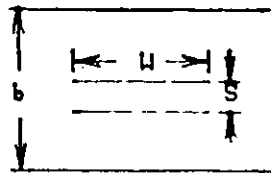
(b)



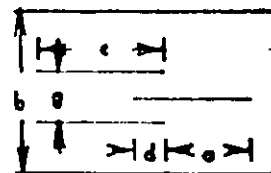
(c)



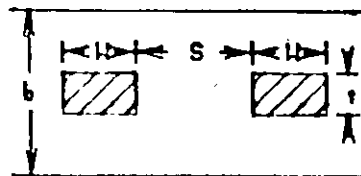
(d)



(e)



(f)



(g)

Figure 4.1 Cross section of various coupled-line configurations

4.3 Coupling with thick rectangular bars:

The thick rectangular bar configuration of coupled lines, illustrated in figure 4.1(g) can be conveniently used where tight coupling between lines is desired. The dimensions of the bars for particular values of Z_{oe} and Z_{oo} can be determined with the aid of the curves shown in figure 4.2(a) & (b). This family of curves is also known as Getsinger's chart[3]. A convenient procedure for using these curves is as follows

First $\Delta C/\epsilon$ is determined using the specified values of Z_{oe} and Z_{oo} or using the equations available for designing filters using coupled rectangular bars. Next a suitable value of t/b is selected and the value of s/b is determined from the corresponding curve shown in figure 4.2(a), The value of W/b is then calculated from the equation

$$W/b = (1-t/b)/2 [C_{oe}/2\epsilon - C_{fe}'/\epsilon - C_f'/\epsilon] \dots\dots(4.1)$$

The value of C_{oe} to use is obtained from specified design equation. The fringing capacitance for the even mode C_{fe}' and fringing capacitance for isolated rectangular bar are read from the curves shown in figure 4.2(a) and 4.2(b) respectively. The fringing and parallel plate capacitances used in the above discussion and the notations W, b, t are illustrated in figure 4.3. The total even mode capacitance of a bar is given by

$$C_{oe}/\epsilon = 2(C_p/\epsilon + C_{fe}'/\epsilon + C_f'/\epsilon) \dots\dots(4.2)$$

and the normalized per-unit-length parallel plate

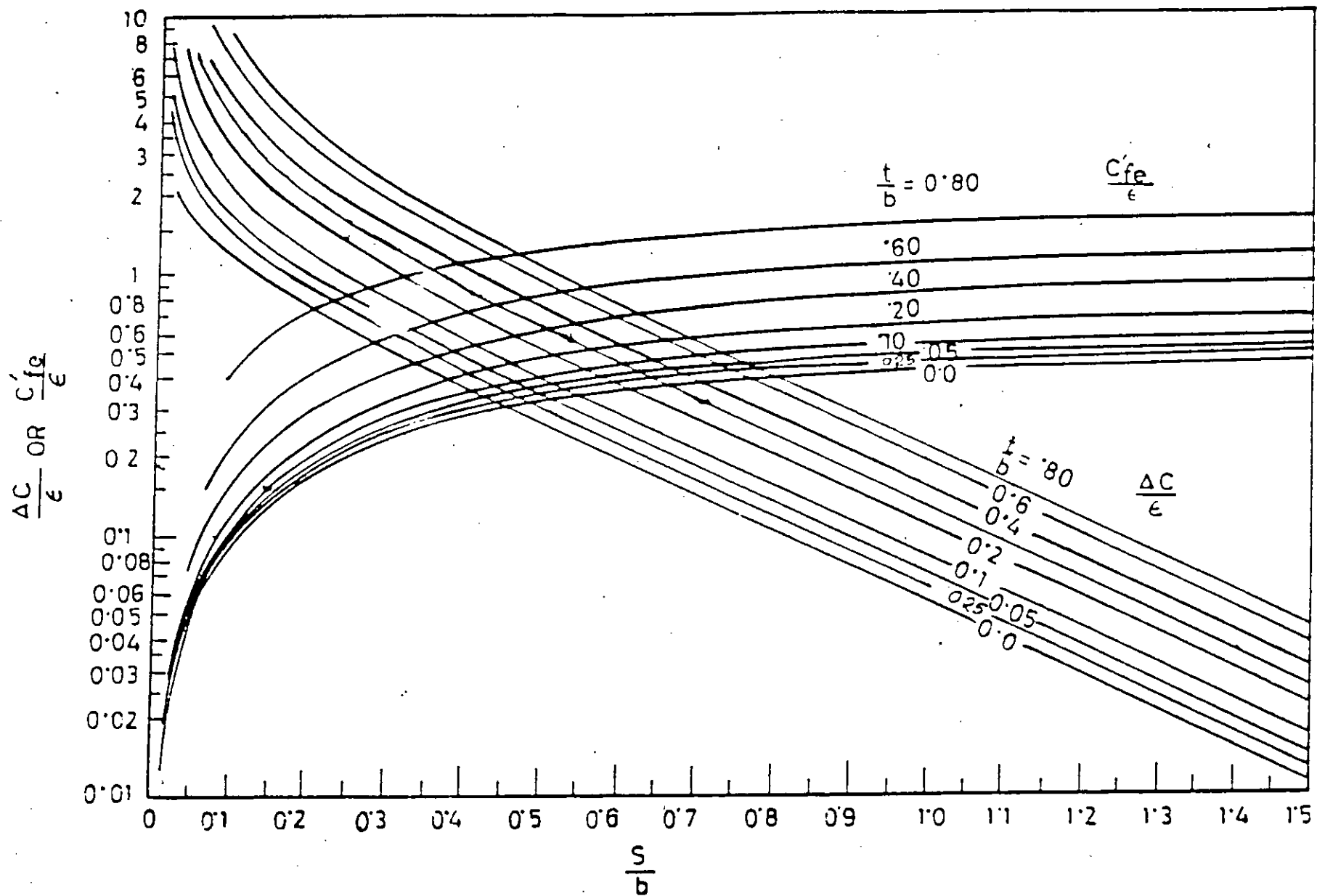


FIG. 4.2(c) NORMALIZED EVEN MODE FRINGING CAPACITANCE C'_{fe}/ϵ AND INTERBAR CAPACITANCE $\Delta C/\epsilon$ FOR COUPLED RECTANGULAR BARS.

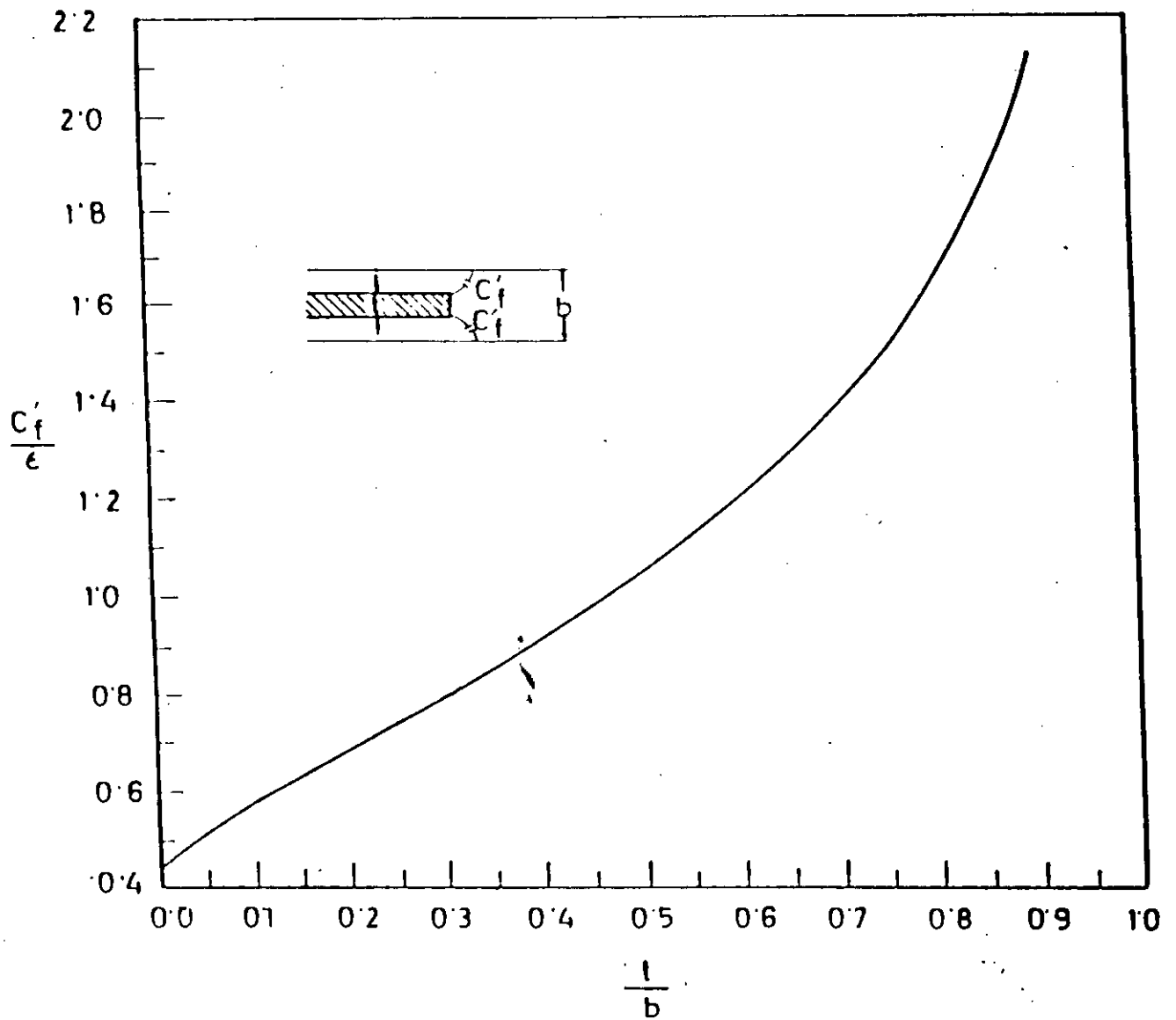


FIG. 4.2(b) NORMALIZED FRINGING CAPACITANCE FOR ISOLATED RECTANGULAR BAR.

capacitance is given by

$$C_p/\epsilon = 2W/(b-t) \quad \text{and} \quad \epsilon = .225\epsilon_r \quad \text{pf/inch}$$

The even mode fringing capacitance is derived by conformal mapping techniques and is exactly in limits of $[W/b/(1-t/b)]$ to infinity. It is believed that when $[W/b/(1-t/b)] > 0.35$, the interaction between the fringing fields is small enough so that the value of C_{oe}/ϵ determined from equation(4.2) is reduced by a maximum of 1.24 percent of its true value. In situations where an initial value of W/b is found from equation (4.1) to be less than $0.35[1-(t/b)]$ so that the fringing fields interact, a new value of W/b can be used where

$$W'/b = [0.07(1-t/b) + W/b]/1.20 \quad \dots\dots(4.3)$$

provided $0.1 < (W'/b)/[1-(t/b)] < 0.35$

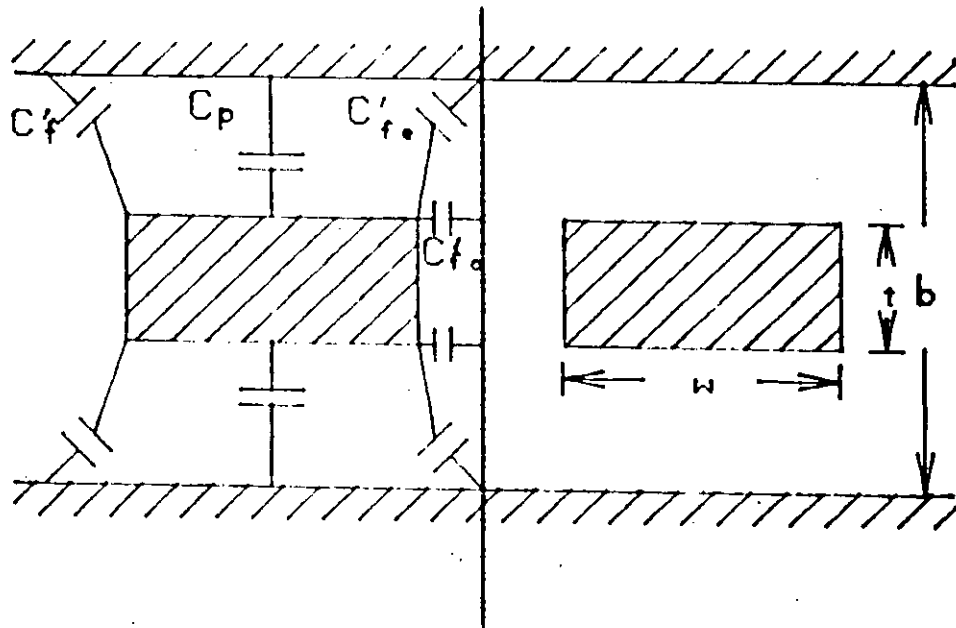


Figure 4.3 Coupled rectangular bars between parallel plates illustrating various fringing and parallel plate capacitances

4.4 Unsymmetrical parallel-coupled lines:

A pair of unsymmetrical parallel-coupled lines and various line capacitances are shown in figure 4.4. Here C_a is the capacitance per unit length between line A and ground, C_{ab} is the capacitance per unit length between line A and line B, while C_b is the capacitance per unit length between line B and ground. When C_a is not equal to C_b , the two lines will have different odd and even-mode admittances. In terms of odd and even mode capacitances, for line A

$$C_{oo}^a = C_a + 2C_{ab} \quad \text{and} \quad C_{oe}^a = C_a \quad \dots\dots(4.4)$$

while for line B

$$C_{oo}^b = C_b + 2C_{ab} \quad \text{and} \quad C_{oe}^b = C_b \quad \dots\dots(4.5)$$

For symmetrical parallel-coupled lines the odd-mode impedances [8] are simply the reciprocals of the odd-mode admittances, and analogously for the even-mode impedances and admittances. However, this is not the case for unsymmetrical parallel coupled lines. The reason behind this lies in the fact that when the odd- and even-mode admittances are computed the basic definition of these admittances assumes that the lines are being driven with voltages of identical magnitude with equal or opposite phase, while the currents in the lines may be of different magnitudes. When the odd- and even-mode impedances are computed, the basic definition of these impedances assumes that the lines are being driven by currents of identical magnitude with equal or opposite phases, while magnitude of the voltages on the two lines may be different. These two

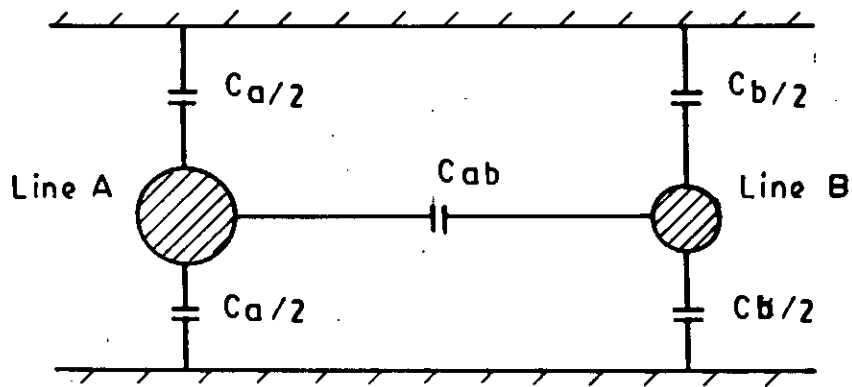


Fig. 4.4 An unsymmetrical pair of parallel coupled lines.

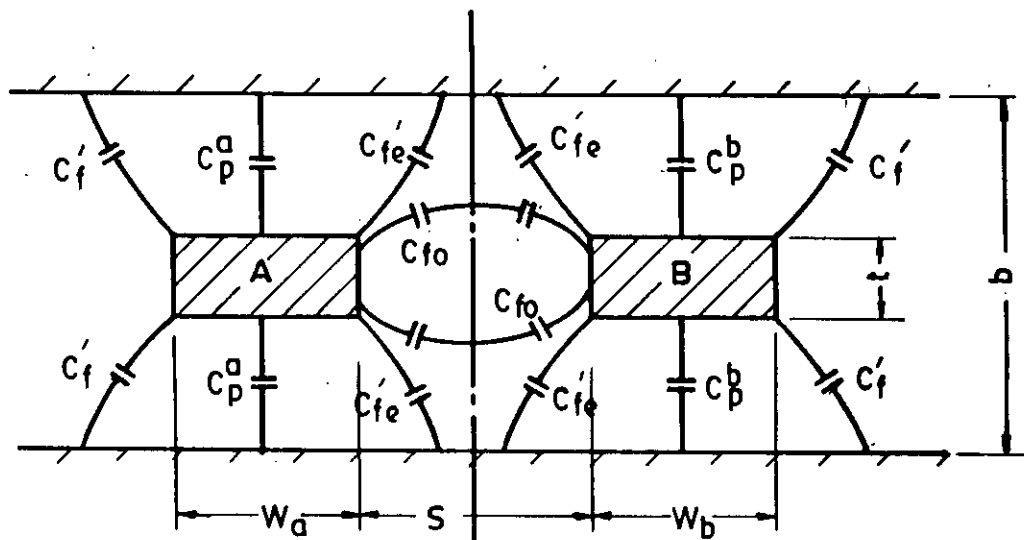


Fig. 4.5 Cross section of unsymmetrical rectangular-bar parallel coupled lines

different sets of boundary conditions can be seen to lead to different voltage current ratios if the lines are unsymmetrical.

Figure 4.5 shows some unsymmetrical parallel-coupled lines which are quite easy to design. Here both bars have the same height, and both are assumed to be wide enough so that the interactions between the fringing fields at the right and left sides of each bar are negligible or at least small enough to be corrected for by the use of equation(4.3). On this basis the fringing fields are the same for both bars, and their different capacitances C_a and C_b to the ground are due entirely to different parallel plate capacitances C_p^a and C_p^b . For the structure shown

$$C_a = 2(C_p^a + C_f' + C_{fe}') \quad \dots\dots(4.6)$$

$$C_{ab} = C_{fo}' - C_{fe}' \quad \dots\dots(4.7)$$

$$C_b = 2(C_p^b + C_f' + C_{fe}') \quad \dots\dots(4.8)$$

Table 4.1 below shows the relations between line admittances and capacitances per unit length of unsymmetrical parallel-coupled lines.

Table 4.1

$$\begin{aligned} Y_{oe}^a &= vC_a, & Y_{oo}^a &= v(C_a + 2C_{ab}) \\ Y_{oe}^b &= vC_b, & Y_{oo}^b &= v(C_b + 2C_{ab}) \\ C_a/\epsilon &= \eta_0 Y_{oe}^a / \sqrt{\epsilon_r}, & C_{ab}/\epsilon &= (\eta_0 / \sqrt{\epsilon_r})(Y_{oo}^a - Y_{oe}^a) / 2 \\ C_b/\epsilon &= \eta_0 Y_{oe}^b / \sqrt{\epsilon_r}, & C_{ab}/\epsilon &= (\eta_0 / \sqrt{\epsilon_r})(Y_{oo}^b - Y_{oe}^b) / 2 \end{aligned}$$

Where, v = Velocity of light in the medium of propagation.

$$c = 1.18 \times 10^{10} / \sqrt{\epsilon_r} \text{ inch/sec.}$$

$$\eta_0 = \text{Intrinsic impedance of free space.}$$
$$= 376.7 \text{ ohms.}$$

$$\epsilon = \text{Dielectric constant.}$$
$$= 0.225 \epsilon_r \text{ pf/inch.}$$

4.5 Arrays of parallel-coupled lines:

The cross section of an array of parallel-coupled lines generally used in Comb-line as well as Interdigital-line filters is shown in figure 4.6. In the structure shown, all of the bars have the same t/b ratio and the other dimensions of the bars are easily obtained by generalizing the procedure described in previous sections.

Here the electrical properties of the structure are characterised in terms of the self capacitances C_k per unit length of each bar with respect to ground and the mutual capacitances $C_{k,k+1}$ per unit length between adjacent bars k and $k+1$. This representation is not necessarily always highly accurate. It is conceivable that a significant amount of fringing capacitance could exist between a given line element, and, say, the line element beyond the nearest neighbour. However, at least for geometries such as that shown, have satisfactory accuracy for applications such as comb-line and Interdigital filter design.

For design of the parallel coupled array structures, equations are available for the normalized self and mutual capacitances per unit length for all the lines in the

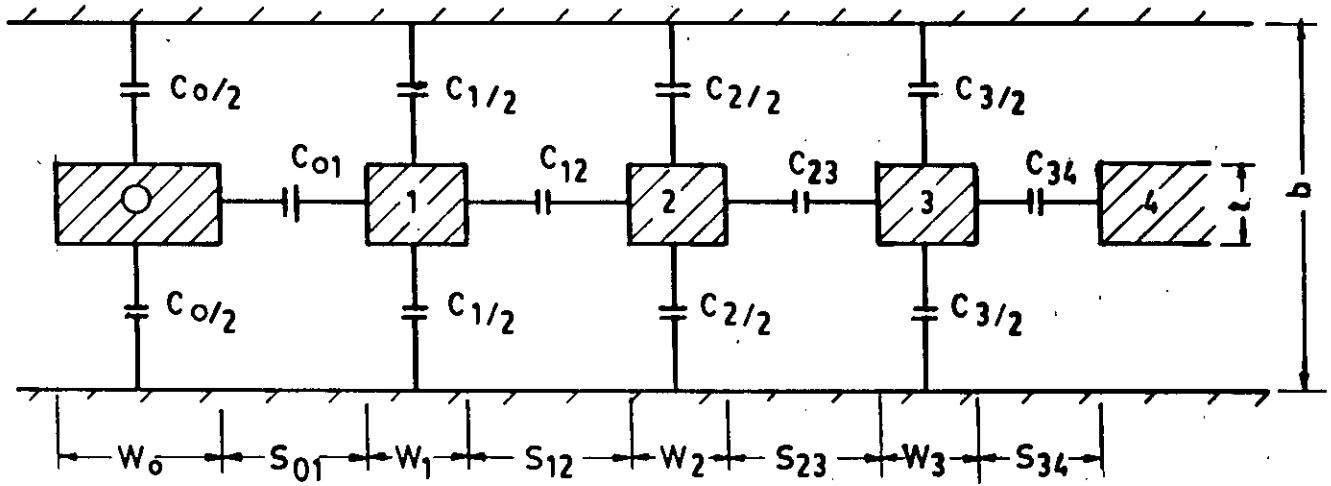


Fig. 4.6 Cross section of an array of parallel coupled lines between ground planes.

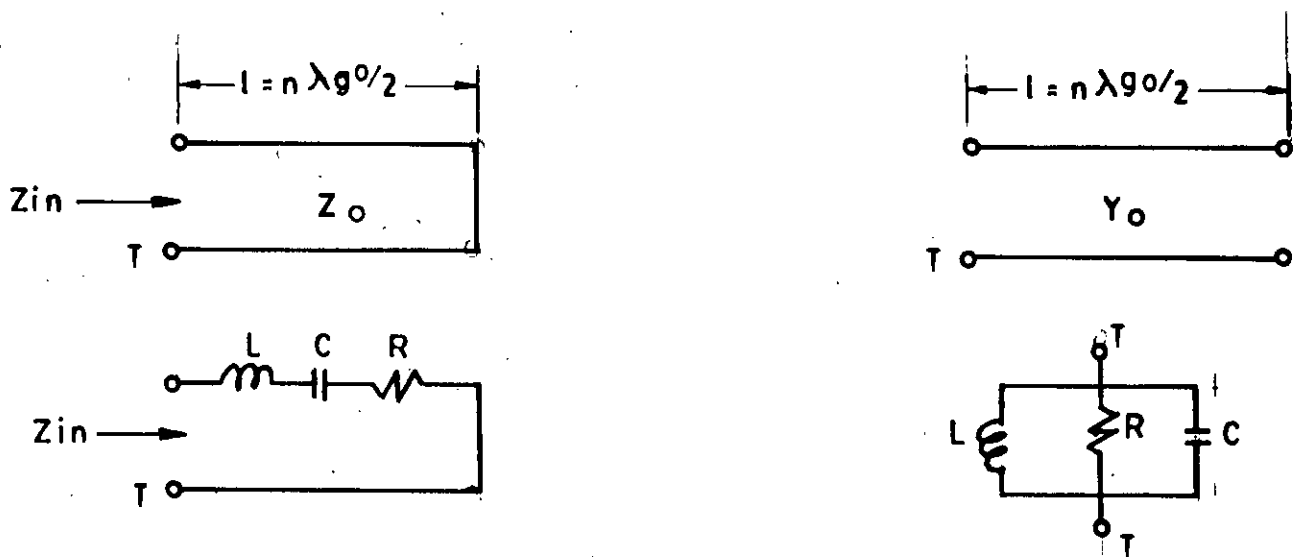


Fig. 4.7 Some transmission line resonators

structure. Then the cross sectional dimensions of the bars and the spacings between them are determined first by taking suitable values for t and b . Then, since

$$(\Delta C)_{k,k+1}/\epsilon = C_{k,k+1}/\epsilon \quad \dots\dots(4.9)$$

Getsinger's charts[3] can be used to determine $S_{k,k+1}/b$. In this manner, the spacings between all the bars are obtained. Also, using Getsinger's Charts, the normalized fringing capacitance $(C_{fe}')_{k,k+1}/\epsilon$ associated with the gaps, between bars is obtained. The normalized width of the k th bar is then calculated from the following equation.

$$W_k/b = [(1-t/b)/2] \{ C_k/2\epsilon - (C_{fe}')_{k-1,k}/\epsilon - (C_{fe}')_{k,k+1}/\epsilon \} \quad \dots\dots\dots(4.10)$$

In the case of the bar at the end of the array (the bar at the far left in figure 4.6), C_{fe}'/ϵ for the edge of the bar which has no neighbour must be replaced by C_f'/ϵ which is determined from figure 4.2(b) i.e. Getsinger's Chart for an isolated bar. Again, if $W_k/b < 0.35 (1-t/b)$ for any of the bars, the width of the bar should be corrected using the approximate formula given in equation (4.3). The need for this correction arises because of the interaction of the fringing fields at opposite sides of a bar, which will occur when a bar is relatively narrow.

4.6 Transmission lines as resonators and its lumped-constant equivalent circuits:

In many microwave filter designs, a length of transmission line [10] terminated in either an open-circuit or

a short-circuit is often used as a resonator. Some resonators of this type are illustrated in figure 4.7 together with their lumped-constant equivalent circuit. It is to be noted that the lumped constant equivalent circuit of the transmission line which is short circuited at one end is the dual of the equivalent circuit of the transmission line with an open circuited termination.

The equivalence between the lumped constant circuits and microwave circuits shown in figure 4.7 is established in the following fashion. The values of the resistance, R, and conductance, G, in the lumped-constant equivalent circuits are determined as the values of these quantities for the various lines at the resonance angular frequency ω_0 . The reactive elements in the lumped constant equivalent circuits are determined by equating the slope parameters of the lumped element circuits to those of the transmission line circuits which exhibit the same type of resonance. Slope parameters are defined in two ways according to the types of resonance leading to reactance slope parameter and susceptance slope parameters. The general definition of the reactance slope parameter x , which applies to circuits that exhibit a series type of resonance, is

$$x = \frac{\omega_0}{2} \left. \frac{dX}{d\omega} \right|_{\omega=\omega_0} \quad \text{ohms} \quad \dots\dots\dots(4.11)$$

And the susceptance slope parameter b , which applies to circuits that exhibit a parallel type of resonance, is

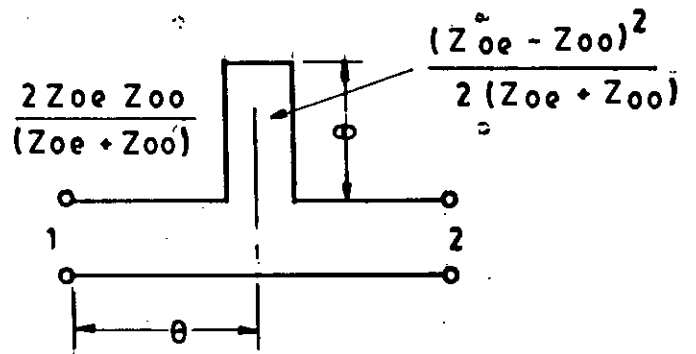
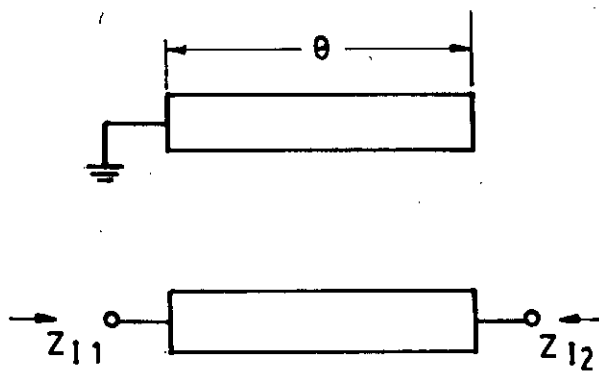
$$b = \frac{\omega_0}{2} \left. \frac{dB}{d\omega} \right|_{\omega=\omega_0} \quad \text{mhos} \quad \dots\dots\dots(4.12)$$

where X and B are the reactance and susceptance components.

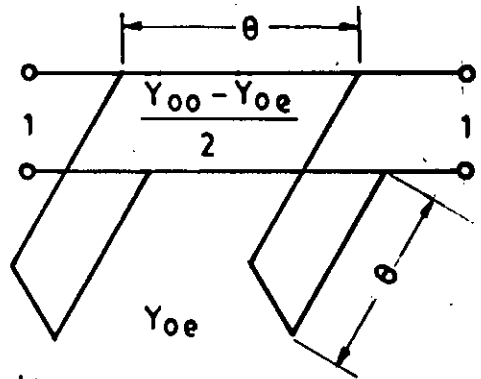
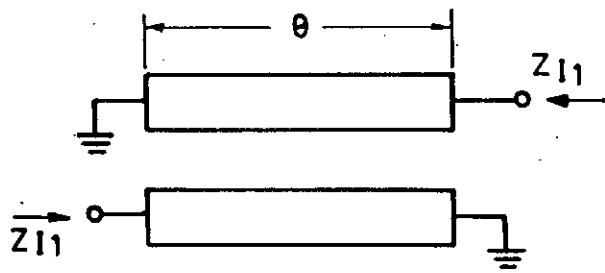
The above general definitions for slope parameters provide a convenient means for relating the resonance properties of any circuit to a simple lumped equivalent circuit such as those shown in figure 4.7. The reactance slope parameter x given by equation (4.11) is seen to be equal to $\omega_0 L = 1/\omega_0 C$ for the equivalent series, lumped-element circuit, while the susceptance slope parameter b is equal to $\omega_0 C = 1/\omega_0 L$ for the equivalent, parallel, lumped-element circuit. These parameters are considerably used in dealing with bandpass and band-stop microwave filters.

4.7 Parallel coupled line filter sections and its equivalent circuits:

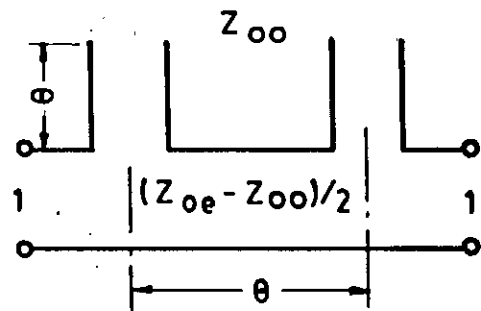
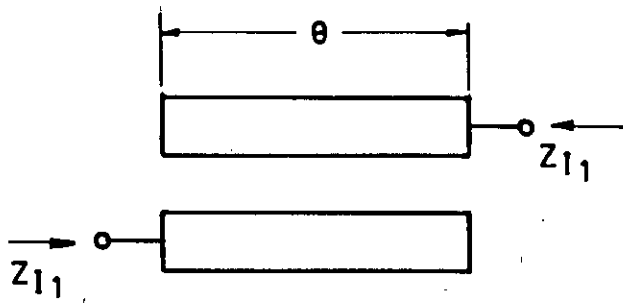
The natural electromagnetic coupling that exists between parallel lines can be used to advantage in the design for filter sections constructed of parallel coupled lines of the types illustrated in figure 4.1. The coupling arrangements that can be obtained from a pair of symmetrical coupled lines by placing open or short-circuits on various terminal pairs are shown in figure 4.8. In this figure, schematic diagrams of single section of different types are shown together with their open-circuit impedances or short-circuit admittances. In addition, equivalent open-wire transmission-line circuits of the coupled transmission line sections are shown beside the corresponding schematic diagram using a two-wire line representation. In each case, the



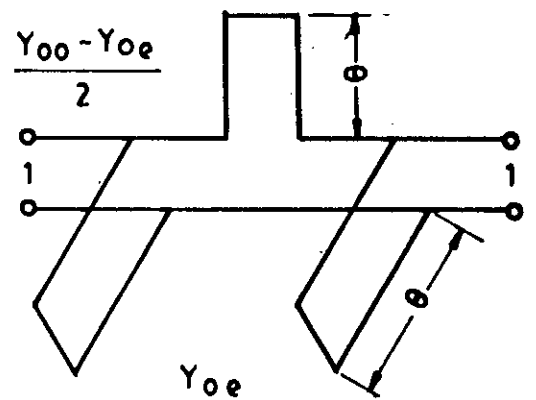
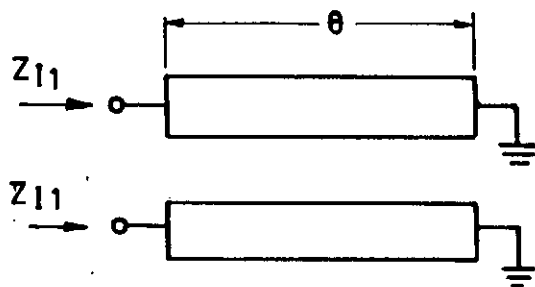
Schematic and equivalent circuit
a) Lowpass



Schematic and equivalent circuit
b) Band pass



Schematic and equivalent circuit
c) Band pass



Schematic and equivalent circuit
d) All stop

Fig. 4.8 Some parallel-coupled line filter sections.

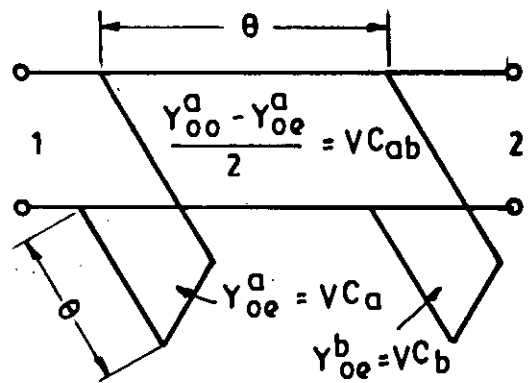
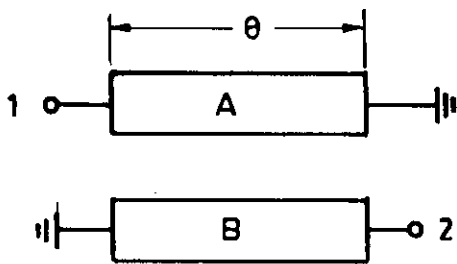
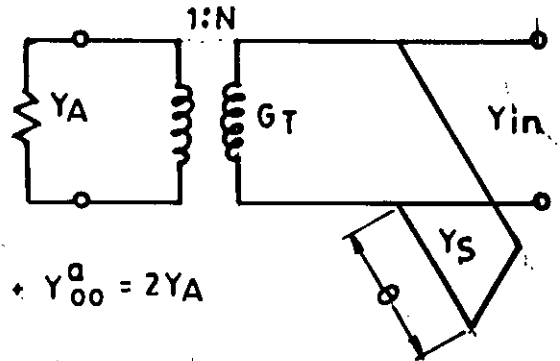
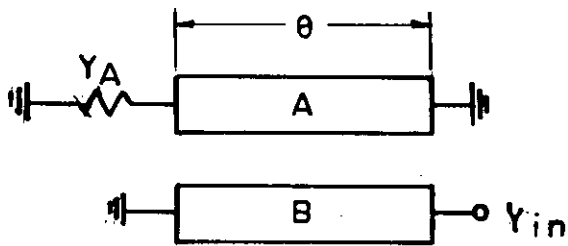


Fig. 4.9 Unsymmetrical parallel coupled line section and its equivalent open wire line section.



Special constraint : $Y_{oe}^a + Y_{oo}^a = 2Y_A$

Here

$$Y_{oo}^a = Y_A \left[\sqrt{G_T/Y_A} + 1 \right]$$

$$Y_{oe}^b = Y_S - Y_A \left[1 - G_T/Y_A \right] + Y_{oe}^a$$

$$Y_S = Y_A \left[\frac{N^2 - 1}{N^2} \right] + Y_{oe}^b - Y_{oe}^a$$

$$N = \text{Turns ratio} = \frac{2Y_A}{Y_{oo}^a - Y_{oe}^a}$$

$$G_T = Y_A/N^2$$

Fig. 4.10 Parallel coupled strip line and equivalent open wire line under the given special constraint

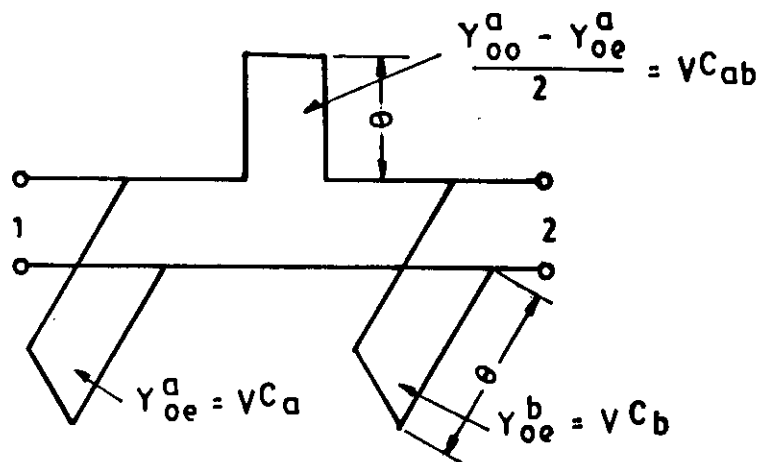
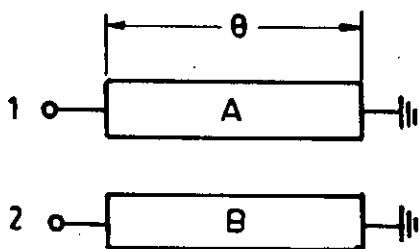


Fig. 4.11 A parallel couple section and its exact equivalent open wire line circuit.

characteristic impedance or admittance of the lengths of transmission line is shown together with the electrical length, θ .

Figure 4.9 shows the same parallel coupled sections as appeared in figure 4.8(b),(c) and (d), but for cases where the strip transmission lines have unsymmetrical cross sections. The line capacitances C_a , C_{ab} and C_b per unit length are as defined earlier. The line capacitances per unit length for the left and right shunt stub in the equivalent open-wire representation are the same as the corresponding capacitances per unit length between line A and ground and line B and ground respectively. And the capacitance per unit length for the connecting line in the open-wire circuit is the same as the capacitance per unit length between lines A and B of the parallel coupled representation. The quantity v associated here is the velocity of light in the medium of propagation.

In the case of circuit in figure 4.9, if the parallel-coupled section is properly terminated, its equivalent open-wire line circuit simplifies in a very useful way. This is illustrated in figure 4.10. When the indicated constraints are applied, the equivalent open-wire circuit reduces to simply an ideal transformer and a single stub. In spite of the constraint equation which is enforced in this circuit, there are still sufficient degrees of freedom so that for specified Y_S and G_T a wide range of Y_A can be accommodated. For this reason, this structure proves quite useful for use

with certain types of bandpass filters for the purpose of effectively realizing a series stub resonator along with obtaining an impedance transformation which will accommodate some desired terminating impedance.

Figure 4.11 shows the parallel coupled section in figure 4.8(d) generalized to cover the case where the two strip lines may be of different widths. The open-wire line structure is equivalent electrically to the strip-line structure. As indicated earlier, parallel coupled structures of this sort are all-stop structures as they stand, but when properly used with lumped capacitances, they become the basis for the Comb-line form of filter.

4.8 Summary :

The characteristics of various types of parallel coupled TEM lines have been illustrated. Defining even mode and odd mode impedance as well as admittance, the relationship of these quantities with the velocity of light in the medium of propagation has been tabulated. A complete procedure to calculate the widths and gaps between adjacent bars using some specific expressions and curves has been described.

CHAPTER-5

Conversion of Prototype filter circuit using (Impedance/Admittance) Inverters

5.1 Introduction:

In deriving design equations for certain type of bandpass filter, it is desirable to convert the prototype low pass filter consisting of both inductances and capacitances into an equivalent form which uses only inductances or capacitances. This is achieved with the aid of the idealized inverters namely Impedance inverter and Admittance inverter or K-inverter and J-inverter[8] as they are otherwise called. Details of these inverters, equivalent form of prototype filter circuit using inverters and some inverter circuits are presented in this chapter.

5.2 Definition of impedance and admittance inverters :

An ideal impedance inverter operates like a quarter-wavelength line of characteristic impedance K at all frequencies. A load impedance connected at one end is seen as an impedance that has been inverted with respect to the characteristic impedance squared at the input. Therefore, if an impedance inverter is terminated in an impedance Z_b on one end, the impedance Z_a seen looking in at the other end is

$$Z_a = K^2 / Z_b \quad \dots\dots\dots(5.1)$$

Alternatively, an idealized admittance inverter is the

admittance representation of the same thing, i.e., it operates like a quarter-wavelength line of characteristic admittance J at all frequencies. Thus, if an admittance Y_b is attached at one end, the admittance Y_a seen looking in the other end is

$$Y_a = J^2 / Y_b \quad \dots\dots\dots(5.2)$$

Using these inverters a prototype filter network can be converted into a convenient form for analysis as has been described in subsequent sections.

5.3 Equivalent forms of Prototype filter using inverters:

Because of the inverting action of the inverter, a series inductance with an inverter on each side looks like a shunt capacitance from its exterior terminals. Likewise, a shunt capacitance with an inverter on both sides looks like a series inductance from its external terminals. This has been illustrated in figure 5.1.

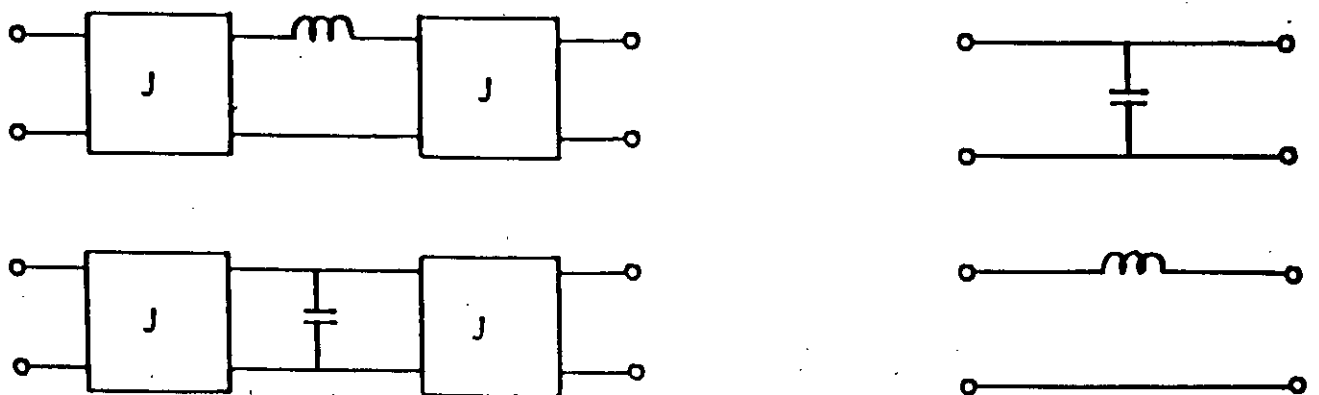
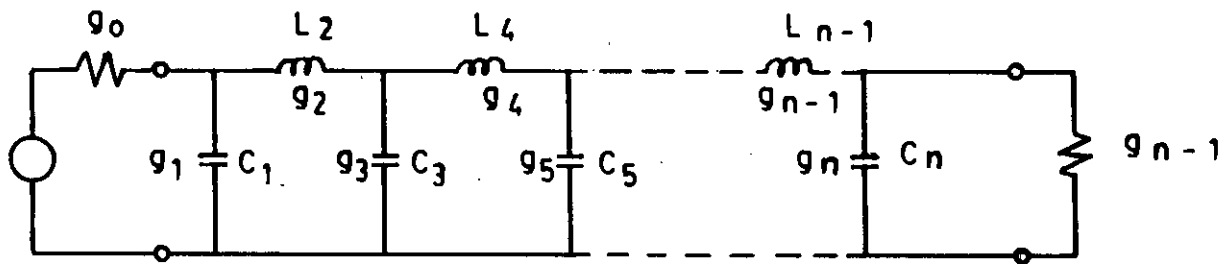
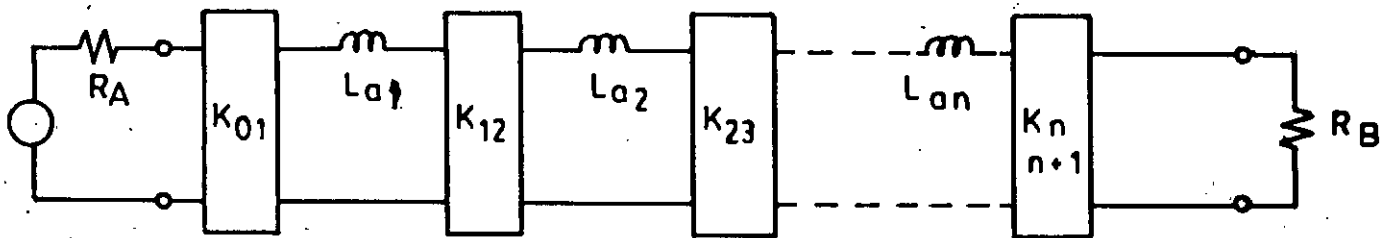


Fig. 5.1 Equivalence of series inductor and shunt capacitors with J-inverters



a) Lowpass prototype filter circuit

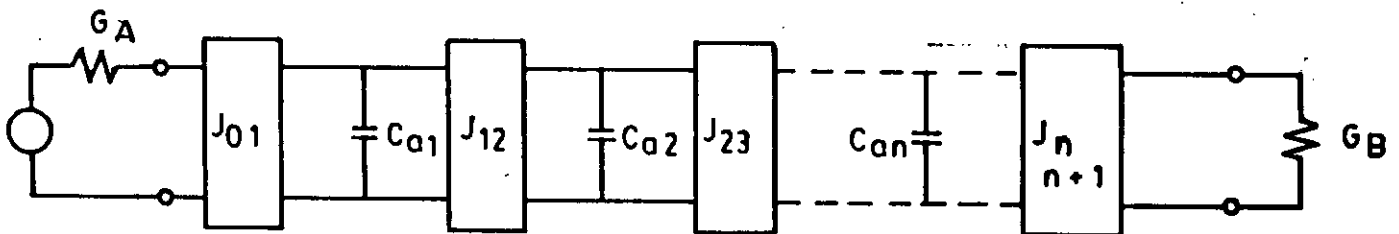


Where,

$$K_{01} = \sqrt{\frac{R_A L_{a1}}{g_0 g_1}}, \quad K_{k, k+1} = \sqrt{\frac{L_{ak} L_{a(k+1)}}{g_k g_{k+1}}}, \quad K_{n, n+1} = \sqrt{\frac{L_{an} R_B}{g_n g_{n+1}}}$$

K = 1 to n-1

b) Modified form using impedance inverter



Where,

$$J_{01} = \sqrt{\frac{G_A C_{a1}}{g_0 g_1}}, \quad J_{k, k+1} = \sqrt{\frac{C_{ak} C_{a(k+1)}}{g_k g_{k+1}}}, \quad J_{n, n+1} = \sqrt{\frac{C_{an} G_B}{g_n g_{n+1}}}$$

K = 1 to n-1

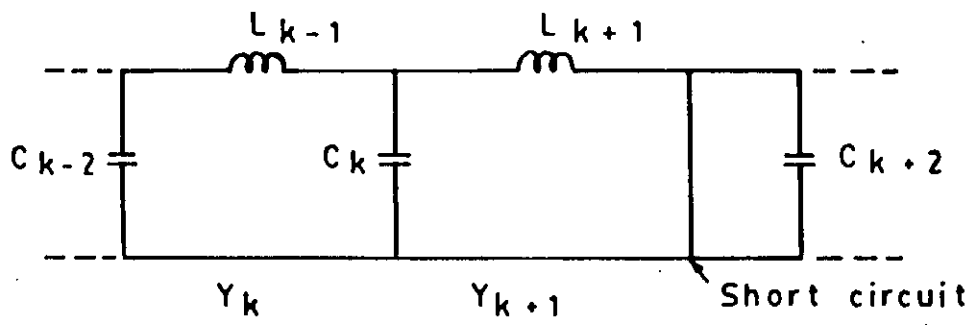
c) Modified form using admittance inverter.

Fig. 5.2 Lowpass prototype circuit and its equivalent forms using inverters

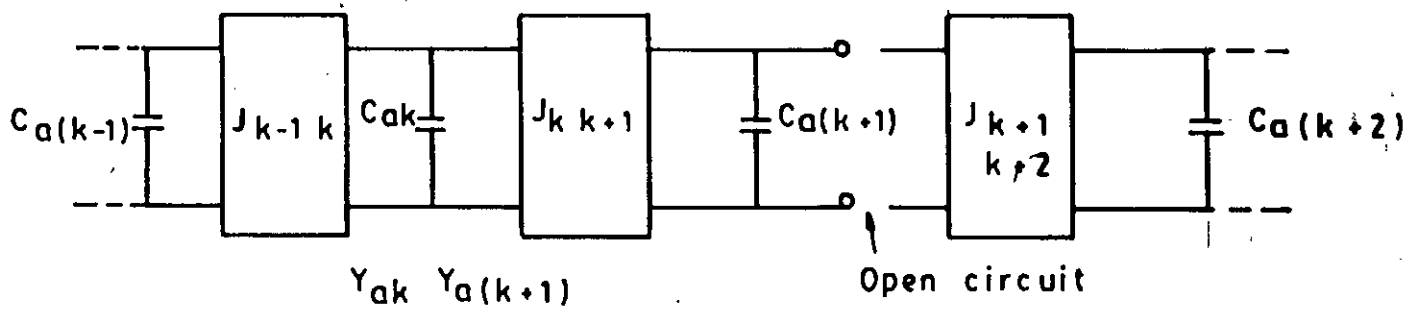
Making use of this property, the prototype circuit shown in figure 5.2(a) can be modified to either of the equivalent forms shown in figure 5.2(b) and (c) which has identical transmission characteristics to the prototype. It is obvious from equation (5.1) and (5.2) that the inverters have the ability to shift impedance or admittance levels depending on the choice of the K or J parameters. For this reason the terminal resistances and the series or shunt reactive components may be chosen arbitrarily with identical response to that of the original prototype provided that the inverter parameters $K_{k,k+1}$ or $J_{k,k+1}$ are specified as indicated by the equations in figure 5.2(b) and (c) respectively. It is to be noted that the g_k values referred to in the equation are the prototype element values.

5.4 Derivation of the expressions for Inverter parameters:

The equations for the inverter parameters as shown with figure 5.2 can be derived by extracting relation between the prototype circuit and the corresponding circuits using inverters. The concept of duality can of course be a way to work it out. A given circuit as seen through an inverter looks like the dual of that circuit. Thus, the admittance seen from the capacitor C_{a1} in figure 5.2(c) is the same as that seen from the capacitance C_1 in figure 5.2(a) except for an admittance scale factor. Similarly the admittances seen from capacitor C_{a2} is identical to that seen from C_3 . In this manner, the admittances in any point of the modified circuit

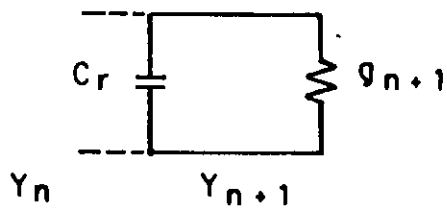


(a)

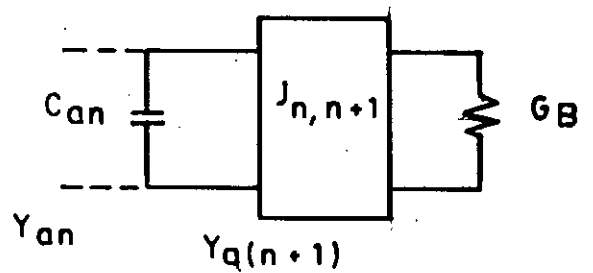


(b)

Fig. 5.3 a) A section of the prototype filter circuit
b) Analogous form with J-inverter



(a)



(b)

Fig. 5.4 (a) End part of the prototype circuit
b) Corresponding part with J-inverter

with admittance inverter may be quantitatively related to the corresponding admittance in the prototype circuit. Since J-inverters are used in the equivalent circuit of comb-line filter only the equation for the J-inverter parameters are derived here. However, the equation for the K-inverter parameters can also be derived in a similar manner considering impedances instead of admittances.

Figure 5.3(a) shows a portion of the low-pass prototype circuit that has been short circuited just after the inductor L_{k+1} while figure 5.3(b) shows the corresponding circuit using J-inverters. The short and hence open circuits are introduced to simplify the derivation of the formula for the inverter parameters, $J_{k,k+1}$

From figure 5.3(a) & (b) we have

$$Y_k = j\omega C_k + 1/j\omega L_{k+1} \dots\dots\dots(5.3)$$

and

$$Y_{ak} = j\omega C_{ak} + J_{k,k+1}^2/j\omega C_{a(k+1)} \dots\dots\dots(5.4)$$

Now Y_{ak} must be identical to Y_k except for an admittance scale change of C_{ak}/C_k . Therefore

$$Y_{ak} = (C_{ak}/C_k)Y_k$$

and hence we get,

$$J_{k,k+1} = \sqrt{(C_{ak}C_{a(k+1)})/C_k L_{k+1}}$$

replacing C_k and L_{k+1} by g_k and g_{k+1} respectively, we obtain,

$$J_{k,k+1} = \sqrt{(C_{ak}C_{a(k+1)})/g_k g_{k+1}} \dots\dots\dots(5.5)$$

Here it is obvious that by moving the positions of the short and open circuit points correspondingly, the same procedure would apply for calculation of the J-parameters for all the

inverters except those at the ends. Hence, equation (5.5) applies for $K = 1, 2, \dots, n-1$.

Considering figure 5.4, we have

$$Y_n = j\omega C_n + 1/g_{n+1} \dots\dots\dots(5.6)$$

and

$$Y_{an} = j\omega C_{an} + J_{n,n+1}^2/G_B \dots\dots\dots(5.7)$$

Again they are identical except a difference in magnitude by the factor C_{an}/C_n . It implies that

$$Y_{an} = (C_{an}/C_n)Y_n$$

and hence we get

$$J_{n,n+1} = \sqrt{(C_{an}G_B/g_n g_{n+1})} \dots\dots\dots(5.8)$$

Also the parameter J_{01} may be evaluated in a similar fashion considering the input end portion of the prototype circuit as well as the corresponding circuit with J-inverter. The equation for the parameter can be obtained as

$$J_{01} = \sqrt{(C_{a1}G_A/g_0 g_1)} \dots\dots\dots(5.9)$$

5.5 Some Inverter Circuits:

A simple form of inverter is a quarter wavelength of transmission line. Such a line obeys the basic impedance inverter definition and that it will have an inverter parameter of $K = Z_0$ ohms, where Z_0 is the characteristic impedance of the line. Of course, a quarter-wavelength of line also serves as an admittance inverter and the inverter parameter will be $J = Y_0$ mhos, where Y_0 is the characteristic admittance of the line.

However, there are numerous other circuits which

operate as inverters. All necessarily give an image phase of odd multiple of ± 90 degrees, and many have good inverting properties over a wider bandwidth than does a quarter-wavelength line. Figure 5.5 shows some inverting circuits specially used as K-inverters i.e. inverters to be used with series type resonators. Those shown in figure 5.5(a) and (b) are particularly useful in circuits where the negative L or C can be absorbed into adjacent positive series elements of the same type so as to give a resulting circuit having all positive elements. While the inverters shown in figure 5.5(c)

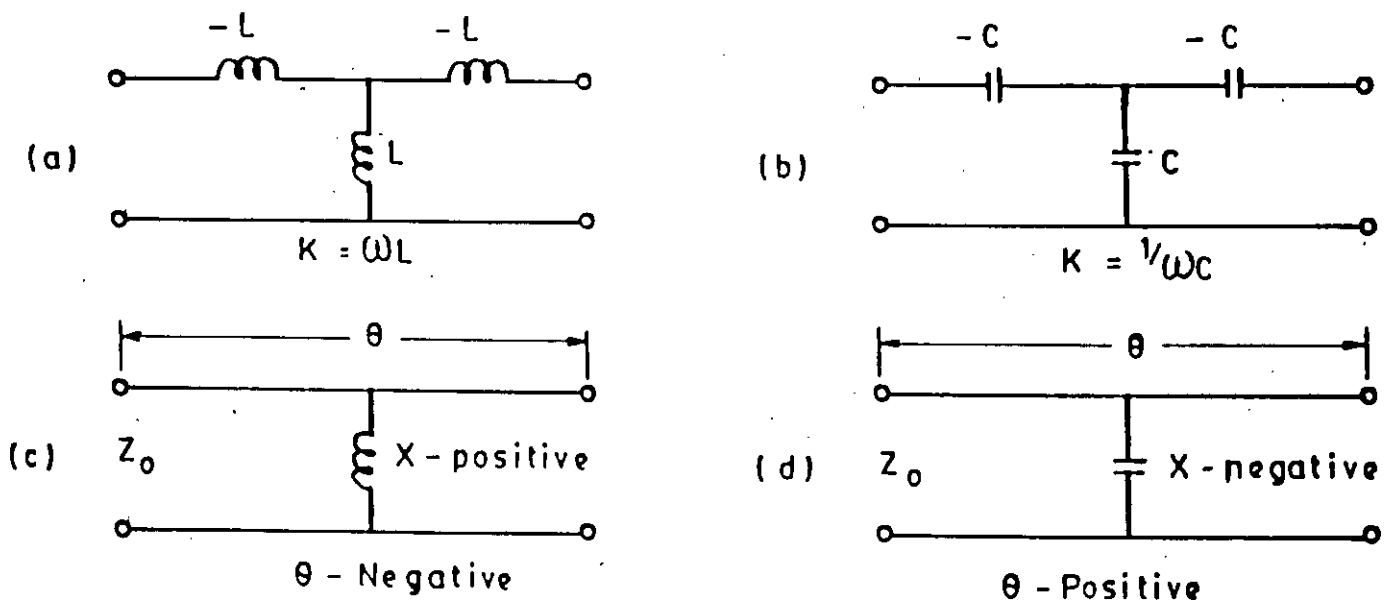


Fig. 5.5 Some K-inverter circuits

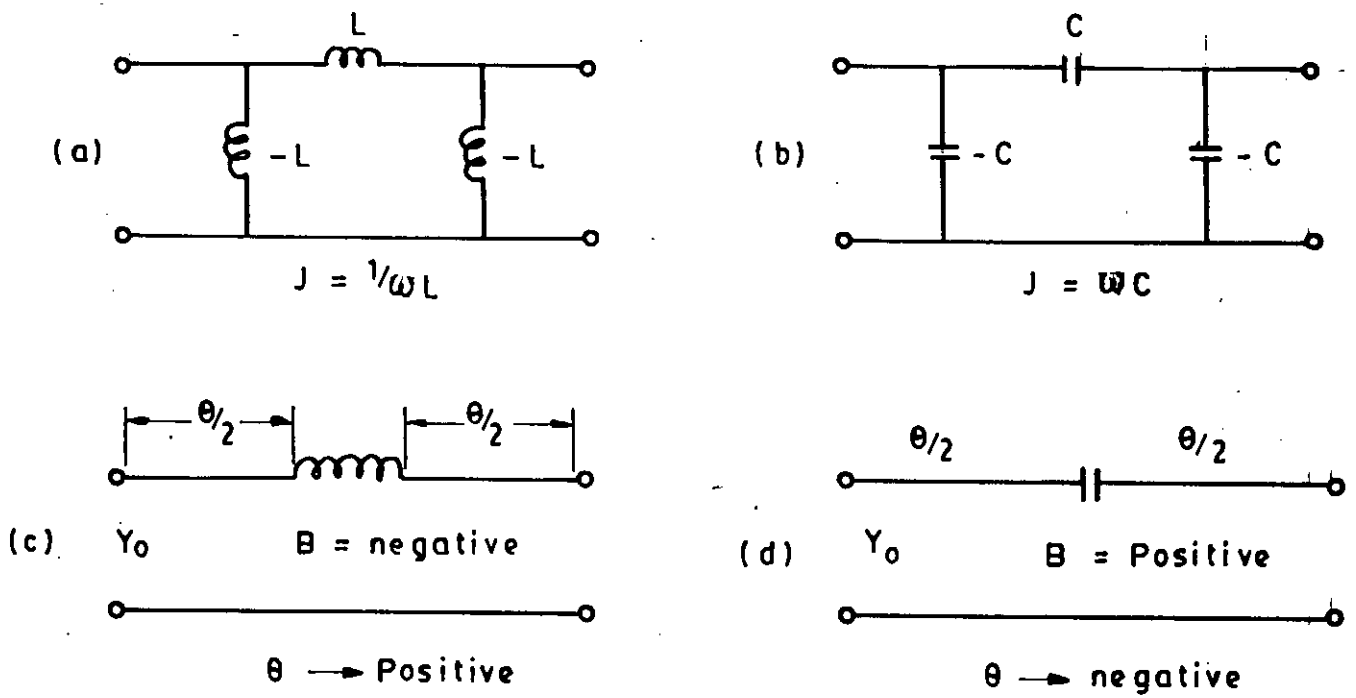


Fig. 5.6 Some J-inverter circuits

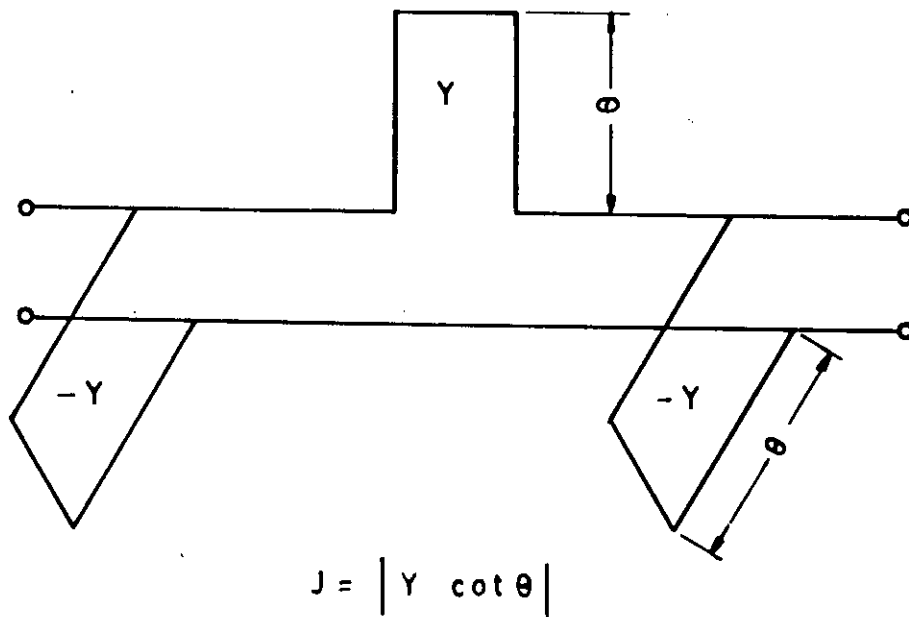


Fig. 5.7 An admittance inverter formed by stubs of electrical length, θ .

and (d) are particularly useful in circuits where the line of positive or negative electrical length, θ can be added or subtracted from adjacent line of the same impedance. The circuits shown at (a) and (c) have an overall image phase shift of -90 degrees while those at (b) and (d) have $+90$ degrees. The impedance inverter parameter K indicated in the figure is equal to the image impedance of the inverter network and i.e. analogous to the characteristic impedance of transmission line.

Some inverting circuits which are of special interest for the use as J-inverters are shown in figure 5.6. Here, the inverter parameters J are the image admittances of the inverter networks. These circuits can also be considered to be the duals of those shown in figure 5.5 as K-inverter circuits.

Figure 5.7 shows yet another form of inverter composed of transmission lines of positive and negative characteristics admittance. The negative admittances are in practice absorbed into adjacent lines of positive admittance.

Many other circuits operate as admittance or impedance inverters. The requirements are that their image impedance be real in the frequency band of operation, and their image phase be some odd multiple of ± 90 degrees.

5.6 Summary :

A method to convert the prototype filter circuit consisting of both series and shunt elements into an

equivalent circuit consisting of either series or shunt elements using the concept of impedance and admittance inverters has been described in details. The derivation of the expressions for J-inverter (admittance inverter) parameters in terms of circuit elements have been developed. Some circuits usually used as impedance inverter and admittance inverter are also presented.

CHAPTER-6

Comb-line geometry and its equivalent circuit

6.1 Introduction:

Comb-line geometry is a popular structure in microwave bandpass filter design and fabrication. The structure contains arrays of parallel lines between ground planes. The resonators in this type of filter consist of TEM-mode transmission line elements that are short-circuited at one end and have a lumped capacitance between the other end of each resonator line element and ground. Comb-line band pass filter and its equivalent circuitry using identical open-wire line and inverters are described in details in the following sections.

6.2 Comb-line bandpass filter :

Theoretically the attenuation through the filter will be infinite at the frequency for which the resonator lines of the comb-line filter are quarter wavelength long. Because of this property, the attenuation above the primary passband will be very high and depending on the electrical length of the resonator line at the passband center, the rate of cut off on the upper side of the passband can be made to be very steep. Comb-line geometry is popular also for its compactness. Moreover, with this structure, adequate coupling can be maintained between resonator elements with sizeable

spacing between resonator lines. Filters of this type can usually be fabricated without using dielectric support materials so that dielectric losses can be eliminated considerably.

A comb-line bandpass filter in strip line configuration is presented in figure 6.1. Here, line 1 to n along with their associated capacitances, C_1^s to C_n^s comprise resonators, while lines 0 and $n+1$ are not resonators but simply part of impedance-transforming sections at the ends of the filter. Coupling between resonators is achieved in this type of filter by way of the fringing fields between resonator lines. Due to the presence of the lumped capacitors, the resonator lines will be less than quarter wave length long at resonance. Also the coupling between the resonators is predominantly magnetic in nature under the aforesaid situation. In absence of the lumped capacitors, the length of the resonator lines would be equal to quarter wavelength long at resonance. As a consequence, the structure would have no passband. Because, without some kind of reactive loading at the ends of the resonator line elements, the magnetic and electric coupling effects would nullify each other. As a result, the comb-line structure would become an all-stop filter.

To avoid the difficult situation described above, it is the usual practice to make the lumped capacitances in this type of filter sufficiently large. As a result, the resonator lines will be nearly $1/8$ wavelength or less long at

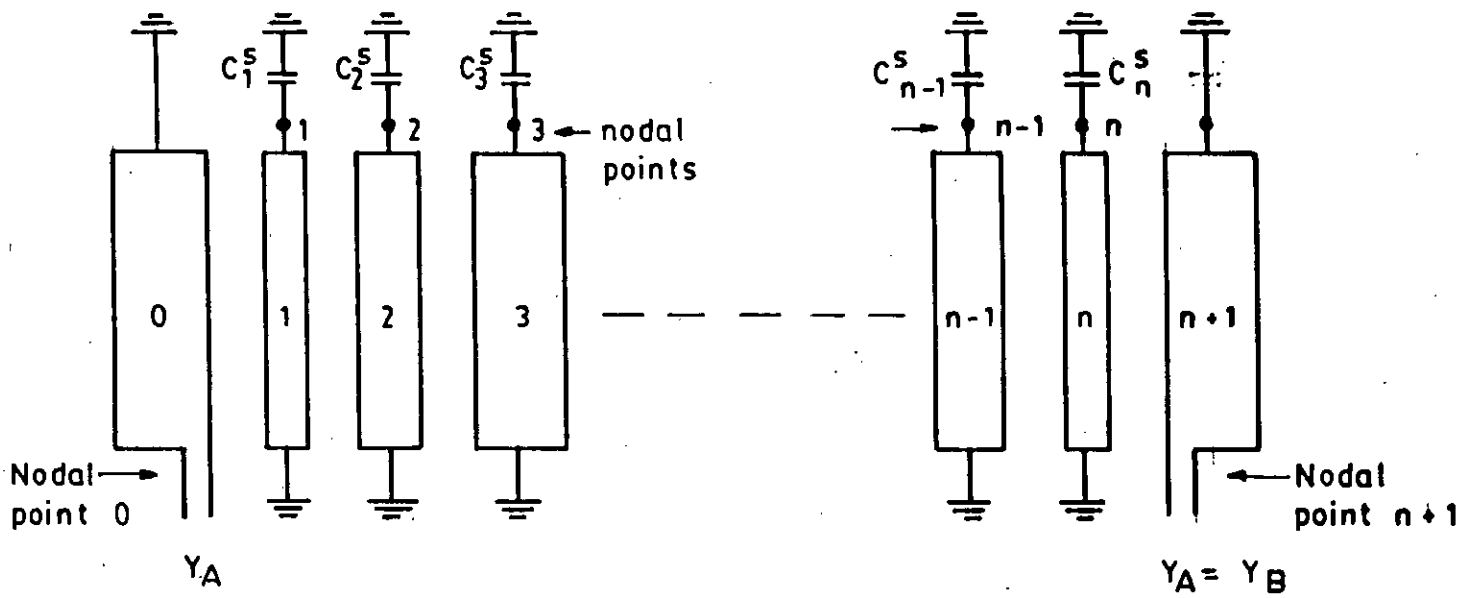


Fig. 6.1 Schematic diagram of comb-line band pass filter

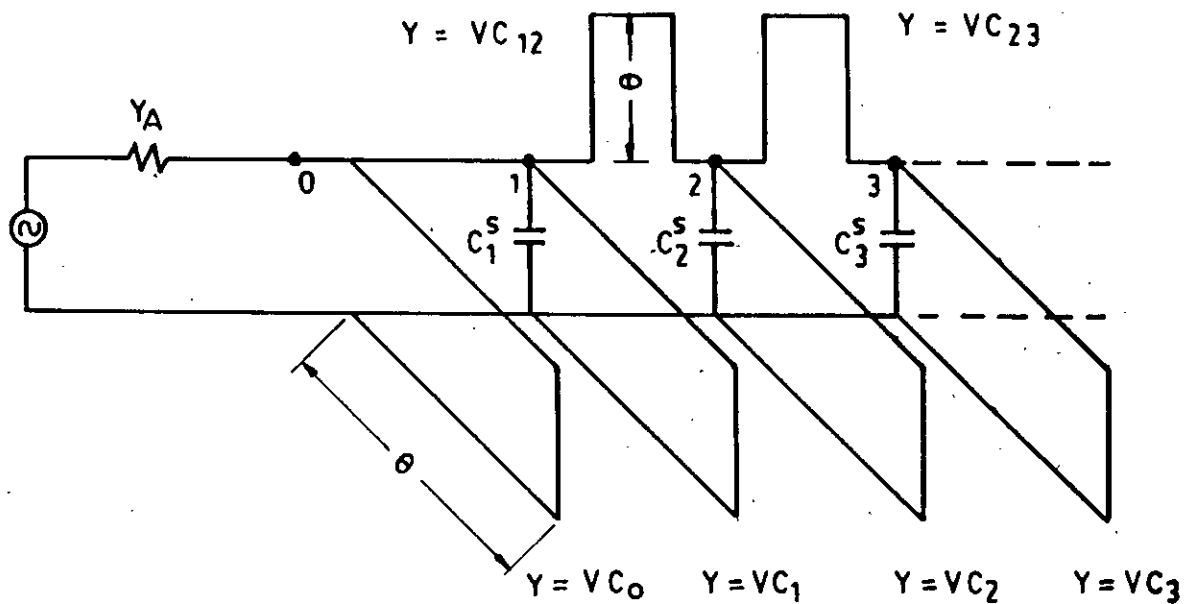


Fig. 6.2 Approximate equivalent circuit of the comb-line filter shown in the fig. 6.1

resonance. Moreover, with sizeable spacings between adjacent lines it offers efficient coupling between resonators. And the resulting filter is relatively small.

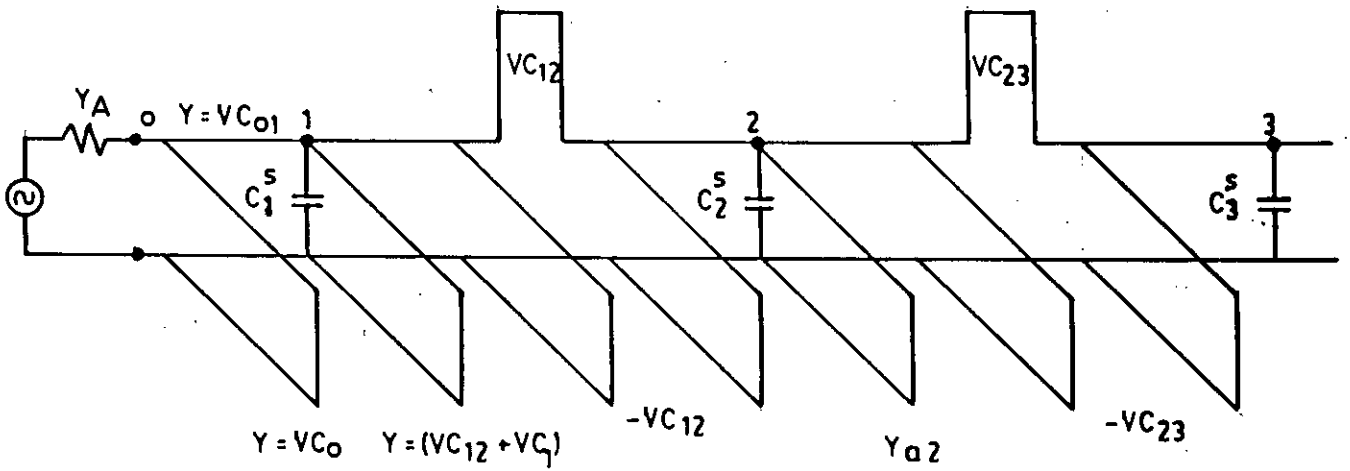
In this type of filter the second pass-band occurs when the resonator line elements are somewhat over one-half wavelength long. So, if the resonator lines are $1/8$ wavelength long at the primary pass-band, the second pass-band will be centred slightly over four times the centre frequency of the first pass-band. If they are made to be less than that at the primary pass-band, the second pass-band will be even further removed. Thus, a very broad stop band above the primary passband can be achieved with Comb-line filter. Besides, proper couplings can be maintained in manufactured filters without unreasonable tolerance requirements.

6.3 Equivalent circuit of Comb-line filter:

An approximate equivalent circuit of Comb-line filter can be obtained by replacing parallel-coupled lines with their electrically equivalent open-wire-line circuit. Using equivalences between parallel-coupled strip lines and open-wire-line circuits as shown in figures 4.8 to 4.11 in chapter 4, such an approximate open-wire-line representation of the Comb-line filter is shown in figure 6.2. Here, it is to be noted that the nodal points in figure 6.2 correspond to the nodal points indicated in figure 6.1. The circuitry between nodal points 0 and 1 in figure 6.2 is specified with the

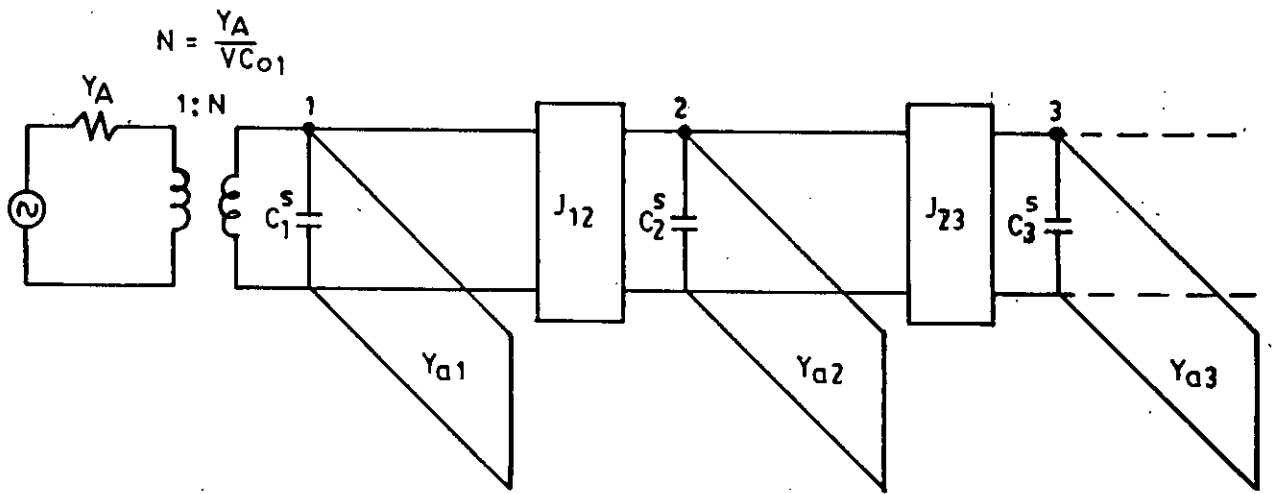
aid of the equivalences shown in figure 4.9 to correspond to the parallel coupled strip lines between nodal points 0 and 1 in figure 6.1. And the circuitry between nodal points 1 and 2, 2 and 3 ,n-1 and n, are specified with the aid of the equivalences shown in figure 4.11 to correspond to the pairs of parallel coupled sections formed by the strip lines connected to nodal points 1 and 2, 2 and 3 etc.

In order to modify the circuit shown in figure 6.2 to a form such that it can be represented using admittance inverter, the series stubs between nodal points 1 and 2, 2 and 3 etc. are incorporated into J-inverters of the form shown in figure 5.7. Thus the equivalent circuit in figure 6.2 modifies to the form shown in figure 6.3. In the rearranged circuit each of the inverters consists of a pi-configuration of a series stub of characteristic admittance $Y = vC_{k,k+1}$, $k=1$ to $n-1$, and two shunt stubs of characteristic admittance $-Y$. So, it is necessary to increase the characteristic admittances of the actual shunt stubs on each side in order to compensate for the negative admittances ascribed to the inverters. This is why shunt stubs 2 to $n-1$ in figure 6.3 now have the admittances $Y_{ak} = v(C_k + C_{k-1,k} + C_{k,k+1})$ instead of just vC_k . The portion of the circuit in figure 6.3 between nodal points 0 and 1 can be converted to a form consisting ideal transformer by use of the simplifying constraint that brings about the properties summarized in figure 4.10 with an additional constraint $vC_0 = Y_A - vC_{01}$. The equivalent circuit of the Comb-line bandpass filter then



Here, $Y_{ak} \quad k = 2 \text{ to } (n-1) = V(C_k + C_{k-1,k} + C_{k,k+1})$

Fig. 6.3 Rearranged form of fig. 6.2 to introduce J-inverter



$$GT = \frac{Y_A}{N^2} \quad Y_{a1} = Y_A \left[1 - \left(\frac{VC_{01}}{Y_A} \right)^2 \right] + V(C_1 + C_{12} - G_0)$$

Fig. 6.4 Rearranged equivalent form of the network shown in fig. 6.3

obtained is as illustrated in figure 6.4.

The equivalent circuit can further be simplified to give a generalized form. This can be achieved by replacing the transformer with the aid of an admittance inverter J_{01} in such a fashion as the terminating admittance G_{T1} in figure 6.4 is specified so that $G_{T1} = J_{01}^2/Y_A$, where the required value for J_{01} is as noted in figure 5.2(e). Finally, the Comb-line bandpass filter takes the generalized equivalent form as represented in figure 6.5. Here, the boxes marked $B_k(\omega)$ represent resonators which exhibit a susceptance characteristic like that of a shunt resonator in the vicinity of ω_0 . The resonator functions $B_k(\omega)$ are defined as

$$B_k(\omega) = \omega C_k^S - Y_{ak} \cot(\theta_0 \omega / \omega_0) \quad \text{--- (6.1)}$$

where θ_0 is the midband electrical length of the resonator lines.

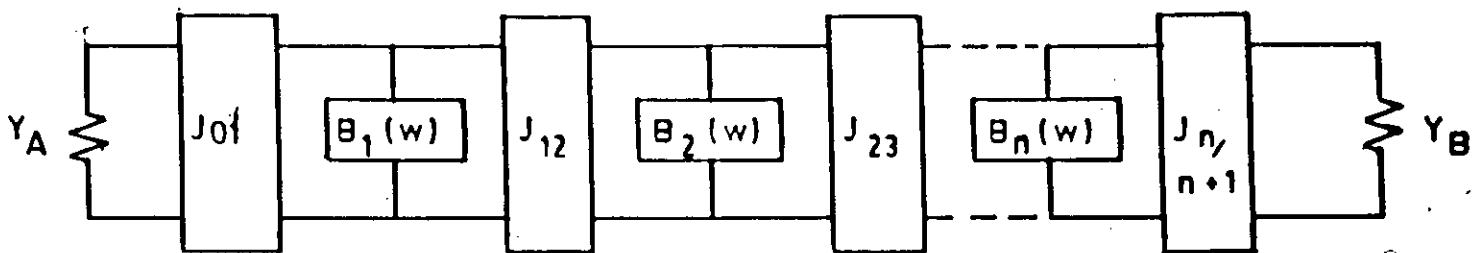


Fig. 6.5 Comb-line bandpass filter represented in the form of generalized bandpass filter network with admittance inverters.

6.4 Summary :

A complete description of the comb-line structure with necessary illustrations has been presented. Various features and advantages of this particular structure for microwave bandpass filter has also been discussed. Equivalent form of the structure using microwave equivalent networks and admittance inverter circuit has been obtained. Finally a generalized form of comb-line bandpass filter is presented.

CHAPTER-7

Design Equations of Comb-line Filter

7.1 Introduction:

Comb-line structure is formed with arrays of parallel lines between ground planes. These lines are also called resonators. In the structure, the coupling between resonators is distributed in nature and the electrical properties of the structure are characterised in terms of self and mutual capacitances. So it is convenient to work out the design of the resonator line in terms of capacitances C_k per unit length of each bar with respect to the ground, and the mutual capacitances $C_{k,k+1}$ per unit length between adjacent bars K and $K+1$. The following sections contains the design equations to calculate these capacitances and other necessary parameters. The procedure to derive the equations are also discussed broadly.

7.2 Design equations:

The equivalent circuit obtained in previous chapter was the combination of shunt resonators and J-inverters. They themselves are defined in terms of self, mutual and lumped capacitances per unit length of the resonator lines, low-pass circuit parameters and some other quantities related to electrical properties of the structure. So, the design equations for comb-line structure is in terms of the said

quantities and parameters. The complete set of equations required to design comb-line band filter are given below. The notations used in the equation are already mentioned in previous chapters.

Design equations in mathematical expressions

Equation for susceptance slope parameters:

$$b_k |_{k=1 \text{ to } n} = Y_{ak} (\cot \theta_o + \theta_o \operatorname{cosec}^2 \theta_o) / 2 \quad \dots\dots\dots(7.1)$$

where θ_o is the electrical length of the resonator elements at midband frequency ω_o .

Equations for terminating admittances are given as:

$$G_{T1} = W b_1 / g_o g_1 \omega_1' \quad \dots\dots\dots(7.2)$$

and

$$G_{Tn} = W b_n / g_n g_{n+1} \omega_1' \quad \dots\dots\dots(7.3)$$

where W is the fractional bandwidth.

The normalized capacitances per unit length between each line and ground can be calculated from the following equations:

$$C_o / \epsilon = (376.7 Y_A / \sqrt{\epsilon_r}) (1 - \sqrt{(G_{T1} / Y_A)}) \quad \dots\dots\dots(7.4)$$

$$C_1 / \epsilon = (376.7 / \sqrt{\epsilon_r}) (Y_{a1} - Y_A + G_{T1} - J_{12} \tan \theta_o) + C_o / \epsilon \quad \dots\dots(7.5)$$

$$C_k / \epsilon |_{k=2 \text{ to } n-1} = (376.7 / \sqrt{\epsilon_r}) (Y_{ak} - J_{k-1,k} \tan \theta_o - J_{k,k+1} \tan \theta_o) \quad \dots\dots\dots(7.6)$$

$$C_n / \epsilon = (376.7 / \sqrt{\epsilon_r}) (Y_{an} - Y_A + G_{Tn} - J_{n-1,n} \tan \theta_o) + C_{n+1} / \epsilon \quad \dots\dots(7.7)$$

$$C_{n+1} / \epsilon = (376.7 Y_A / \sqrt{\epsilon_r}) (1 - \sqrt{(G_{Tn} / Y_A)}) \quad \dots\dots\dots(7.8)$$

where ϵ is the absolute dielectric constant of the medium of propagation and ϵ_r is the relative dielectric constant.

The normalized mutual capacitances per unit length between adjacent lines are given by :

$$C_{01}/\epsilon = (376.7Y_A/\sqrt{\epsilon_r}) - C_0/\epsilon \quad \dots\dots\dots(7.9)$$

$$C_{k,k+1}/\epsilon \quad k=1 \text{ to } n-1 = (376.7/\sqrt{\epsilon_r})(J_{k,k+1}\tan\theta_0) \quad \dots\dots(7.10)$$

$$C_{n,n+1}/\epsilon = (376.7Y_A/\sqrt{\epsilon_r}) - C_{n+1}/\epsilon \quad \dots\dots\dots(7.11)$$

The lumped capacitances are obtained from:

$$C_k^s \quad k=1 \text{ to } n = (Y_{ak}\cot\theta_0)/\omega_0 \quad \dots\dots\dots(7.12)$$

Also the J-inverter parameters can be calculated from the equation:

$$J_{k,k+1} \quad k=1 \text{ to } n-1 = (W/\omega_1') [\sqrt{(b_k b_{k+1}/g_k g_{k+1})}] \dots\dots(7.13)$$

7.3 Derivation of the design equations:

The comb-line filter design equations can be derived by use of the approximate, open-wire line representation and other equivalent circuits obtained in chapter 6 following the out lines given by Cohn[1]. Derivation of all the equations listed in section 7.2 are presented below.

The expression for J-inverter parameters shown in equation (7.13) can be derived by exploiting the expression for the same parameters obtained in chapter 5 for a low pass prototype circuit. Using lowpass to bandpass transformation in the same circuit the required expression is available with simple mathematical manipulation. The lowpass circuit with J-inverters as shown in figure 5.2(c) can be transformed to a corresponding lumped - element band pass circuit using the frequency transformation

$$\omega' = (\omega_1'/W) \{ (\omega/\omega_0) - (\omega_0/\omega) \} \quad \dots\dots\dots(7.14)$$

where $W = (\omega_2 - \omega_1)/\omega_0$ and $\omega_0 = \sqrt{(\omega_2 \omega_1)}$

ω' , ω are the lowpass and bandpass radian frequency

variables respectively. Then the shunt reactances $\omega' C_{ak}$ in figure 5.2(c) take the form

$$(\omega_1'/W)[(\omega/\omega_0) - (\omega_0/\omega)]C_{ak}$$

It can be rearranged as

$$C_{rk}\omega - 1/L_{rk}\omega$$

where $C_{rk} = \omega_1' C_{ak} / W\omega_0$ and $L_{rk} = W/\omega_1' \omega_0 C_{ak}$

Thus the lowpass circuit of figure 5.2(c) is transformed to the bandpass circuit as illustrated in figure 7.1 below.

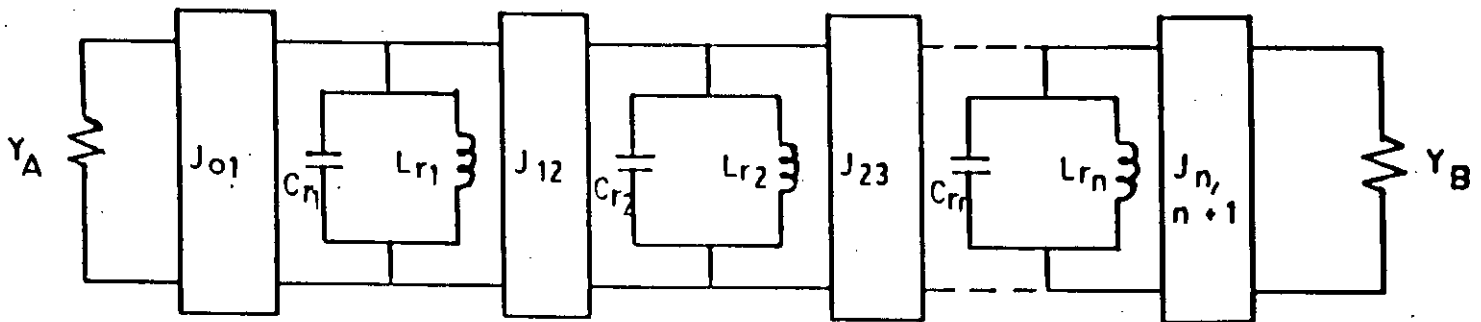


Fig. 7.1: Bandpass filter network obtained from lowpass prototype using frequency transformation.

The shunt elements in the above circuit is equivalent to the resonators in comb-line structure. Here , the resonator function is given by

$$B_k(\omega) = C_{rk}\omega - 1/L_{rk}\omega \quad \text{--- (7.15)}$$

Now, the resonator slope parameter i.e. the susceptance slope parameter is given by

$$\begin{aligned} b_k &= \frac{\omega_0}{2} \left. \frac{dB_k(\omega)}{d\omega} \right|_{\omega=\omega_0} \quad \text{--- (7.16)} \\ &= C_{rk}\omega_0 \\ &= (\omega_1'/W)C_{ak} \end{aligned}$$

Therefore, $C_{ak} = (W/\omega_1')b_k \quad \text{--- (7.17)}$

Substituting this value of C_{ak} in the expression for J-inverter parameter obtained in chapter 5, we get

$$J_{k,k+1} = (W/\omega_1')\sqrt{(b_k b_{k+1}/g_k g_{k+1})} \quad \text{--- (7.18)}$$

The J-inverters used in the equivalent circuit of comb-line bandpass filter is of the form as shown in figure 5.7. The negative shunt admittances required for these inverters are lumped with the resonator capacitances to yield somewhat smaller net shunt capacitance actually used in constructing the filter. However, in the case of the inverters between the end resonators and the terminating admittances, this procedure does not work since there is no way of absorbing the negative admittance that would appear across the resistive terminations. This difficulty directly limits the value of k in the above expression for J-inverter parameters from 1 to n-1. Thus, we can write

$$J_{k,k+1} \quad k=1 \text{ to } n-1 = (W/\omega_1')\sqrt{(b_k b_{k+1}/g_k g_{k+1})} \quad \text{--- (7.19)}$$

Now, the expressions for the end inverters can be obtained

directly from equations (5.9) and (5.10) by replacing the low pass reactance values with the respective transformed band pass values. Then we get

$$J_{01} = \sqrt{(Wb_1 Y_A / \omega_1' g_0 g_1)} \text{ and } J_{n,n+1} = \sqrt{(Wb_n Y_A / \omega_1' g_n g_{n+1})}$$

The difficulty in analysis mentioned above can be avoided by analyzing the end couplings in a different way. This method of analysis for the end couplings leads to the deduction of the expression of terminating admittance. Looking left from resonator 1 in figure 7.1 into the inverter J_{01} , the terminating admittance appears

$$\begin{aligned} G_{T1} &= J_{01}^2 / Y_A \\ &= Wb_1 / \omega_1' g_0 g_1 \end{aligned} \quad \text{--- (7.20)}$$

Similarly, we can deduce

$$G_{Tn} = Wb_n / \omega_1' g_n g_{n+1} \quad \text{--- (7.21)}$$

The equations for the susceptance slope parameters and lumped capacitances can be deduced considering the behaviour of resonators at midband frequency. At resonance, the influence of resonator functions $B_k(\omega)$ becomes null. we have

$$B_k(\omega) = \omega C_k^S - Y_{ak} \cot(\theta_o \omega / \omega_o) \quad \text{--- (7.22)}$$

at $\omega = \omega_o$, we require that $B_k(\omega_o) = 0$, which calls for

$$C_k^S = (Y_{ak} \cot \theta_o) / \omega_o \quad \text{--- (7.23)}$$

Now, the susceptance slope parameter is defined as

$$\begin{aligned} b_k &= (\omega_o / 2) \frac{d}{d\omega} B_k(\omega) \Big|_{\omega=\omega_o} \\ &= (\omega_o / 2) \frac{d}{d\omega} [\omega C_k^S - Y_{ak} \cot(\theta_o \omega / \omega_o)] \\ &= (\omega_o / 2) [(Y_{ak} \cot \theta_o) / \omega_o + (\theta_o Y_{ak} \operatorname{cosec}^2 \theta_o) / \omega_o] \\ &= (Y_{ak} / 2) (\cot \theta_o + \theta_o \operatorname{cosec}^2 \theta_o) \end{aligned} \quad \text{(7.24)}$$

The slope parameter is meant only for the resonators. Hence

the value of k is limited between 1 and n , i.e. the number of resonators, so we can write

$$b_{k|k=1 \text{ to } n} = (Y_{ak}/2)(\cot\theta_0 + \theta_0 \operatorname{cosec}^2\theta_0) \quad \text{--- (7.25)}$$

and

$$C_{k^s|k=1 \text{ to } n} = (Y_{ak} \cot\theta_0)/\omega_0 \quad \text{--- (7.26)}$$

The equation describing the mutual capacitances between resonator line elements can be deduced taking into account the equivalent circuit shown in figure 6.3 and its reorganized form as shown in figure 6.4. Here the J-inverter parameters are given by

$$J_{k,k+1} = vC_{k,k+1} \cot\theta_0 \quad \text{--- (7.27)}$$

From the above equation we can get the expression for mutual capacitances per unit length between resonator lines as

$$C_{k,k+1} = (J_{k,k+1} \tan\theta_0)/v \quad \text{--- (7.28)}$$

Again from table 4.1 which displays the relations of parallel coupled lines, we can easily obtain

$$v = \sqrt{(\epsilon_r)}/\epsilon\eta_0 \quad \text{--- (7.29)}$$

hence

$$C_{k,k+1} = (\epsilon\eta_0/\sqrt{\epsilon_r})(J_{k,k+1} \tan\theta_0)$$

or, $C_{k,k+1}/\epsilon = (376.7/\sqrt{\epsilon_r})(J_{k,k+1} \tan\theta_0) \quad \text{--- (7.30)}$

The expression for the J-inverter parameter used to deduce the above equation is due to the inverters $J_{12}, J_{23}, \dots, J_{n-1,n}$ shown in figure 6.4 because of identical construction and defining equation. But the end inverters i.e. J_{01} and $J_{n,n+1}$ are made of different structure. It has also got defining equation different from the others. So, the value of k in the above expression is obviously limited between 1 and

(n-1). Thus, we obtain the equation for the normalized mutual capacitance per unit length between the resonator lines as

$$C_{k,k+1}/\epsilon'_{k=1 \text{ to } n-1} = (376.7/\sqrt{\epsilon_r})(J_{k,k+1}\tan\theta_0) \quad \text{---(7.31)}$$

Now the equation for the mutual capacitance between the end bars and their adjacent resonators is to be deduced exploiting the special constraints mentioned in figure 4.10 under section 4.6 of chapter 4. Consider the end bar and its adjacent resonator i.e. the rectangular bar marked 0 and 1 in figure 6.1, we can write

$$vC_{01} = (Y_{00}^o - Y_{0e}^o)/2 \quad \text{---(7.32)}$$

using the special constraint $Y_{0e}^a + Y_{00}^a = 2Y_A$

and the usual phenomena $Y_{0e}^a = vC_a$

here Y_A is the terminating admittance as mentioned elsewhere.

we can rearrange the above equation as

$$\begin{aligned} vC_{01} &= (2Y_A - Y_{0e}^o - Y_{0e}^o)/2 \\ &= Y_A - vC_o \end{aligned}$$

$$\text{or, } C_{01} = \epsilon\eta_o Y_A/\sqrt{\epsilon_r} - C_o$$

$$\text{Therefore, } C_{01}/\epsilon = 376.7Y_A/\sqrt{\epsilon_r} - C_o/\epsilon \quad \text{--- (7.33)}$$

Similarly, we can obtain for the other end

$$C_{n,n+1}/\epsilon = 376.7Y_A/\sqrt{\epsilon_r} - C_{n+1}/\epsilon \quad \text{--- (7.34)}$$

The self capacitances per unit length of the resonator lines can be obtained by considering the admittances of the shunt stubs rearranged to introduce J-inverters as shown in figure 6.4. Since each of the inverters consist of a pi configuration having a series stub of characteristic admittance Y and two shunt stubs of characteristic admittance -Y, it is necessary to increase the characteristic

admittances of the actual shunt stubs on each side in order to compensate for the negative admittances ascribed to the inverters. For this reason shunt stubs will have the admittances as follows

$$Y_{ak} = v(C_k + C_{k-1,k} + C_{k,k+1})$$

$$\text{or, } vC_k = Y_{ak} - vC_{k-1,k} - vC_{k,k+1}$$

$$\begin{aligned} \text{or, } C_k/\epsilon &= \eta_0 Y_{ak} / \sqrt{\epsilon_r} - C_{k-1,k}/\epsilon - C_{k,k+1}/\epsilon \\ &= (376.7/\sqrt{\epsilon_r})(Y_{ak} - J_{k-1,k} \tan \theta_0 - J_{k,k+1} \tan \theta_0) \dots (7.35) \end{aligned}$$

The above analysis is justified for the shunt stubs 2 to (n-1) in figure 6.3, which in fact provides the range of the subscript k. So, we get the equation for the normalized self capacitance per unit length of the resonator line elements as

$$C_k/\epsilon; k=2 \text{ to } n-1 = (376.7/\sqrt{\epsilon_r})(Y_{ak} - J_{k-1,k} \tan \theta_0 - J_{k,k+1} \tan \theta_0) \dots (7.36)$$

Since the equation obtained above does not give the self capacitance of the end bars as well as the adjacent resonators, we require different equations for them. The equations valid for them are as deduced below.

Let us consider the portion upto node 1 of the circuit shown in figure 6.4 isolated from the rest. Under this condition, from the equivalence shown in figure 4.10, the admittance of the shunt is supposed to be

$$Y_{a1} = Y_A [(N^2 - 1)/N^2] + Y_{oe}^1 - Y_{oe}^0 \dots (7.37)$$

But, since it is integrated with the rest of the circuit, in order to accommodate the negative shunt admittance $-vC_{12}$ introduced to form the inverter J_{12} , the admittance of the stub must be increased by the same amount. Hence, the

accurate expression for the said admittance should be

$$Y_{a1} = Y_A[(N^2-1)/N^2] + Y_{oe}^1 - Y_{oe}^0 + vC_{12} \quad \dots\dots(7.38)$$

$$= Y_A[1-G_{T1}/Y_A] + vC_1 - vC_0 + vC_{12} \quad (\text{since } N^2=Y_A/G_T)$$

or, $C_1/\epsilon = (\eta_0/\sqrt{\epsilon_r})(Y_{a1} - Y_A + G_{T1} - J_{12}\tan\theta_0) + C_0/\epsilon \dots\dots(7.39)$

Therefore,

$$C_1/\epsilon = (376.7/\sqrt{\epsilon_r})(Y_{a1} - Y_A + G_{T1} - J_{12}\tan\theta_0) + C_0/\epsilon$$

Similarly, we can deduce $\dots\dots(7.40)$

$$C_n/\epsilon = (376.7/\sqrt{\epsilon_r})(Y_{an} - Y_A + G_{Tn} - J_{n-1,n}\tan\theta_0) + C_{n+1}/\epsilon \dots\dots(7.41)$$

Finally the expression for the self capacitance of the end bars can be obtained from the equation describing the mutual capacitance between the end bar and the adjacent resonator. we have already deduced

$$C_{o1}/\epsilon = 376.7Y_A/\sqrt{\epsilon_r} - C_0/\epsilon \quad \dots\dots(7.42)$$

rearranging the above equation we get

$$C_0/\epsilon = 376.7Y_A/\sqrt{\epsilon_r} - C_{o1}/\epsilon \quad \dots\dots(7.43)$$

Now the characteristic admittance of the inverter J_{o1} in the equivalent circuit shown in previous chapter can be obtained as $J_{o1} = \sqrt{vC_{o1}}$. It implies that.

$$C_0/\epsilon = 376.7Y_A/\sqrt{\epsilon_r} - 376.7J_{o1}/\sqrt{\epsilon_r} \quad \dots\dots(7.44)$$

$$= (376.7/\sqrt{\epsilon_r})(Y_A - (G_{T1}Y_A)) \quad (\text{since } G_{T1}=J_{o1}^2/Y_A)$$

Thus we obtain,

$$C_0/\epsilon = (376.7/\sqrt{\epsilon_r})Y_A[1 - \sqrt{(G_{T1}/Y_A)}] \quad \dots\dots(7.45)$$

In a similar fashion, we can deduce

$$C_{n+1}/\epsilon = (376.7/\sqrt{\epsilon_r})Y_A[1 - \sqrt{(G_{Tn}/Y_A)}] \quad \dots\dots(7.46)$$

7.4 Summary :

Equations showing various capacitances associated with

the comb-line structure and equations of some other parameters necessary to design bandpass filter in comb geometry are listed in this chapter. Derivation of all the equations considering relevant circuits and equivalent networks has been carried out with brief descriptions.

CHAPTER-8

Design of the experimental filter

8.1 Introduction:

By now we are in a position to go for the design of an experimental five resonator Comb-line bandpass filter. Various terms, parameters and quantities discussed in previous chapters will now be used to compute necessary dimensions in order to realize the filter physically. It has already been mentioned earlier that the Comb-line filters contain arrays of parallel lines between ground planes. So, the design of the experimental filter must be directed to obtain various dimensions of the line elements comprising the array as well as the separating distances between adjacent elements. This objective is achieved in steps together with the selection of low-pass prototype filter parameters from Saal's catalogue [12]. The design of the experimental comb-line filter under consideration is presented in details in the following section.

8.2 Design Procedure:

In the design procedure, the lumped-element prototype filter parameters are used to achieve bandpass filter having approximately the same response properties. Thus, using a lumped-element prototype having a Chebychev response characteristics, the corresponding band-pass filter response

will also be Chebychev in nature. Figure 8.1 shows the low-pass prototype circuit under consideration. The corresponding band-pass filter circuit which can be obtained directly from the prototype by a low-pass to bandpass transformation discussed in chapter 2 is shown in figure 8.2. Note that the five reactive elements in the prototype circuit is transformed into five resonators in the corresponding band-pass circuit as has been explained in chapter 2.

The band-pass filter circuit contains both series and shunt resonators. Such type of structure is difficult to realize practically. In order to facilitate the practical realization of the filter, the series resonators in the above structure is transformed into shunt resonators using admittance inverters as has been discussed in chapter 5. The equivalent circuit thus obtained is illustrated in figure 8.3. Series resonators (L_2, C_2) and (L_4, C_4) are now shunt resonators like (L_1, C_1) etc. and incorporated in $B_2(\omega)$ and $B_4(\omega)$.

To carry out the design of a five resonator comb-line bandpass filter using the design formulas discussed in previous chapter, the lowpass prototype filter parameters g_0, g_1, \dots, g_6 and the cut off point are selected first. Next the terminating line admittance, the midband electrical length of the resonator line, the fractional bandwidth and the normalized line admittances must all be specified properly. Usually it is convenient to make the midband electrical length equal to $\pi/4$ radians or less. The choice of

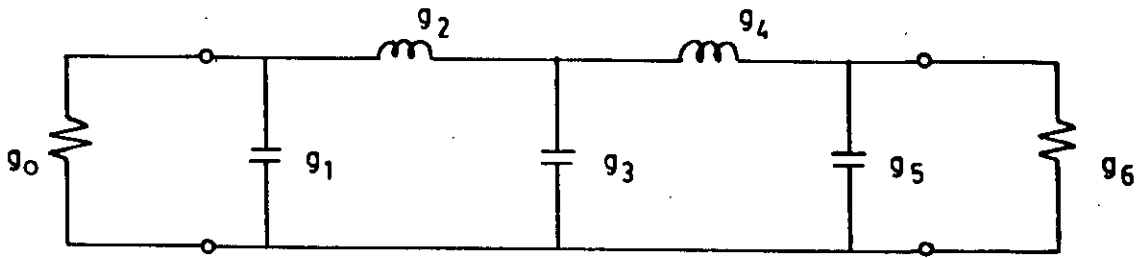


Fig. 8.1 A five element lowpass prototype filter circuit having cheby ev response

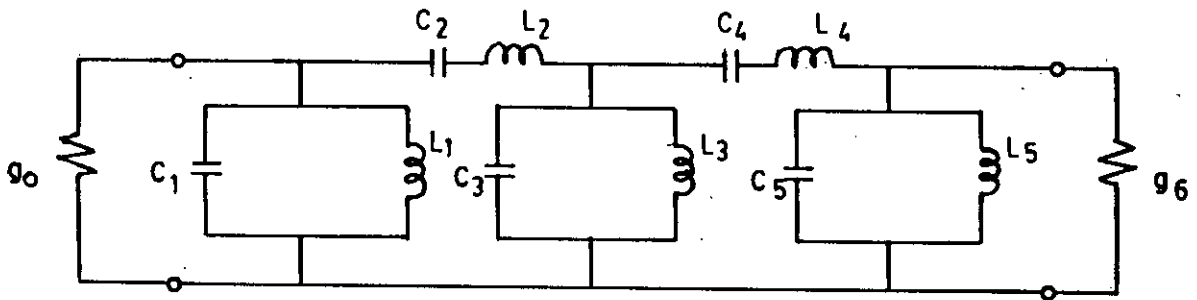


Fig. 8.2 A five resonator bandpass filter circuit corresponding to the lowpass prototype shown in fig. 8.1

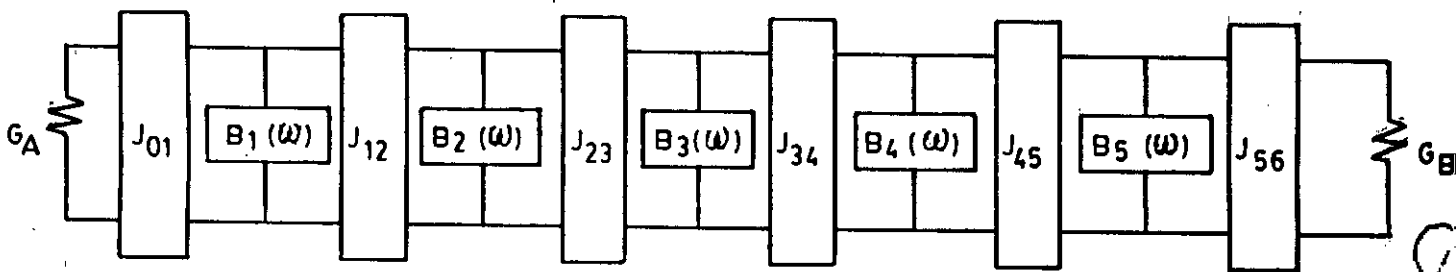


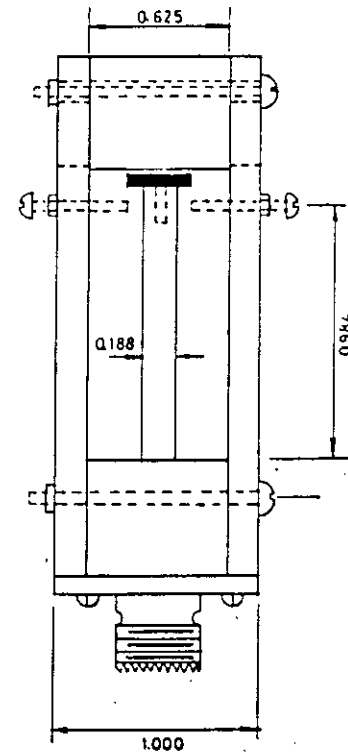
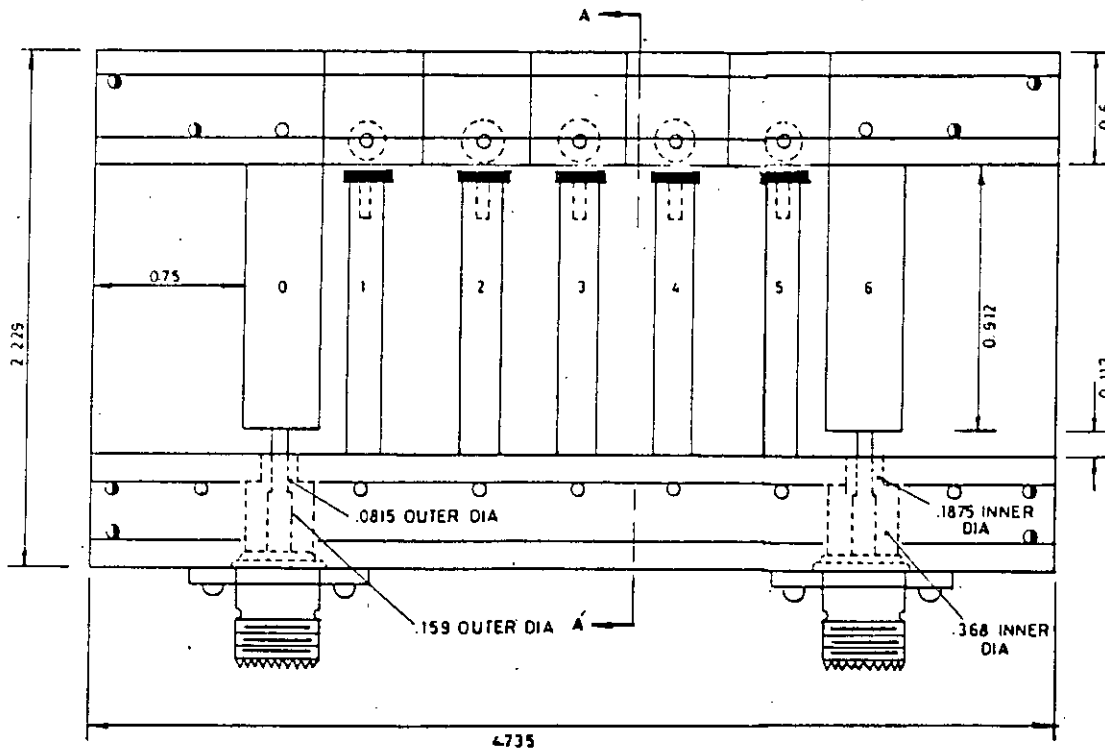
Fig. 8.3 Equivalent network of the five resonator bandpass filter circuit using admittance inverter.

WIDTHS OF RECTANGULAR BARS:

$W_0 = 0.353 = W_6$
 $W_1 = 0.151 = W_5$
 $W_2 = 0.192 = W_4$
 $W_3 = 0.195$

SEPARATION BETWEEN RECTANGULAR BARS:

$S_{01} = 0.109 = S_{56}$
 $S_{12} = 0.328 = S_{45}$
 $S_{23} = 0.387 = S_{34}$



SECTION A-A

FIG. 8.4 DRAWING OF THE EXPERIMENTAL FIVE-RESONATOR COMBLINE FILTER

(All dimensions are in inch)

the resonator line admittance fixes the admittance level within the filter. The term line admittance is interpreted physically as the admittance of line k with the adjacent lines $(k-1)$ and $(k+1)$ grounded. Then the dimensions of the resonators and the spacings between adjacent resonators is obtained from Getsinger's chart [3] by computing the required capacitance values using the equations given in chapter 7. Table below summarizes various parameters selected and used in the design of the experimental five resonator Comb-line bandpass filter.

Low-pass prototype filter parameters

$$g_0 = 1, g_1 = 0.9732, g_2 = 1.372, g_3 = 1.803,$$

$$g_4 = 1.372, g_5 = 0.9732, g_6 = 1$$

$$\text{Terminating admittance, } Y_A = 0.02 \text{ mho}$$

$$\text{Midband electrical length of resonator line, } \theta_0 = \pi/4 \text{ rad.}$$

$$\text{Fractional bandwidth, } W = 0.10$$

$$\text{Normalized line admittance, } (Y_{ak}/Y_A) = 0.677$$

$$\text{Separation between ground plates, } b = 0.625 \text{ inch.}$$

$$\text{Thickness of resonator line element } t = 0.188 \text{ inch.}$$

$$\text{Passband Chebychev ripple} = 0.1 \text{ dB.}$$

8.3 Computation of widths of rectangular bars and separation between adjacent bars:

The cross-section of an array of parallel-coupled lines used in a comb-line filter is similar to that as shown in figure 4.6. In the structure, all the bars have the same

thickness giving same t/b ratio. The other cross-sectional dimensions of the bars can be obtained with the aid of the Getsinger's charts after computing the values of normalized self and mutual capacitances per unit length of the line elements using the respective equations given in previous chapter. Since,

$$(\Delta C)_{k,k+1}/\epsilon = C_{k,k+1}/\epsilon \quad \dots \dots (8.1)$$

Getsinger's charts shown in figure 4.2(a) can be used for the specific value of t/b (which is 0.3 for the design under consideration) to determine $S_{k,k+1}/b$. In this manner, the spacings $S_{k,k+1}$ between all the bars are obtained. At the same time, using the chart shown in the same figure, the normalized fringing capacitances, $(C_{fe}')_{k,k+1}$ associated with each gap, $S_{k,k+1}$ between the bars is obtained. The normalized width of the k th bar is then calculated from the equation as follows:

$$W_k/b = [(1-t/b)/2] \{ (C_k/\epsilon)/2 - (C_{fe}')_{k-1,k}/\epsilon - (C_{fe}')_{k,k+1}/\epsilon \} \quad \dots \dots (8.2)$$

In case of the bars at the ends of the array (i.e. bar 0 and 6 in figure 6.1), C_{fe}'/ϵ for the edge of the bar that has no neighbour must be replaced by C_f'/ϵ i.e. the normalized fringing capacitance for an isolated bar which is directly available from the plot show in figure 4.2(b). Then width of bar 0 should be calculated as

$$W_0/b = (1-t/b)/2 \{ (C_0/\epsilon)/2 - C_f'/\epsilon - (C_{fe}')_{01}/\epsilon \} \dots (8.3)$$

Also the width of bar 6 is calculated in a similar fashion.

Various parameters thus computed in the design of the experimental five resonator comb-line band-pass filter are given in table 8.1 below.

Table 8.1

k	$(J_{k,k+1})/Y_A$	C_k/ϵ	$C_{k,k+1}/\epsilon$	C_k^S (*10 ⁻¹²)	W_k (inch)	$S_{k,k+1}$ (inch)
0	0.000	5.281	2.252	0.000	0.353	0.109
1	0.075	2.953	0.567	1.445	0.151	0.328
2	0.055	4.116	0.416	1.445	0.192	0.386
3	0.055	4.266	0.416	1.445	0.195	0.386
4	0.075	4.116	0.567	1.445	0.192	0.328
5	0.000	2.953	2.252	1.445	0.151	0.109
6		5.281		0.000	0.353	

A complete diagram of the experimental filter hence designed is illustrated in figure 8.4.

8.4 Summary :

Procedure to design a five resonator comb line filter taking lumped low-pass filter parameters from published paper has been presented. Selection of parameters and quantities other than the low pass element values has also been discussed. Physical dimensions of the resonator elements were calculated following the procedure discussed in chapter four. Computed results has been tabulated.

CHAPTER-9

Fabrication and Measurement of the Experimental Filter

9.1 Introduction:

In order to establish the validity of the design technique developed in this work and described in previous chapters, an experimental filter has been constructed and tested by measuring the insertion loss characteristics of the filter. Details of fabrication and the method of measurement is described in subsequent sections.

9.2 Fabrication of the experimental filter:

A complete drawing of the filter with the dimensions was presented in figure 8.4 in the previous chapter. An experimental filter has been constructed by machining and cutting brass plates. The cross sectional view of the filter shows that the resonator elements are flanked by two cover plates which are meeting the purpose of ground plates. These ground plates were made by cutting and machining brass plates with less effort as the dimensions were large enough and precision could be obtained easily. But the cutting and machining of the resonator elements and the pieces in between were not that easy. Since the dimensions of these pieces were in fraction of inches upto third decimal place it took much attention and careful machining to obtain accuracy in making these small pieces. Five resonator elements and two

transformer elements of identical thickness but different widths were cut from a brass plate having a thickness of 0.25 inch and machined carefully to obtain proper dimensions according to the design. And the adjustable blocks ensuring proper separations between transforming elements and resonators and responsible for the lumped capacitance were made of a 0.50 inch thick brass plate. In order to make the total thickness of the physically realized filter equal to 1.0 inch, each of the cover plates were made of brass plates having a thickness of 0.25 inches. Finally the machined pieces were arrayed in the designed fashion and tied together with flat-top machine screws made of brass. With a view to make communication with the instruments connected at the input and output terminals two RS SO 239 sockets were set at the respective transformer elements. Figure 8.4 clearly shows the connection of these connectors to the input and output transformer elements. Photographs of the constructed filter without the top cover plate are shown in next two pages, in fig. 9.7 and fig. 9.8

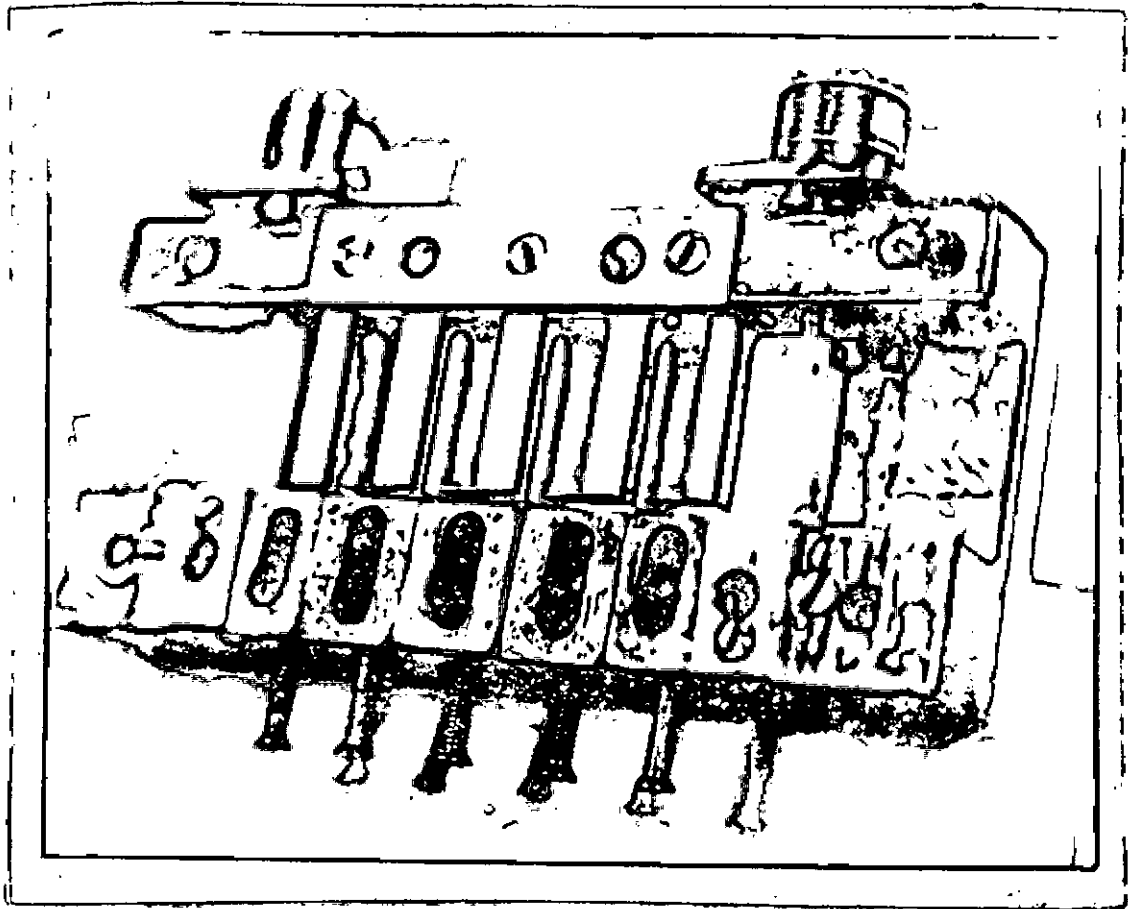


Fig. 9.7 Photograph of the constructed filter
with top cover plate removed.

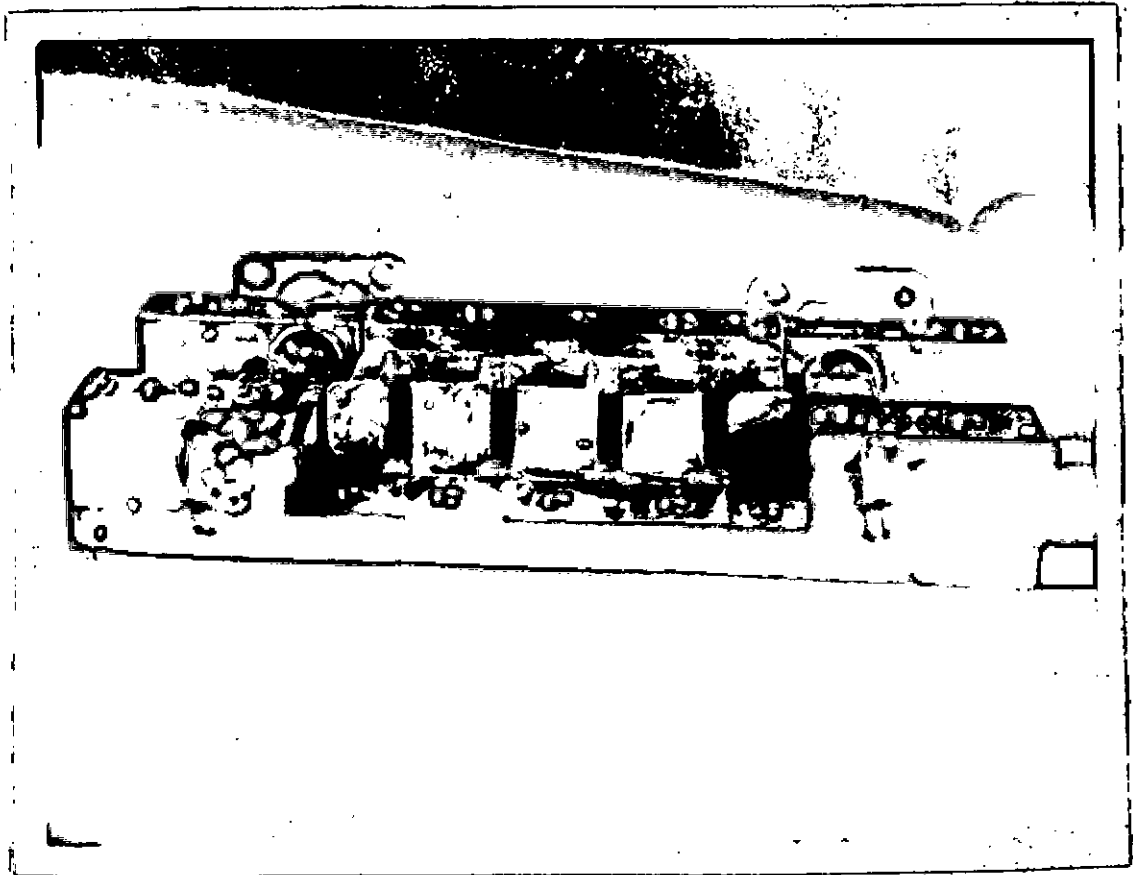


Fig. 9.8 Photograph of the constructed filter with top cover plate and the sliding blocks removed.

9.3 Measurement of Insertion loss characteristics:

The block diagram of the arrangement for measuring the insertion loss of a filter by means of a power meter and thermistor mount is shown in figure 9.1. Before going into the measurement let us have a brief discussion on the measuring arrangement. The arrangement consists of a hp-430C microwave power meter and a 477B coaxial thermistor mount as shown in figure 9.2. With the help of this arrangement average power upto 10 mW may be measured if the frequency range is within 10 mc/s to 10 Gc/s. The thermistor is a resistive device capable of dissipating radio frequency power and can change resistance using the thermal energy absorbed. It has a negative co-efficient of temperature and is constructed generally of a small amount of semiconducting material suspended by two fine wires. The hp 477B coaxial thermistor mount is designed to operate at 200 ohm resistance with negative temperature coefficient.

In this measuring arrangement the thermistor mount forms one leg of a self balancing bridge of the power meter. The power meter contains such a bridge, a 10.8 Kc oscillator, a d.c. bias circuit and a meter circuit. Initially, the thermistor element is connected to the instrument bridge circuit keeping the bias off but is not connected to the r.f. power source. The thermistor mount bridge is balanced when the element changes from its cold resistance to its operating resistance. The change takes place as the element absorbs power from the oscillator and d.c. power from the

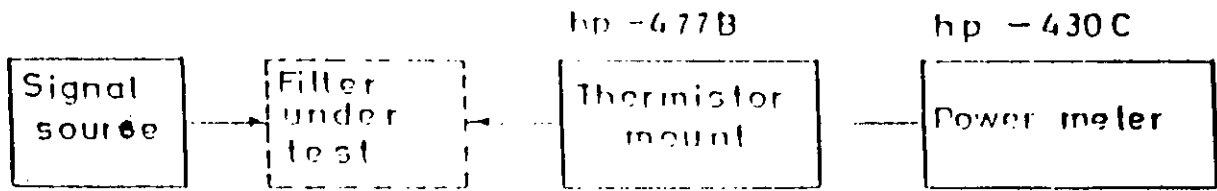


Fig. 9.1. Block diagram of the set-up for the measurement of insertion loss of filters by using power meter and thermistor mount.

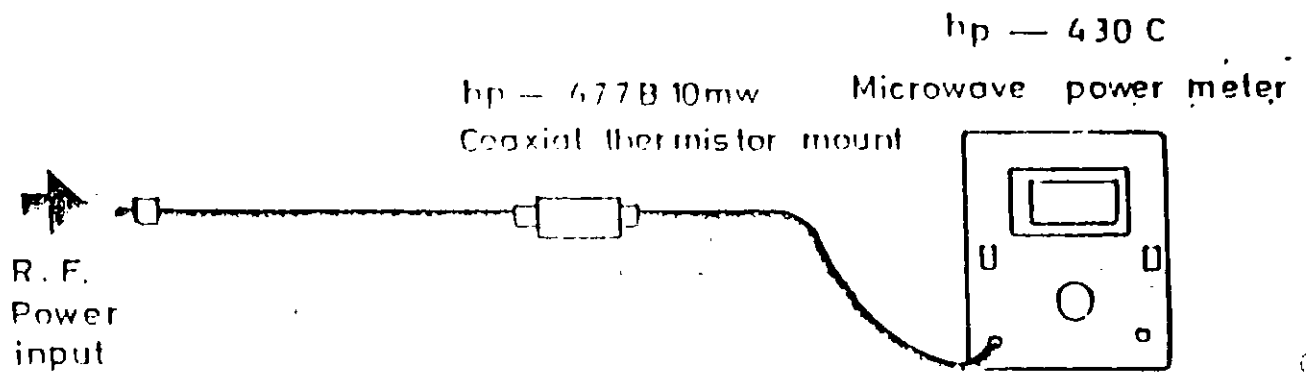


Fig 9.2. Arrangement for measuring average power.

bias circuit of the power meter.

Now, we intend to measure the insertion loss characteristics of the constructed experimental comb-line bandpass filter. To achieve this, the input and output power of the filter were measured at different frequencies within the passband using the power meter and thermistor mount. This was done in the following manner. First, the indicator of the power meter is set zero by means of zero setting knobs. The power range indicator is kept at 10 mW position. The r.f. power source is then connected to the thermistor mount. The thermistor element absorbs the external r.f. power, gets heated, and changes its resistance which unbalances the bridge. This action causes the output from the oscillator inside the power meter to decrease to accommodate the external r.f. power through the thermistor element. The meter circuit inside the power meter measures the amount of this power decrease from the oscillator of the power meter and displays the result of measurement over a calibrated scale as the power increase due to the external r.f. source. This power is noted as input power. Then the filter whose insertion loss characteristics is to be measured is inserted in between the r.f. power source and the thermistor mount. The power now indicated by the needle on the calibrated display board is noted as the output power. Repeating this procedure readings were taken at different frequencies within the passband. Output power being very low outside the pass band, it was measured by keeping the power range indicator of the power

meter at 0.1 mW position. Then the ratio of the output power to the input power is calculated and the insertion loss is calculated in dB.

Following the procedure described above, three sets of readings were taken. First set was taken immediately after assembling the filter without proper tuning. Second set of readings were taken creating proper tuning by following the tuning method described in section 9.4. Third set of readings were taken under same tuning condition with the connection to the input and output terminals of the filter interchanged. Insertion loss in dB for all the individual readings of the three sets of observations were calculated and are tabulated in appendix-C, appendix-D and appendix-E. The curves of insertion loss against frequency are plotted using three sets of readings and are presented in figures 9.4, 9.5 and 9.6 respectively. The theoretical plot of the insertion loss is shown in figure 9.3.

It is obvious from the measured plots that tuning plays a significant role in this type of filters. Without proper tuning the desired response can not be obtained. It means the lumped capacitance between one end of the resonators and the ground has significant influence on the response of the filter. A little variation of the values of these capacitances changes the performance including shifting the position of the pass band.

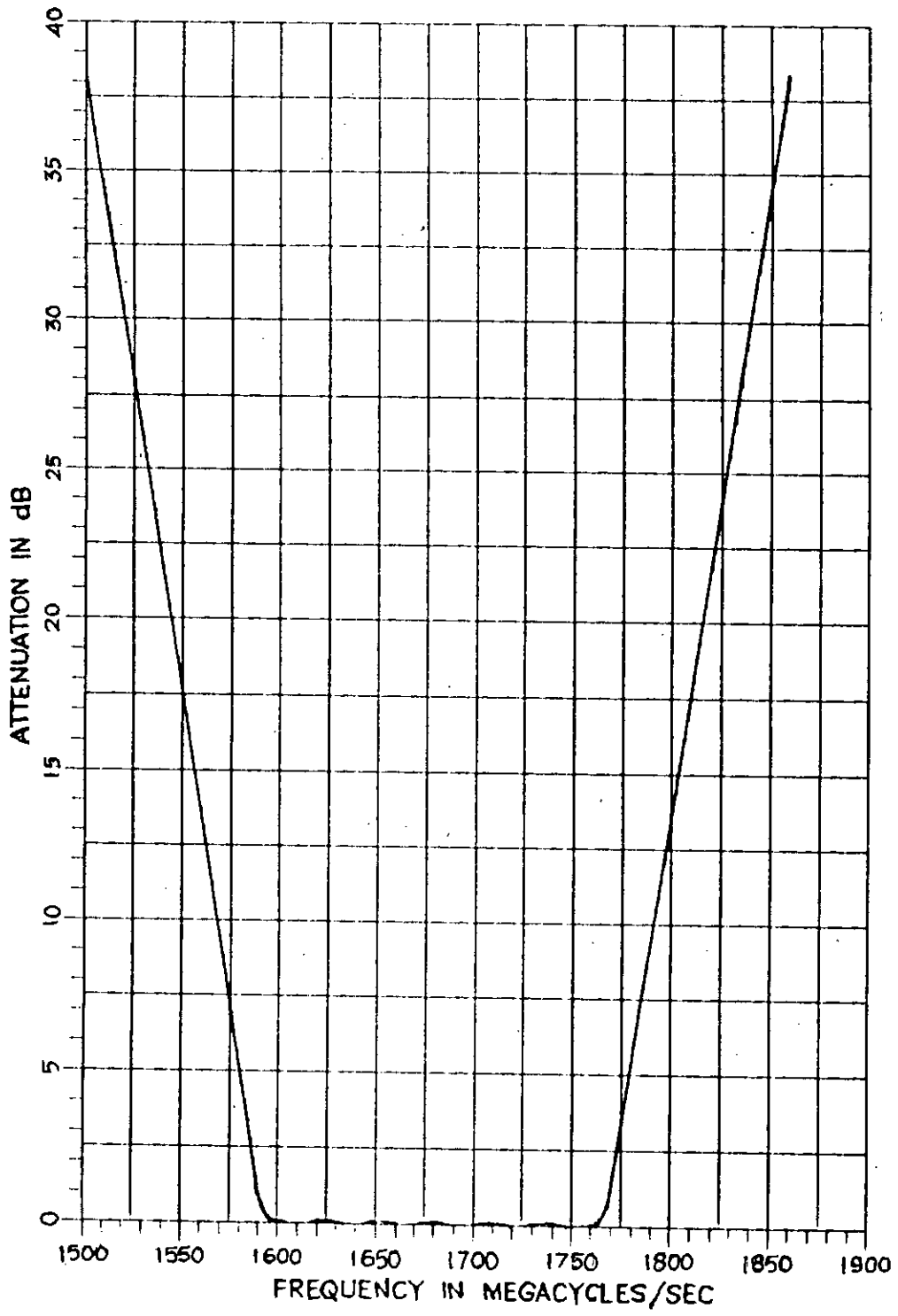


Figure 9.3 Theoretical attenuation characteristics of the combline bandpass filter.

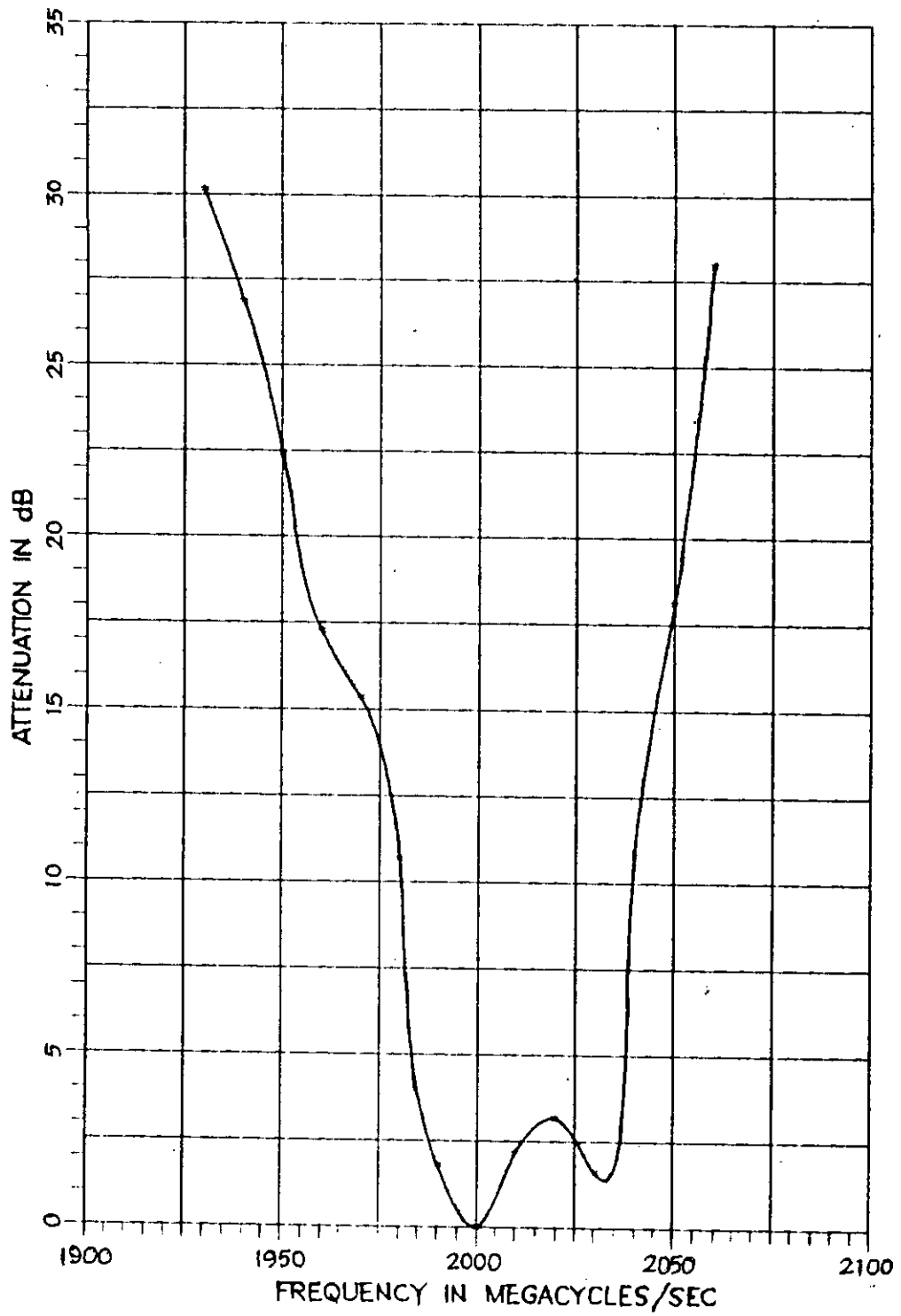
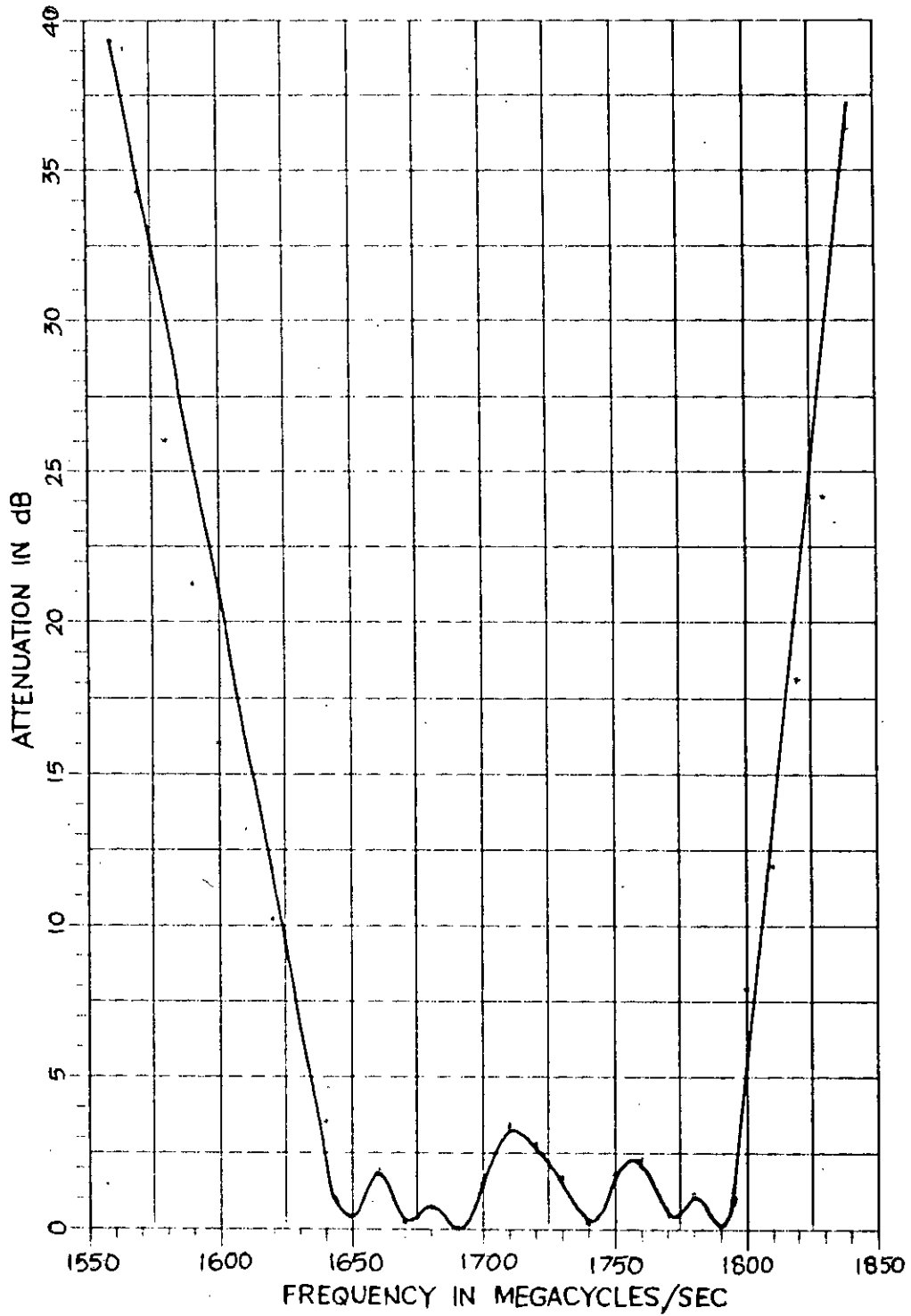


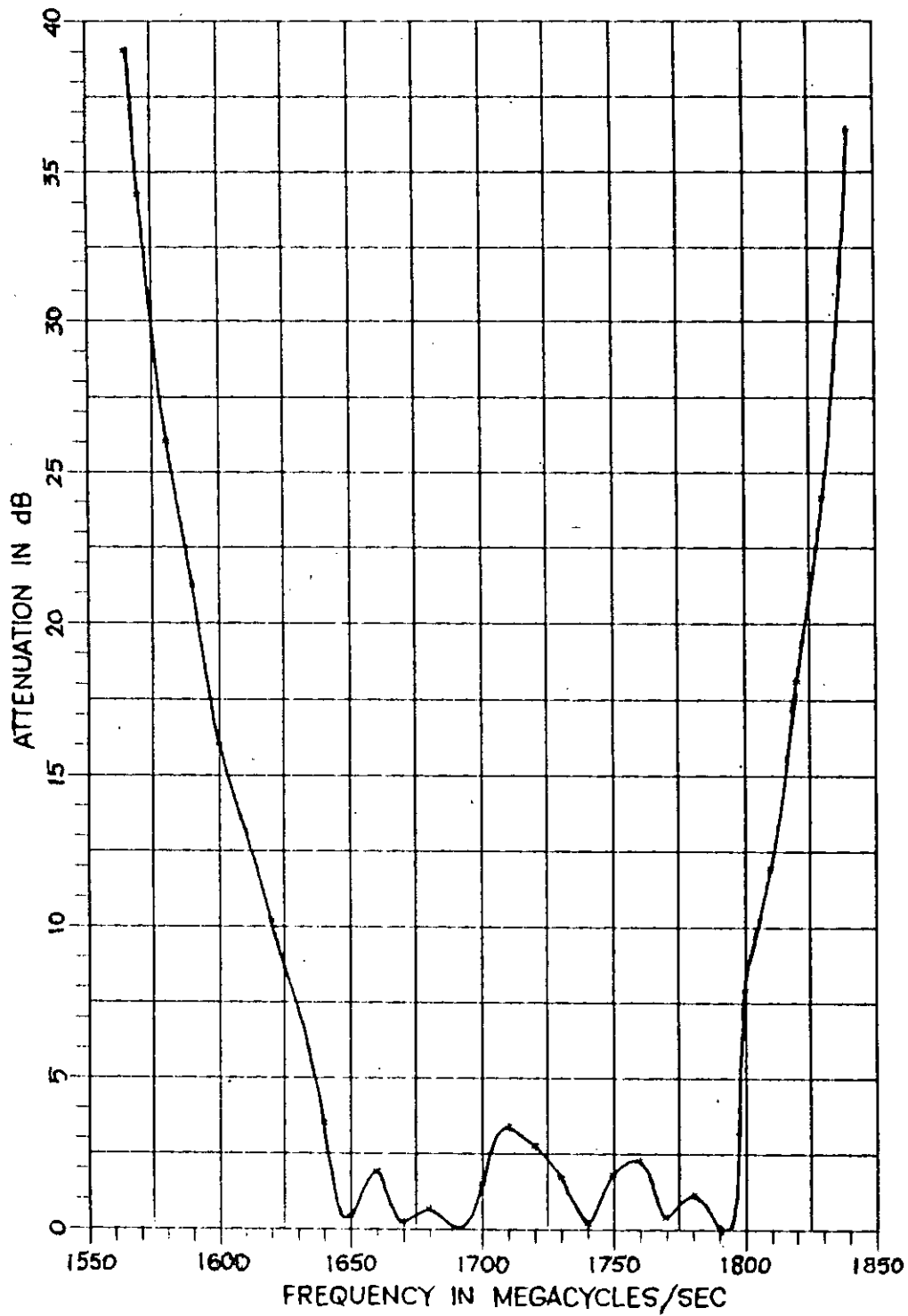
Figure 9.4 Measured insertion loss against frequency curve of the fabricated filter before tuning.



(a)

Figure 9.5 Measured insertion loss against frequency curve of the fabricated filter after tuning.

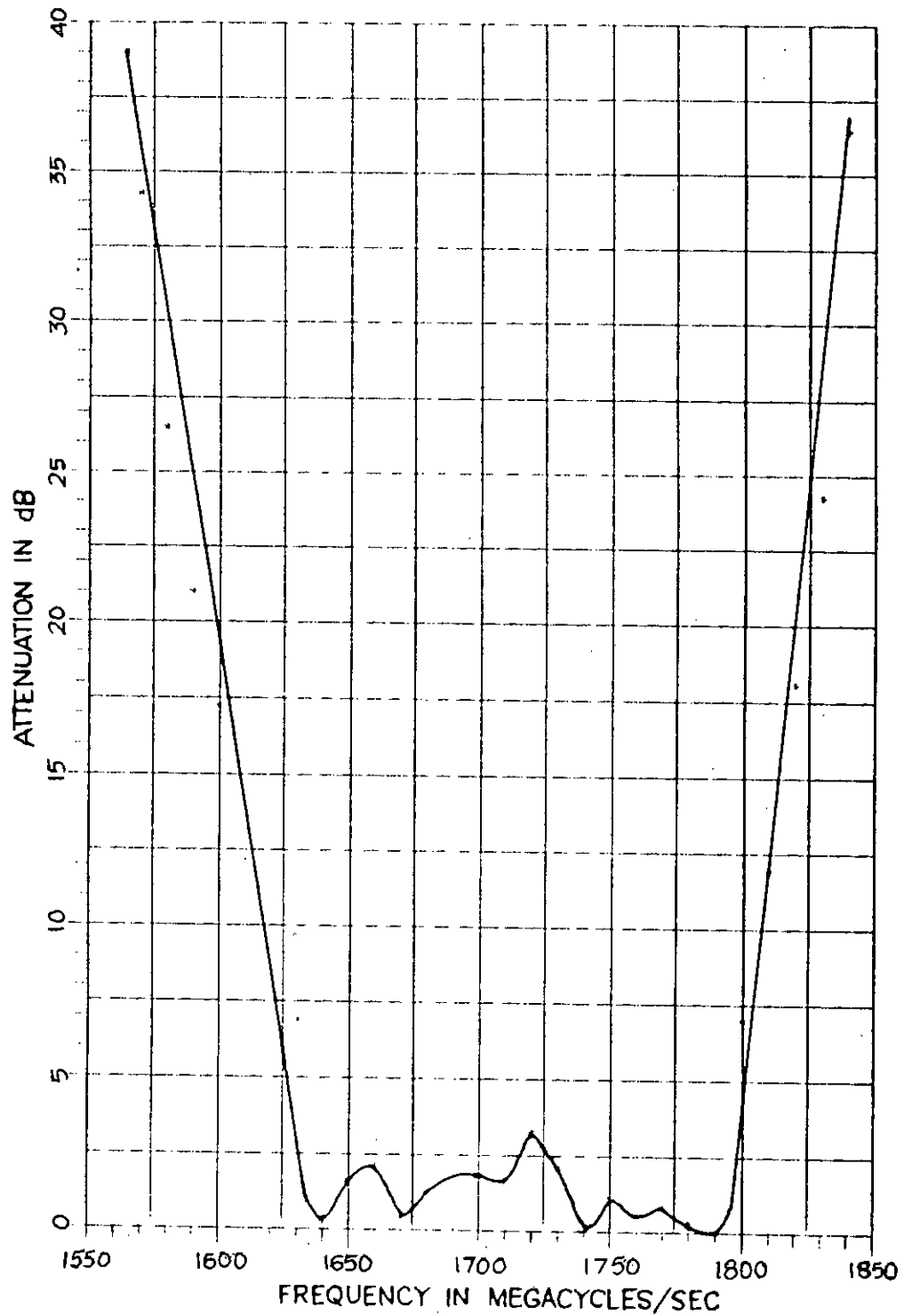
(a) Approximate representation



(b)

(b) Exact representation

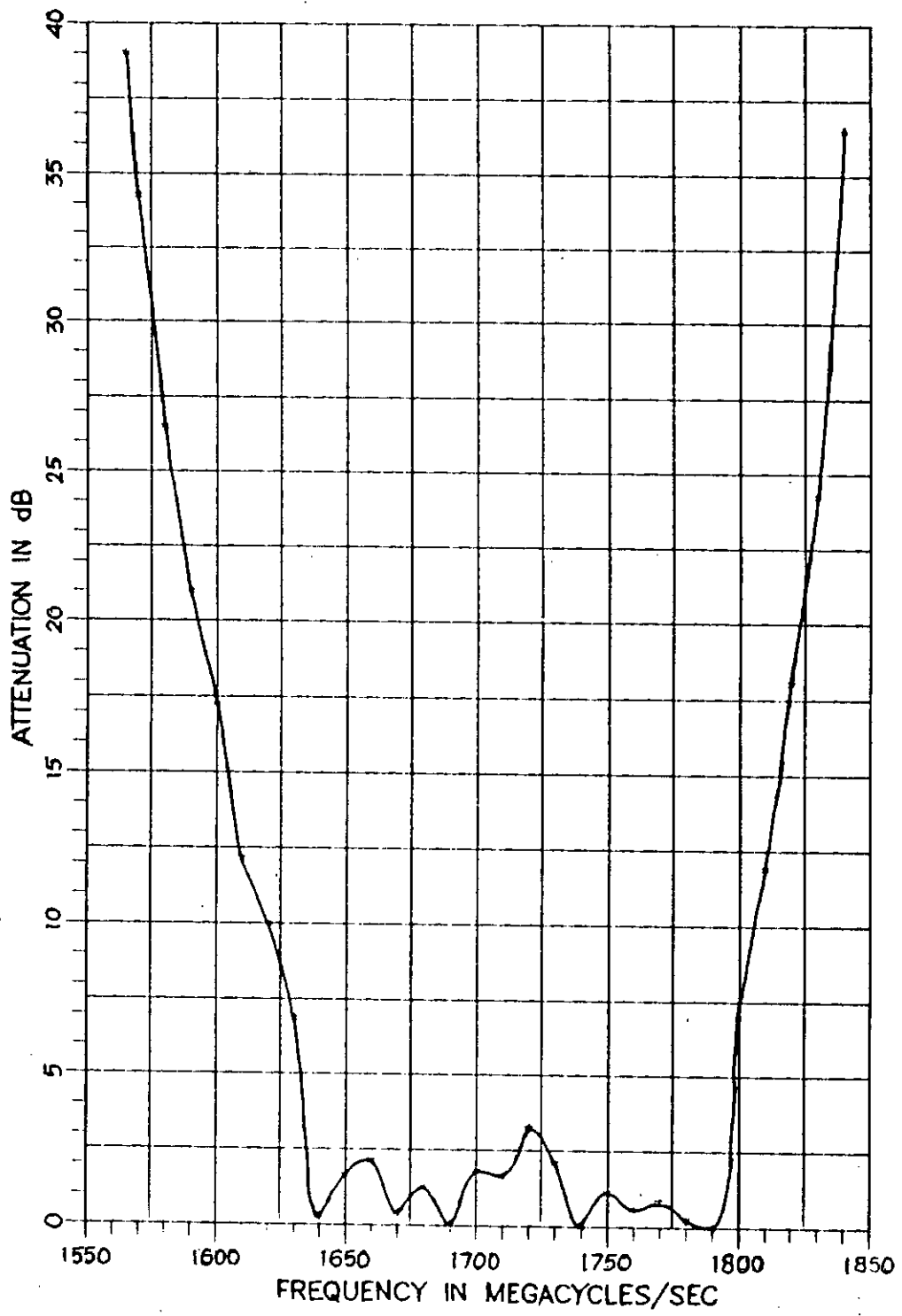




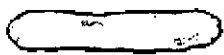
(a)

Figure 9.6 Measured insertion loss against frequency curve of the fabricated filter after tuning with connection to the input and output terminals interchanged.

(a) Approximate representation



(b)

(b) Exact representation 

9.4 Method of tuning:

The filter has been tuned with the grounded sliding blocks, each of which form one side of the parallel plate lumped capacitances connected at the open circuited tip of each of the resonators. Since the structure has symmetry so it was thought that for a five resonator the tuning should be done by sliding the blocks with resonator lines 1 and 5 first, then lines 2 and 4, and then line 3. In this way by small incremental changes a first tuning was obtained. Usually such a tuning procedure requires a sweep generator and display system, or a Network Analyzer, or a Time Domain Reflectometer(TDR) system so that one can observe the effect of the adjustments on the passband and stopbands simultaneously. Unfortunately only discrete frequency measurement system with a power meter is available in the laboratory. As a result it was not possible to observe the effect of any adjustment over the entire passband. However, tuning was done by first improving the attenuation value at a frequency near the lower bandedge and then at another frequency near the upper bandedge. The process was continued on those two fixed frequencies until no further improvements could be obtained.

9.5 Summary :

Construction of the experimental filter has been described. Method of measurement and the working principles with brief description of measuring instruments are also

given in this chapter. Measured attenuation characteristics of the constructed filter under two tuning conditions have been presented. Tuning procedure used to obtain desired response has been discussed.

CHAPTER-10

Discussions and Conclusions

A method has been developed for designing narrow band microwave bandpass filter in this work. In this method a Chebychev lumped low-pass prototype has been transformed to distributed bandpass filter. Such a distributed bandpass filter contains both series and shunt resonators. Using admittance inverter and other microwave equivalent network of shunt resonator, ultimately the equivalent network of the filter is obtained in the form of coupled TEM lines in comb geometry.

Following the realization procedure developed in this work, a bandpass filter is designed and constructed for a center frequency of 1680 MHz with 10% bandwidth i.e. a bandwidth of 168 MHz. The filter is designed to have a maximum passband attenuation of 0.10 dB. The attenuation characteristics measured after tuning are shown in figure 9.5 and figure 9.6. Both these plots were supposed to be identical since the calculated dimensions of the resonators and the transformer elements are symmetrical. But a little variation is observed between the two curves. This is due to the fact that the physical dimensions of the transformer elements as well as the identical resonators could not be made exactly equal. Moreover gap between resonators could not be maintained identical and thereby symmetry was lost to a

little extent resulting a little variation between the curves. The measured attenuation characteristics obtained after tuning shows that the maximum passband attenuation is about 3.25 dB and the bandwidth is around 160 MHz and the midband frequency is 1715 MHz. So, it is observed that the maximum passband attenuation is more than the theoretically predicted value and the center frequency has increased by 2.08% while the bandwidth remained almost equal to the desired value. If a comparison is made between the attenuation curves of the filter before and after tuning, it is observed that tuning improves the response to a large extent.

The filter was constructed by machining brass plates. A high degree of accuracy in physical dimension is required for the construction of this type of filters. Introduction of inaccuracy to physical dimension of resonator or transformer element influences the overall performance highly. Such as a little inaccuracy introduced in the lengths of resonator elements changes the center frequency. Increase in length of resonator decreases the value of the center frequency while a little bit of decrease in length increases the value of the center frequency. Here it is to be noted that a small change in length of the resonator lines causes a significant change in the center frequency. This is probably the reason behind the shifting of the center frequency of the experimental filter.

Another area responsible for introducing error is the

Getsinger's chart. Curves of ΔC against s/b in figure 4.2(a) shows that a change in the spacing between the lines(s) causes considerable change in mutual capacitance between lines (ΔC). It is very likely that due to the inaccuracy of machining some error may be introduced in the interbar spacings. This causes a change in the value of mutual capacitance which intern causes a change in the response of the filter. Moreover during measurement it has been observed that lumped capacitance between the resonator and ground has got a sensitive effect on the response of the filter. Slight adjustment of the grounded sliding block by means of tuning screw changes the response very much. The influence of the sliding blocks nearest to the input and output transformer element on the response is highly remarkable. Since these blocks were not identical in shape and size, it may be responsible to some extent for the variation in the attenuation characteristics of the filter.

The setting of input and output connectors to the respective transformer element was a difficult job. For the connection between the transformer element and the connector it was necessary to construct a coaxial transmission line of 50 ohm. But due to the lack of accuracy in physical dimension and for the fact that the central conductor may become eccentric with the outer conductor of the transmission line, the characteristic impedance may not remain 50 ohm. In fact, due to the difficulty faced in machining and setting it was next to impossible to maintain a high degree of accuracy at

those connections. As a result at the input and output ports impedance mismatch may be present. This type of impedance mismatch is very much unwanted. It causes an increase in loss in the passband. At the same time loss of power in the connectors itself increases attenuation in the pass-band. Moreover, theoretically this type of filter should be constructed with materials having infinite conductivity. The brass plates used for the construction of the filter were purchased from local market and were not meant for this kind of work. This ordinary brass material may also cause some loss in the passband.

Taking into consideration the availability of materials and fabrication facilities, it can be said that the discrepancies that appeared between the theoretical and measured characteristics was very much within tolerable range. Even it can be concluded that utilizing the existing facilities filters in the GHz frequency range can be designed and constructed with satisfactory measured performance and the experimental filter was more or less in good agreement with theory.

Suggestions for future work

The design method presented in this work is valid for Chebyshev filters only. It is worthwhile investigating the possibility of extending this method for elliptic-function bandpass filters and seeing whether for elliptic function also one can obtain similar physically realizable combine geometry. This remains to be done in future.

References

- [1] J.T.Bolljahn and G.L.Matthaei, "A Study of the Phase and Filter Properties of Arrays of Parallel Conductors Between Ground Planes." Proceedings of the IRE, Vol.50, March,1962. pp.299-311.
- [2] G.L. Matthaei, "Interdigital Band-Pass Filters." IRE Transactions on Microwave Theory and Techniques, PGMTT-10, November, 1962. pp.479-491.
- [3] W.J.Getsinger, "Coupled Rectangular Bars Between Parallel Plates." IRE Transactions on Microwave Theory and Techniques, PGMTT-10, January,1962. pp.65-72.
- [4] R.J. Wenzel, "Exact Theory of Interdigital Band-Pass Filters and Related Coupled Structures." IEEE Transactions on Microwave Theory and Techniques, Vol.MTT-13,No.5, September,1965. pp.559-575.
- [5] M.C.Horton and R.J.Wenzel, "The Digital Elliptic Filter - A compact Sharp-Cutoff Design for Wide Band-Stop or Bandpass Requirements." IEEE Transactions on Microwave Theory and Techniques, Vol. MTT-15,No.5, May, 1967, pp.307-314.
- [6] J.D. Rhodes, "The Half-Wave Stepped Digital Elliptic Filter." IEEE Transactions on Microwave Theory and Techniques,Vol.MTT 17, No.12, December,1969.pp.1102-1107.
- [7] R. E. Collin, "Foundations for Microwave Engineering." McGraw-Hill International Book Comp. pp.398-404,410-415.

- [8] G.L. Matthaei, L. Young, E.M.T. Jones, "Microwave Filters, Impedance Matching Networks and Coupled Structures." McGraw-Hill, New York, 1964. pp.49-59, 144-149, 174-197, 217-229.
- [9] H. Ozaki and J. Ishii, "Synthesis of a Class of Strip-Line Filters," IRE Transactions on Circuit Theory, PGMTT-5, June, 1958. pp.104-109.
- [10] E.M.T. Jones and J.T. Bolljahn, "Coupled-Strip-Transmission-Line Filters and Directional Couplers." IRE Transactions on Microwave Theory and Techniques, April, 1956. pp.75-81.
- [11] S.B. Cohn, "Direct-Coupled-Resonator Filters." Proceedings of the IRE, Vol. 45, February, 1957, pp.187-196.
- [12] R. Saal, "Der Entwurf Von Filtern mit Hilfe des Kataloges Normierter Tiefpasse." Telefunken, G.m.b.H., Backney/Wurtemberg, W.Germany, 1964.
- [13] A. L. Lance "Introduction to Microwave Theory and Measurements." McGraw-Hill Book Company, New York. pp.244-255.

Appendix-A

```

                Program to calculate line parameters
10 dim g(7),b(7),j(7,7),c(7,7),cs(7),ya(7)
20 rem comblin filter design.
30 rem open "a:dfile.app" for output as #3: close #3
40 cls
50 lprint "designing a 5 resonator comblin filter with chebychev
   characterstic"
60 pi = 3.14159: print "dummy";pi;sin((pi*60)/180)
70 epsilon0=8.854*10^12: epsilon=1
80 epsilon=epsilon0*epsilon
90 g(1)=1:g(2)=.9732:g(3)=1.372:g(4)=1.803:g(5)=1.372:g(6)=.9732:g(7)=1
100 f1=1.57*10^9: f2=1.8*10^9
110 fo=1.68*10^9
120 wo=2*pi*fo
130 wlu=2*pi*f1
140 wllp=1
150 lambda=(3*10^10/fo)/2.54
160 wl=1: wb=.1: ya1=.02
170 lprint "f1="; f2=";f2;";fo=";fo
180 for k=2 to 6: b(k)=.87*ya1: ya(k)=.677*ya1: next k
190 ya(1)=1/50: ya(7)=1/50
200 theta0=pi/4: b=.625: t=.188: rho=.1
210 rem wl=2*pi*1.1*10^9
220 ap=10*log(1-rho^2)
230 lprint "maxm. passaband attenuation=";ap;"db"
240 lprint "rho=";rho;"; w=";wb
250 for k=2 to 6
260 b(k)=ya(k)*((1/tan(theta0))+theta0*(1/sin(theta0))^2)/2
270 next k
280 gt2=wb*b(2)/(g(1)*g(2)*wllp)
290 for k=2 to 5
300 j(k,k+1)=(wb/wllp)*sqr((b(k)*b(k+1))/(g(k)*g(k+1)))
310 next k
320 gt6=wb*b(6)/(g(6)*g(7)*wllp)
330 c(1,1)=(376.7*ya1/sqr(epsilon))*((1-sqr(gt2/ya1))
340 c(2,2)=(376.7*ya1/sqr(epsilon))*ya(2)/ya1-1+(gt2/ya1)-
   (j(2,3)/ya1)*tan(theta0))+c(1,1)
350 for k=3 to 5
360 c(k,k)=(376.7*ya1/sqr(epsilon))*((ya(k)/ya1)-
   (j(k-1,k)/ya1)*tan(theta0)-(j(k,k+1)/ya1)*tan(theta0)): next k
370 c(7,7)=(376.7*ya1/sqr(epsilon))*((1-sqr(gt6/ya1))
380 c(6,6)=(376.7*ya1/sqr(epsilon))*((ya(6)/ya1)-1+(gt6/ya1)-
   (j(5,6)/ya1)*tan(theta0))+c(7,7)
390 c(1,2)=376.7*ya1/sqr(epsilon)-c(1,1)
400 for k=2 to 5
410 c(k,k+1)=(376.7*ya1/sqr(epsilon))*((j(k,k+1)/ya1)*tan(theta0))
420 next k
430 c(6,7)=376.7*ya1/sqr(epsilon)-c(7,7)
440 for k=2 to 6: cs(k)=(ya(k)*(1/tan(theta0)))/wo: next k
450 lprint "lowpass parameters:"
460 lprint "g(1...7):"g(2);g(3);g(4);g(5);g(6);g(7)
470 lprint "j inverter impedances j12...j67:"
```



```

480 lprint j(1,2)/ya1;j(2,3)/ya1;j(3,4)/ya1;j(4,5)/ya1;j(5,6)/ya1;
      j(6,7)/ya1
490 lprint "-----"
500 lprint "coupling capacitances:"
510 lprint c(1,2);c(2,3);c(3,4);c(4,5);c(5,6);c(6,7)
520 lprint "-----"
530 lprint "self capacitances:"
540 lprint c(1,1);c(2,2);c(3,3);c(4,4);c(5,5);c(6,6);c(7,7)
550 lprint "-----"
560 lprint "lumped capacitances:"
570 lprint "cs(1...7):"
580 lprint cs(1);cs(2);cs(3);cs(4);cs(5);cs(6);cs(7)
590 lprint "-----"
600 lprint "za=1/ya= ";/ya1;"; za1=1/ya1=";1/ya(1);" za2=";1/ya(2);"
      za3=";1/ya(3);" za4=";1/ya(4);"za5=";1/ya(5);" za6=";1/ya(6);"
      za7=";1/ya(7)
610 lprint "-----"
620 lprint"lambda=";lambda;";lambda/4=";lambda/4;"; lambda/8=";
      lambda/8; "inch"

```

Appendix-B

Program to calculate widths of rectangular bars

```

10 dim cc(7,7),s(7,7),m(6),fc(7,7),w(7),sc(7)
20 rem comblne filter desine
30 rem open "a:dfile.app" for output as #3: close #3
40 cls
50 lprint "calculation of widths of rectangular bars and fringing
      capacitances using getsinger's charts"
60 t=.188: b=.625: I=.8
70 lprint "fringing capacitance for an isolated rectangular bar
      from getsinger's chart(for t/b=.3),I=.8"
80 cc(1,2)=2.252879: cc(2,3)=.567379: cc(3,4)=.416847:cc(4,5)=.416847:
      cc(5,6)=.567379: cc(6,7)=2.252879
90 m(1)=.175: m(2)=.525: m(3)=.62: m(4)=.62: m(5)=.525: m(6)=.175
100 fc(1,2)=.225: fc(2,3)=.56: fc(3,4)=.62: fc(4,5)=.62: fc(5,6)=.56:
      fc(6,7)=.225
110 for k=1 to 6: s(k,k+1)=m(k)*b: next k
120 sc(1)=5.281121: sc(2)=2.953934: sc(3)=4.116291: sc(4)=4.266824:
      sc(5)=4.116291: sc(6)=2.953934: sc(7)=5.281121
130 w(1)=b*.5*(1-.3)*((.5*sc(1))-I-fc(1,2))
140 for k=2 to 6: w(k)=b*.5*(1-.3)*((.5*sc(k))-fc(k-1,k)-fc(k,k+1)):
      next k
150 w(7)=b*.5*(1-.3)*((.5*sc(7))-fc(6,7)-I)
160 lprint "separation between rectangular bars:"
170 lprint s(1,2);s(2,3);s(3,4);s(4,5);s(5,6);s(6,7); "inchs"
180 lprint "-----"
190 lprint "widths of rectangular bars:"
200 lprint w(1); w(2); w(3); w(4); w(5); w(6); w(7); "inchs"

```

Appendix-C

Measured attenuation characteristics
of the constructed filter. (Before tuning)

Frequency (in MHz)	Attenuation (in dB)
1930	30.15
1940	26.85
1950	22.46
1960	17.28
1970	15.37
1980	10.68
1990	1.80
2000	0.00
2010	2.16
2020	3.17
2030	1.63
2040	10.91
2050	18.12
2060	28.05

Appendix-D

Measured attenuation characteristics
of the constructed filter (After tuning)

Frequency (in MHz)	Attenuation (in dB)	Frequency (in MHz)	Attenuation (in dB)
1565	39.03	1710	3.39
1570	34.25	1720	2.76
1580	26.02	1730	1.69
1590	21.25	1740	0.20
1600	16.02	1750	1.82
1610	13.17	1760	2.30
1620	10.21	1770	0.40
1630	9.37	1780	1.16
1640	3.50	1790	0.06
1650	0.44	1800	7.92
1660	1.91	1810	11.97
1670	0.23	1820	18.12
1680	0.70	1830	24.15
1690	0.00	1840	36.37
1700	1.51		

Appendix-E

Measured attenuation characteristics of the
constructed filter after tuning with the
connection to the input and output terminals interchanged.

Frequency (in MHz)	Attenuation (in dB)	Frequency (in MHz)	Attenuation (in dB)
1565	39.00	1710	1.63
1570	34.25	1720	3.25
1580	26.50	1730	2.09
1590	21.00	1740	0.00
1600	17.26	1750	1.14
1610	12.15	1760	0.56
1620	10.00	1770	0.84
1630	6.87	1780	0.26
1640	0.30	1790	0.00
1650	1.64	1800	6.99
1660	2.12	1810	11.90
1670	0.41	1820	18.06
1680	1.28	1830	24.25
1690	0.00	1840	36.45
1700	1.82		

